Fall 2021

Optimization and Application of Electrochemical Probes for Neurotransmitter Detection

Colby E. Witt

OPTIMIZATION AND APPLICATION OF ELECTROCHEMICAL PROBES FOR NEUROTRANSMITTER DETECTION

by

Colby E. Witt

Bachelor of Science
Francis Marion University, 2017

Submitted in Partial Fulfillment of the Requirements

For the Degree of Doctor of Philosophy in

Chemistry

College of Arts and Sciences

University of South Carolina

2021

Ph.D. Committee:

Parastoo Hashemi, Major Professor

Susan Richardson, Committee Member

Sheryl Wiskur, Committee Member

Ana Pocivavsek, Committee Member

Tracey L. Weldon, Interim Vice Provost and Dean of the Graduate School

DEDICATION

To the strong personalities that helped to shape me. To the teachers who inspired me. To the animals who were used throughout this body of work.

ACKNOWLEDGEMENTS

First, I would like to thank my incredible advisor, Dr. Parastoo Hashemi. You have taught me how to do science with integrity and how to stand up for what I believe in. You have shown me how to be a great mentor and I will carry that with me forever. I would like to thank my committee members: Dr. Susan Richardson, Dr. Sheryl Wiskur and Dr. Ana Pocivavsek for their advice and kindness over the years but I would mostly like to thank them for challenging me to be a better scientist. Another special thanks should be extended to Mrs. Mia Junkins, Dr. Jessica McCutcheon and Professor Lisa Pike for igniting my passion for chemistry, research and teaching during my career as a student. Without their encouragement, I would not be where I am today.

I would like to take the time to thank the members of the Hashemi Lab for everything they have taught me over the years. I would like to thank Ou for her mentorship and guidance. She was the first person to truly believe in my scientific abilities and has been a great friend and confidant. I would like to thank Jordan H. for teaching me everything I know about fundamental electrochemistry and for teaching me to work hard and play harder. I would like to thank Shane for finally teaching me where the elusive medial forebrain bundle is located and for being a great "workplace acquaintance". I would like to thank Alyssa and Melinda for guiding me through my first animal surgeries. I would like to thank Anna Marie for eagerness to always bounce ideas with me and for always being the person I could talk to about the latest TV shows. Thank you for going through the ups and downs with me during this whole dissertation process; we are forever bonded

because of this shared stress. I would like to thank Brenna for the endless coffee breaks and every conversation about science and life in general; you're a true friend, buddy. I would like to thank Sergio for all the codes he has written for analyzing my basal data and for the wonderful friendship that has blossomed. I would like to thank Lauren B. and Melissa for always being ready to help and allowing me the opportunity to sharpen my teaching and communication skills through their training. However, my tenure in the Hashemi Lab would not be complete without my "science babies". Thank you to Lauren H, Fariha, Jordan C, you guys were my first mentees and it has been amazing to get to know you all and see you guys blossom into successful young women in science. Specifically, I would like to thank Lauren H. for all of her hard work that is featured throughout this dissertation; I couldn't have done all this without you. Navid, Ian, Dee Dee, Kayla, and Morgan for letting me teach you and ultimately learning and growing alongside me. To my "science babies" being your mentor has been one of my greatest joys. I am so excited to see what amazing things you all do.

I would like to thank the people outside of the lab who have made an impact on my Ph.D. work by keeping me sane and in good mental health. I would like to thank the friends I have made on the way: Dayla, Madeleine, Rhiannon, Jennifer, Katy P, Katie H, Will and Ryan. Thank you for the distractions, the advice and, ultimately, your friendship. I would also like to take the time to thank some lifelong friends for their years of encouragement, love, support and helping me through every "mental breakdown" I've had along the way: Adam, Kyndell, Caroline, Caitlyn E., Christina, Ashlei B, Megan, Latara, Latia, Amanda, Lucas, Kaitlyn S, Ashleigh S and Whitley—thanks you all for everything.

Finally, I would like to thank my family for the unwavering support. To my mom and dad, Sandra and Roy, thank you for being my rock. Thanks for showing me what real love looks like, for always pushing me to better myself and for accepting me for who I am. To my brother, Corbin, thank you for being my best friend. Thank you for challenging me and teaching me throughout the years. To my grandparents, Caroline (Peggy), Jimmy and Ann, thank you for encouragement and for pushing me to always strive to do my best work and shoot for the stars. I would be nowhere without my family. This is for you all; I hope I make you guys proud!

ABSTRACT

The brain is a complex matrix that is difficult to study. Signaling molecules, neurotransmitters, are constantly being released and sequestered back into neurons within milliseconds to facilitate communication and normal function, a process called neurotransmission. There are few analytical techniques available to selectively probe such a dynamic system, and even fewer can detect these discrete changes in real-time. In order to make robust measurements in the brain you need speed, sensitivity, selectivity and small probe size, which are encompassed by fast-voltammetry with microelectrodes. Traditional fast-voltammetry at carbon fiber microelectrodes (fast-scan cyclic voltammetry (FSCV)) requires background subtraction to overcome the large capacitive currents generated from scanning at such a high rate, therefore crucial basal information is lost. To capture this previously lost information, fast-scan controlled adsorption (FSCAV) was developed for serotonin detection *in vivo*. Serotonin is tightly regulated in the brain and thought to mark affective disorders, therefore it is crucial to develop and cultivate new tools to better understand this biomarker. Recently, our lab has employed FSCAV to understand niche mechanisms of action and regulatory processes of the central nervous system regarding serotonin. Here, we discuss improvements towards basal serotonin detection with FSCAV by first modifying CFMs to improve sensitivity and stability over prolonged periods of time and then demonstrate their use in elucidating the effects of antidepressants on tonic serotonin levels. These efforts have indeed improved our own measurements of serotonin and have clearly shown that exploiting the *in vivo* environment can improve biomarker

detection and thus shows promise as a methodology to be adopted across the fast-voltammetry community.

PREFACE

This dissertation is closely based on the following refereed publications:

Chapter 2: Holmes, J., **Witt, C. E.**, Keen, D., Buchanan, A. M., Batey, L., Hersey, M. & Hashemi P. "Glutamate Electropolymerization on Carbon Increases Analytical Sensitivity to Dopamine and Serotonin: An Auspicious *In Vivo* Phenomenon in Mice?" — *Accepted* — Analytical Chemistry

Chapter 3: **Witt, C. E.**, Mena, S., Honan, L. E., Visentin, M., Batey, L, Robins, N., Ou, Y. & Hashemi, P. "Novel, User-Friendly Experimental and Analysis Strategies for Fast Voltammetry: 2. Next Generation FSCAV Serotonin Measurements." — *In Preparation* — ACS Measurement Science AU.

Chapter 4: **Witt, C. E.**, Mena, S., Berger, S. N., Parke, B., Hersey, M., Ou, Y., Honan, L. E., Fadel, J. and Hashemi, P. "Voltammetric Assessment of the Effects of Different Antidepressants Types on In Vivo Serotonin." — *In Preparation* — Frontiers in Neuroscience.

Chapter 5: **Witt, C.E.**, Islam, F., Honan, L. E., Mena, S., Ou, Y. & Hashemi, P. "FSCAV Parameter Optimization for Improved Definition and Temporal Resolution of Ambient Serotonin Oscillations." — *In Preparation* — Analytical Methods.

TABLE OF CONTENTS

LIST OF TABLES

LIST OF FIGURES

LIST OF SYMBOLS

R^2	Coefficient of Determination
Q(t)	Charge of Serotonin Faradaic Peak
t	Time
Q0	Position of Exponential in the Cartesian Axis
Qf	Position of Exponential in the Cartesian Axis
k	Exponential Constant
t63%	Time Constant
X	Vector of Inputs of Nodes

LIST OF ABBREVIATIONS

AAs ..... Amino Acids

Ads ..... Antidepressants

AFM ..... Atomic Force Microscopy

AMPA ..... Alpha-amino-3-hydroxy-5-methyl-4-isoxazoepropionic Acid

ANN ..... Artificial Neural Network

Asp ..... Aspartate

CFMs ..... Carbon Fiber Microelectrodes

CNS ..... Central Nervous System

CV ..... Cyclic Voltammogram

Cys ..... Cysteine

DA ..... Dopamine

DATS ..... Dopamine Transporters

DNR ..... Dorsal Raphe Nucleus

ESCIT ..... Escitalopram

FIA ..... Flow Injection Analysis

FSCAV ..... Fast-Scan Controlled Adsorption Voltammetry

FSCV ..... Fast-Scan Cyclic Voltammetry

GABA ..... Gamma Aminobutyric Acid

Glu ..... Glutamate

Gly ..... Glycine

GAD ..... Glutamate Decarboxylase

i.p. ..... Intraperitoneal

Lys ..... Lysine

MAOIs ..... Monoamine Oxidase Inhibitors

mTOR ..... Mammalian Target of Rapamycin

NA ..... Nafion

NE ..... Norepinephrine

NETS ..... Norepinephrine Transporters

NMDA ..... N-methyl-D-aspartate

NN ..... Neural Networks

NRIs ..... Norepinephrine Reuptake Inhibitors

OCTS ..... Organic Cation Transporters

PBS ..... Phosphate-Buffered Saline

PEDOT ..... Poly-(3,4-Ethylenedioxythiophene)

PGA ..... Polyglutamic Acid

PMAT ..... Plasma Monoamine Transporter

RMSE ..... Root Mean Square Error

ROS ..... Reactive Oxygen Species

SEM ..... Standard Error of the Mean

SEM ..... Scanning Electron Microscopy

SERTs ..... Serotonin Transporters

SSRIs ..... Serotonin Selective Reuptake Inhibitors

SWC ..... Sliding Window Correlation

TCAs ..... Tricyclic Amines

Trp ..... Tryptophan

Tyr ..... Tyrosine

5-HT 5-Hydroxytryptamine/Serotonin

5-HIAA ..... 5-Hydroxyindoleacetic Acid

Chapter 1: Introduction

NEUROTRANSMISSION

The brain comprises a complex chemical system that changes on a rapid time scale. These rapid-fire chemical changes are underpinned by neurotransmission. Neurotransmission is mediated *via* small molecules known as neurotransmitters/neuromodulators (eg. dopamine (DA), serotonin (5-HT), histamine (HA)) and occurs though a few general steps. The transmitter is synthesized in the presynaptic neuron,[1] packaged into vesicles and released into the synaptic cleft *via* calcium(II)-initiated exocytosis.[2] The transmitter then binds to either postsynaptic receptors or to presynaptic autoreceptors allowing neuronal commination to propagate or terminate through a given circuit. Finally, the signal is terminated *via* reuptake of the neurochemical back into the presynaptic neuron and/or extra- or intra-cellular catabolism.

The fundamental processes neurotransmission are of interest because dysfunctions in neurotransmission are implicated in neuropsychiatric disorders, such as depression. Fundamentally, it is important to understand how these neuromodulators function rapidly (phasic release) and control homeostasis on a slower time scale (ambient levels).

NEUROTRANSMITTERS

Neurotransmission is mediated by essential amino acids (AAs) found in the extracellular space. AAs have a duality about them, they serve as the building blocks for neurotransmitters[3-5] such as serotonin, dopamine and norepinephrine, and they act on their

own to propagate signals.[6-8] Of notable interest are glutamate, gamma aminobutyric acid (GABA) and glycine, which play a large role in the mediation of neurotransmission by functioning as excitatory and inhibitory neurotransmitters.[9-11] As glutamate is the precursor of GABA *via* glutamate decarboxylase (GAD) mediated metabolism,[12, 13] it illustrates the vital need for these two neurotransmitter systems to have a balanced interaction in order to maintain homeostasis within the central nervous system (CNS). This homeostasis is mediated by the release of neuromodulators and is initiated with glutamate by binding to its receptor types causing a conformational change, an influx of Na^+ and efflux of K^+ and hence neuronal signaling.[14] In contrast, GABA inhibits signal propagation by hyperpolarization of the postsynaptic neuron.[15] Serotonin and dopamine function *via* volume transmission. Unlike the tightly regulated glutamate and GABA, neurochemicals released *via* volume transmission can diffuse outside of the synapse and directly influence (*i.e.* activate receptors, causing signaling cascades) larger areas of the brain. These types of messengers are called the neuromodulators.

NEUROTRANSMITTER DYSFUNCTION – THE MONOAMINE HYPOTHESIS OF DEPRESSSION

When neurotransmission is not at homeostasis, there are serious disease implications. Since the turn of the 20th century, decades of work have centered on trying to understand the chemical underpinnings of depression, which is also the focus of our lab's work. Primary contenders for being implicated in the depressed state were the monoamines: serotonin, dopamine and norepinephrine. This idea brought forth "The Monoamine Hypothesis of Depression" and states that one or a combination of these three

monoamines are dysregulated in some capacity in the depressed state.[22] This hypothesis was constructed from early pharmaceutical efforts to target these modulators. Clinicians noted that compounds targeting the serotonergic system were found to provide the most relief in patients.[23] This particular class of drugs became known as selective serotonin reuptake inhibitors (SSRIs) due to their method of action.[22, 24] SSRIs bind to the serotonin transporters to prevent the reuptake of the serotonin back into the presynaptic neuron; this is thought to increase the ambient levels of serotonin in the extracellular space[25] and thus has been shown to alleviate depressive symptoms in some patients.[26] This improvement in symptoms, along with SSRI having the least severe side effects[27] has placed serotonin as a key biomarker for depression. **Figure 1.1** depicts the pathology for SSRI termination of reuptake by various transporters: specifically, this model is based off SSRIs mode of action.

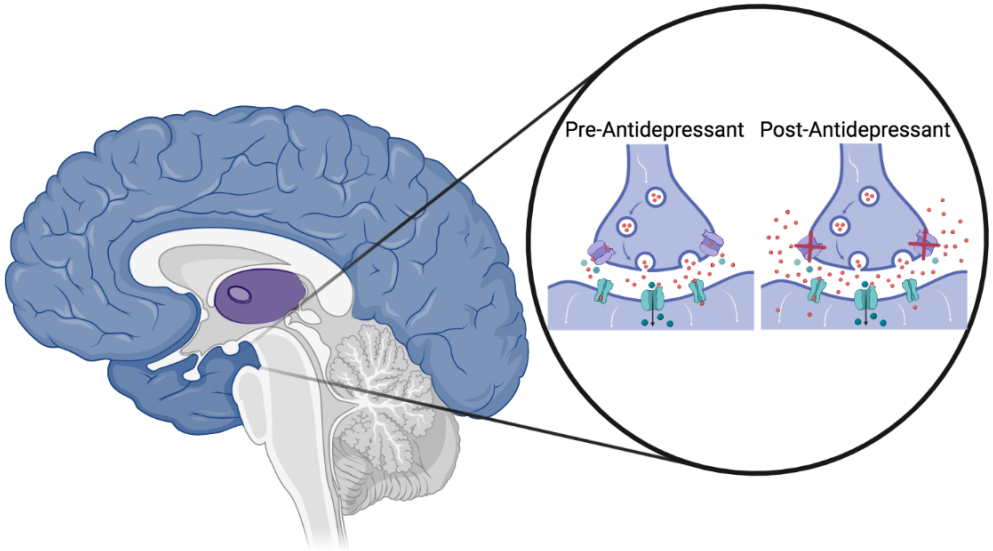

Figure 1.1. Antidepressant "Mode of Action" Scheme. This schematic shows a cartoon of a zoomed in feature of the brain: individual synapses. Pre-antidepressant, there are fewer red molecules in the synaptic cleft and far fewer escaping into the extracellular space. Upon antidepressant administration, "post-antidepressant", the transporters for reuptake of the red molecules have been blocked, resulting in a large increase to the number of red molecules in the synaptic and the extracellular space. This is the general mode of action for SSRIs. (Image made in Biorender).

Serotonin has 14 receptors types: 7 inhibitory and 7 excitatory G-protein coupled receptors and 1 excitatory ligand gated ion channel (5-HT_3). Most of these receptors are postsynaptic; however, there are two notable presynaptic receptors: 5-HT_{1A} and 5-HT_{1B}.[37] Activation initiates a negative feedback loop, this is one method of serotonin regulation. Three other major mechanisms exist to prevent the excess release of serotonin into the cellular space: 1) Uptake 1, serotonin is reuptaken into the presynaptic neuron by serotonin transporters (SERTS)[38-40], 2) Uptake 2, serotonin is reuptaken into other neurons by monoamine transporters (dopamine transporters (DATS), norepinephrine transporters (NETS), and organic cation transporters (OCTS)[38-41], 3) degradation of serotonin *via* monoamine oxidase (MAO).[42, 43] Serotonin has long been known to be electroactive, however, studying this molecule remains difficult. Unlike dopamine, serotonin is tightly regulated due to this molecule's natural tendency to be pushed toward reuptake mechanisms and its metabolism pathways.[44]

EXISTING ANTIDEPRESSANTS AND FRONTIER TREATMENTS

Drug discovery to treat depression has dwindled since the advent of SSRIs in the late 70s with the release of Prozac.[24] There are two-fold reasons for this: 1) new drugs have failed to improve the efficacy rates of existing drugs and 2) the full biochemical mechanism of depression is not known and thus there are no pre-clinical screening tools to test the potential efficacy of new drugs.[68] As of now, a patient presenting with depressive-like symptoms is given a questionnaire and based of the discretion of the physician a diagnosis is made and an antidepressant may be prescribed.[69] The common classes of antidepressants include SSRIs, norepinephrine reuptake inhibitors (NRIs), monoamine oxidase inhibitors (MAOIs) and, more recently, atypical antidepressants. The monoamine hypothesis of

depression was recently revised to include the interactions of glutamate and GABA with the emergence of atypical antidepressants like ketamine.[70-72] Ketamine, also a drug of abuse, has emerged as an atypical antidepressant of interest due to its potential rapid relief of depressive phenotypes.[72, 73]

NEUROCHEMICAL DETECTION

It is very difficult to develop better drugs for depression because the underlying chemistry of depression is unknown because it is hard to measure neurotransmitters such as serotonin. For many decades, electrochemical measurements of serotonin were limited to *ex vivo* preparations such as cerebral spinal fluid or tissue slice preparations. To better understand the dynamics of neuronal communication, neuroscientists and neurochemists have used a variety of tools to answer some complex questions. Because the *in vivo* environment is dynamic and has a small homeostatic window, the tools that are used to answer these fundamental questions must be cover the "Four S's" defined by Lama *et al*: sensitivity, selectivity, size and speed.[53] In order to be an optimal candidate for *in vivo* analysis, the technique should meet all 4 of the S's. Promising techniques have emerged to look at serotonin's roles in the brain including microdialysis[45-48], chronoamperometry[49-51], and fast voltammetry, [38, 44, 52-58] reviewed below.

Microdialysis

Traditionally, microdialysis has been used in the neuroscience community to quantify ambient levels of neurotransmitters from the *in vivo* environment and has been viewed as the gold-standard technique for ambient detection. This technique works by perfusing solution to the probe surface and allowing analytes diffuse through semi permeable membrane. Microdialysis is on its own, a sampling technique and needs to be

paired with separation technique for true detection and quantification. Though microdialysis has been proven to be a useful technique, it is not without drawbacks. The primary issue is the size of the probes themselves, (on average 200-250 μM in diameter).[74] The size of this probe causes damage to the brain by being much larger than the intercapillary distance (~30 μM).[75, 76] This damage elicits an immune response and, thus, microdialysis may not capture the true ambient state for neurotransmission. Fast voltammetry provides itself as an attractive alternative due to its small probe size, biocompatibility (carbon probe), and the fast temporal resolution.

Fast-Scan Cyclic Voltammetry (FSCV)

In the early 1980s, the Wightman lab, along with collaborators, created a new niche tool to study the transmission of dopamine in real time[77]; they later coined this technique fast scan cyclic voltammetry (FSCV) at carbon fiber microelectrodes (CFMs).[77] CFMs offer a self-renewing surface, are biocompatible, adsorb cations, and are cheap and sustainable.[78-81] CFMs have been shown to be stable over time thereby making them a great tool for *in vivo* studies. Since the advent of FSCV, the method has been employed to study dopamine neurotransmission dynamics and has also been adapted to study other neurotransmitters. For example, in 2009, FSCV was first utilized to rapidly measure serotonin on a sub-second timescale *in vivo*.[52] FSCV detection of serotonin has been used to study sex differences within the serotonergic system[57], to understand reuptake dynamics of serotonin back in to the presynaptic neuron[38], to monitors serotonin's dynamic phasic changes to antidepressants[44, 54, 57, 58], and to predict tissue architecture[58].

FSCV detection of serotonin *in vivo* is accomplished thus; a serotonin selective waveform (+0.2 V to +1.0V to -0.1V to +0.2V, 1000V/s)[21] is applied to an electrode implanted in the CA2 region of the hippocampus (CA2: AP:-2.91, ML:+3.35, DV-2.5) at 10 Hz. The current is measured at each potential along the ramp and the output is a color plot generated using custom software. The data are analyzed from false color where green is indicative of oxidation and blue is indicative of reduction. First extrapolated from vertical view from the color pot we will see the signature cyclic voltammogram (CV) for serotonin where its oxidation will occur at 0.7 V while its reduction will occur at 0.0 V.[21] The primary purpose this CV serves is to both identify and qualify the that we have found serotonin. Second, we can extrapolate physiological data by taking a horizontal view of the color plot. This generates a current vs. time plot can be extrapolated from this color plot showing the change in the amount of serotonin in the extracellular space over time. This can be converted into concentration by using a calibration factor.[52] The method is background subtracted due to the very fast scan rate generating a large non-Faradaic current.[82] Therefore, a change must be induced to visualize serotonin's redox processes: this is accomplished *in vivo* by way of electrical stimulation of the medial forebrain bundle (MFB: AP:-1.58, ML:+1.00, DV:-4.80).[52, 82] FSCV is an unquestionably powerful method for *in vivo* neurotransmitter analysis, but the major limitation is that it is a background-subtracted technique, meaning one will only be able to see relative changes in serotonin concentration respect to a low activity state before stimulation (absolute concentration). To combat this and to measure true extracellular concentration, a new technique was created in 2013.

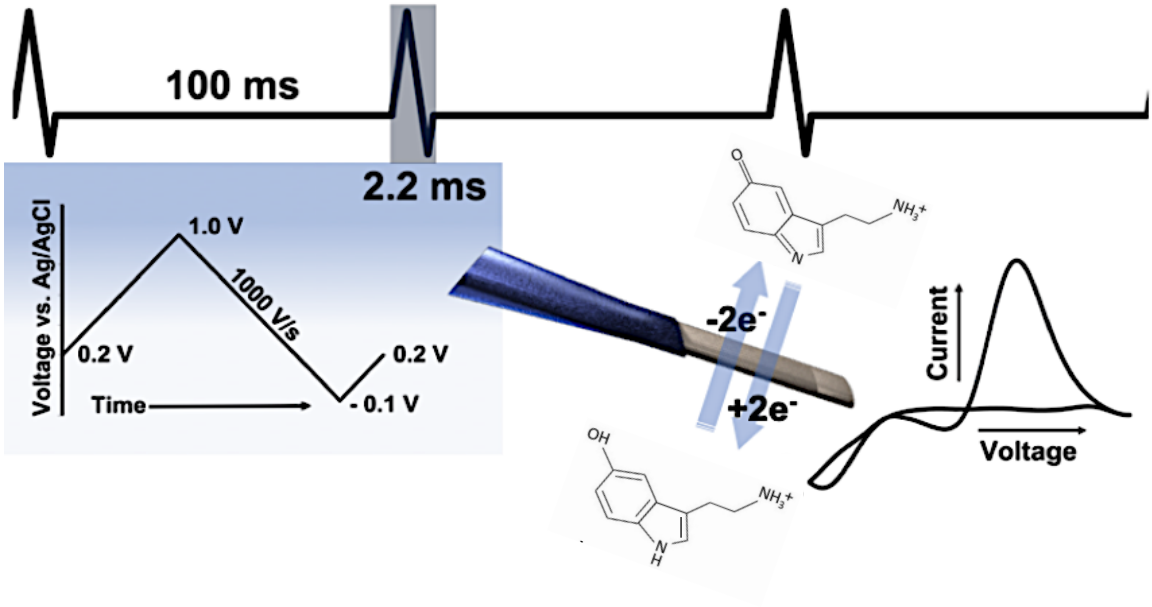

Figure 1.2. FSCV Scheme. To the CFM surface, the serotonin specific waveform is applied. This is a selective way to monitor the oxidation and reduction of this promiscuous analyte. A signature CV for serotonin is displayed with in the figure.

Fast-Scan Controlled Adsorption Voltammetry (FSCAV)

Fast-Scan Controlled-Adsorption Voltammetry (FSCAV), was developed first to measure ambient extracellular levels of dopamine in the absence of an electrical stimulus.[83] These *in vitro* experiments showed promise and FSCAV soon moved *in vivo* in 2015.[55] This method was later modified to measure ambient serotonin.[56] FSCAV is analogous to the principles of stripping voltammetry and is performed in three steps: 1) the serotonin waveform is applied at 100 Hz to minimize adsorption to the electrode surface; 2) a fixed potential (0.2 V) is then applied for 10 secs, (the time is calibrated for maximum adsorption of analyte to the electrodes surface); 3) the waveform is then reapplied and the first signature cyclic voltammogram collected is used to quantify ambient serotonin concentration. The concentration is found *via* post-calibrations of the electrodes. The CVs are unfolded and the oxidation peak for serotonin is integrated to obtain a charge value

(pC). Charge is then converted to concentration (nM). The temporal resolution of this method is 1 minute, and is a great improvement over other techniques for basal measurements which, on average, have the temporal resolution of 10s of minutes.[84-86] **Figure 1.3** depicts the 3 steps of FSCAV data acquisition and shows the signature color plots and cyclic voltammogram for serotonin analysis. By combining FSCV and FSCAV, we now have a multi-purpose tool for measuring the subtle changes of the serotonergic system *in vivo*. This allows for a dual lensed approach to understand serotonins role in depression and how antidepressants effect this neurotransmitters nuances[57].

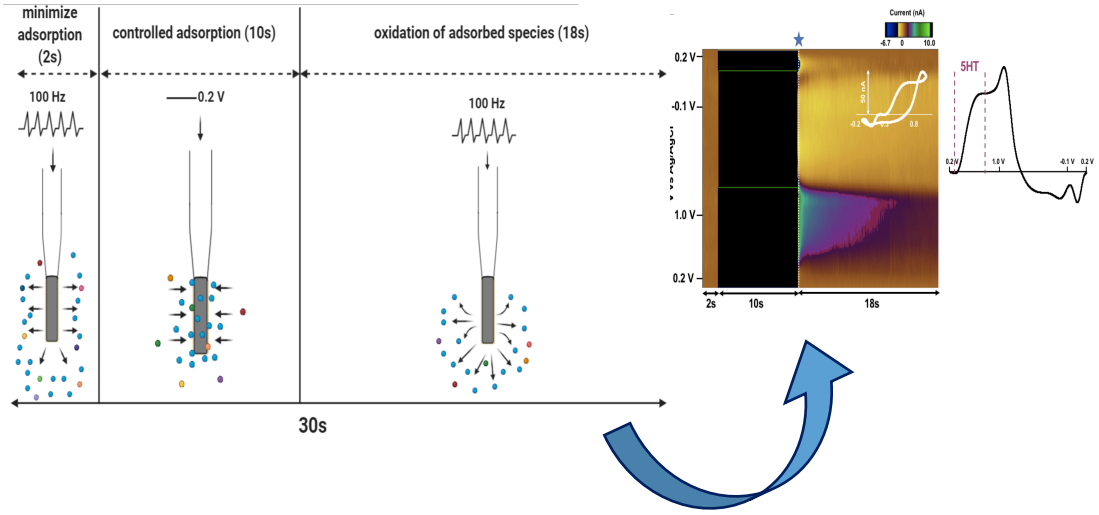

Figure 1.3. FSCAV Scheme. From left to right, the steps of FSCAV are displayed. 1) 2 s to minimize adsorption to the electrodes surface. 2) 10 seconds of controlled adsorption held at 0.2 V to allow for serotonin and other molecules to migrate toward the surface while repelling major metabolites and interferences such as 5-Hydroxyindoleacetic acid. 3) Rapid oxidation of serotonin on the electrode surface. This is selective for serotonin because of the waveform that has been reapplied (the Jackson waveform). An example color plot, CV and integrated oxidation peak are shown next to the blue arrow of the FSCAV schematic

These techniques have uncovered a plethora of knowledge of serotonins role and function in the diseased state. One important nuanced discovery was the ability to understand the mechanism that controls ambient fluctuations of serotonin oscillations.[59, 60]

Serotonin oscillations are linked to extracellular processes. It is known that too much serotonin leads to serotonin syndrome, whereas too little serotonin is linked to depression.[61-64] So, there are fine-tuning mechanisms that balance the serotonergic system to ensure a healthy level is maintained. It is thought that this fine-tuning mechanism can be related back to the receptors that are found on presynaptic and postsynaptic neurons: autoreceptors and heteroreceptors, respectively.[65-67] These receptors often mediate modulatory signaling, or in the case of autoreceptors, initiate a feedback loop inhibiting neurotransmitter release. It has also been noted that these oscillation patterns can be pharmacologically manipulated.[59, 60, 67]

Carbon Fiber Surface Modification

It is clear that sensitivity is an issue for detection of low levels of serotonin in vivo, and while our laboratory's expertise are these measurements, a more sensitive electrode may facilitate broader adoption of the method by the greater community. Surface modification of CFMs has aided the specificity and sensitivity of FSCV measurements. Serotonin detection has historically employed the use of a cation exchange polymer, Nafion. This has been used to limit biofouling, repel serotonin's precursors and metabolites, and has been shown to increase sensitivity toward serotonin analysis.[52, 87, 88] Though Nafion has been shown to initially increase sensitivity toward serotonin, it has been noted that within the first 20 minutes in a biological matrix there is a 35% loss in sensitivity.[89] Other surface treatments have been explored for improving sensitivity toward other important monoamines including poly-(3,4-ethylenedioxythiophene) (PEDOT)[16], acid-treatment[90], and by over oxidizing the surface of the carbon fiber by extending the potential widow of the waveform that is being applied past 1.1 V[91]. However, we have

found great success by investigating the effects of highly concentrated extracellular amino acids. Our work has focused on understanding the effects of glutamate on the sensitivity of our electrode toward serotonin. We have found that by electropolymerizing glutamate to the electrodes surface that we gain a 2-fold increase in sensitivity. However, we note in our previous work that glutamate my not be the only contributor to this auspicious phenomenon. The work in this thesis goes to further study amino acid treatments and directly uses these novel treatments to improve ambient detection of serotonin.

Scope of Dissertation

This dissertation aims to highlight the versatility, strength and adaptability of fast-voltammetric analysis for the serotonergic system.

Chapter 2: This published article presents a multifaceted approach towards characterizing glutamate coated CFMs. Imaging techniques confirm the presence of a non-uniformed layer of this new auspicious coating. We also note the increase to analyte sensitivity (dopamine and serotonin) due to this new surface modifications.

Chapter 3: This chapter describes novel and robust amino acid surface treatment to improve ambient serotonin detection using FSCAV. This chapter aims to make serotonin detection and analysis more user-friendly.

Chapter 4: Here we utilize fast voltammetry to study four classes of antidepressants and their effects on the serotonergic system. This is accomplished by analyzing stimulated release of the serotonin system and ambient levels of serotonin during the time of drug administration. We will also describe the response of histamine and its modulation of serotonin to elicit a mechanism to explain why there is no change in stimulated release of serotonin is observed, but a robust increase in ambient levels is seen

upon an acute does of ketamine. This chapter also explores the formation and characterization of a novel antidepressant, selenium-fluoxetine. This new antidepressant aims to increase the ambient levels of serotonin by acting as both a traditional antidepressant and an anti-inflammatory drug. We explore the phasic changes associated with this novel treatment and compare it to its traditional analog.

Chapter 5: This chapter will introduce serotonin oscillatory patterns and presents experimental paradigms to increase the frequency of data acquisition during fast-scan controlled adsorption voltammetry to better define these patterns described. We will also propose a rational for these tight fluctuations in ambient serotonin *via* pharmacological and mathematical means.

Chapter 6: This conclusion chapter will highlight the major findings of this body of work. First, creating methods for better ambient analysis for serotonin and secondly, understanding pharmacological manipulations in their phasic release, ambient transmission and oscillatory changes. Finally, this work shows future direction for faster serotonin basal data acquisition. In doing so, this work has gone to show the versatility of fast-voltammetry for serotonin measurements, all while creating more user-friendly methods for the expansion of serotonin analysis using this unique tool. This chapter will also discuss future directions.

Chapter 2: Glutamate Electropolymerization on Carbon Increases Analytical Sensitivity to Dopamine and Serotonin: An Auspicious *In Vivo* Phenomenon in Mice?[1]

[1]Holmes, J., Witt, C. E., Keen, D., Buchanan, A. M., Batey, L., Hersey, M. & Hashemi P. Accepted. Glutamate Electropolymerization on Carbon Increases Analytical Sensitivity to Dopamine and Serotonin: An Auspicious *In Vivo* Phenomenon in Mice? *Analytical Chemistry*

ABSTRACT

Carbon is the material of choice for electroanalysis of biological systems, being particularly applicable to neurotransmitter analysis as carbon fiber microelectrodes (CFMs). CFMs are most often applied to dopamine detection; however, the scope of CFM analysis has rapidly expanded over the last decade with our laboratory's focus being on improving serotonin detection at CFMs, which we achieved in the past via Nafion modification. We began this present work by seeking to optimize this modification to gain increased analytical sensitivity toward serotonin under the assumption that exposure of bare carbon to the *in vivo* environment rapidly deteriorates analytical performance. However, we were unable to experimentally verify this assumption and found that electrodes that had been exposed to the *in vivo* environment were more sensitive to evoked and ambient dopamine. We hypothesized that high *in vivo* concentrations of ambient extracellular glutamate could polymerize with a negative charge onto CFMs and facilitate response to dopamine. We verified this polymerization electrochemically and characterized the mechanisms of deposition with micro- and nano-imaging. Importantly, we identified that the application of 1.3 V as a positive upper waveform limit is a crucial factor for facilitating glutamate polymerization, thus improving analytical performance. Critically, information gained from these dopamine studies were extended to an *in vivo* environment where a 2-fold increase in sensitivity to evoked serotonin was achieved. Thus, we present here the novel finding that innate aspects of the *in vivo* environment are auspicious for detection of dopamine and serotonin at carbon fibers, offering a solution to our goal of an improved fast-scan cyclic voltammetry serotonin detection paradigm.

INTRODUCTION

Carbon electrodes are uniquely amenable for biological analyses, in particular detection of neurochemicals in dynamic and complex media. The carbon surface is biocompatible and versatile (easily fashionable into multiple configurations); a variety of available carbon forms provide an extensive catalogue of electroanalytical opportunities.[1−4] Within neurochemical analysis with this material, carbon fiber microelectrodes (CFMs) are particularly popular.[5,6] For several decades, fast-scan cyclic voltammetry (FSCV) at CFMs has been employed to study dopamine in the context of pathologies such as addiction and Parkinson's disease.[7−9] In tandem to this work, the electrochemical properties governing the FSCV response toward dopamine have been well explored, including the regenerative ability of carbon, electron transfer kinetics, and adsorption interactions at the carbon fiber surface interface.[10−14]

In the last decade, the scope of FSCV has been expanded to analytes other than dopamine.[15−20] In our laboratory, we pioneered FSCV for serotonin and applied these measurements *in vivo*.[21,22] We have used the method over the last 10 years to investigate serotonin dynamics in a variety of *in vivo* scenarios including probing neurochemistry between sexes, analyzing the effects of antidepressants, investigating mouse models of disease, and mapping the biochemical architecture in different brain regions.[23−27] However, serotonin detection with CFMs remains niche because serotonin signaling is highly regulated *in vivo*, with very low evocable concentrations (low nM range compared to 10 μM evoked dopamine).[28] Furthermore, the primary serotonin metabolite, 5-hydroxyindole acetic acid (5-HIAA), rapidly electropolymerizes on the electrode surface and reduces the *in vivo* signal response.[22,29−31] Our approach to facilitating serotonin detection has been to

modify the electrode surface a priori with Nafion, a sulfonated tetrafluoroethylene-based cation exchange polymer, that preconcentrates serotonin and repels 5-HIAA.[22]

There has, in recent years, been incongruity in the community about an optimal Nafion modification procedure,[31–35] and there have been reports of alternative polymer modifications (such as poly(3,4-ethylenedioxythiophene) (PEDOT)).[36–38] Thus, we sought to further improve FSCV's sensitivity toward serotonin by optimizing a Nafion modification protocol that would facilitate broader adoption of the method. However, before we could assess the effects of the polymer coating, we encountered an unusual phenomenon. Specifically, we were unable to replicate a key assumption in the field that sensitivity toward monoaminergic cations decreases after electrode implantation into brain tissue.[29,31] We found that after *in vivo* implantation, electrodes were significantly more sensitive to dopamine using both FSCV and fast-scan controlled-adsorption voltammetry (FSCAV). The rationale that electrodes should be less sensitive to dopamine after *in vivo* implantation is that polymerization of proteins and metabolites (such as 5-HIAA) makes the surface less accessible to dopamine. Using the same rationale, we considered which brain chemicals had the potential to interact with the electrode creating a positive effect for dopamine detection. Glutamate is a ubiquitous neurotransmitter, present at high concentrations throughout the brain. This amino acid has been shown previously to electropolymerize, forming polyglutamic acid (PGA) on carbon surfaces, via a radical-initiated mechanism.[39–42] PGA possesses an overall negative charge at biological pH; thus, we postulated that a PGA coating on CFMs might improve sensitivity toward dopamine. Indeed, we found that electrodes electrochemically pretreated in glutamate solution displayed significantly better analytical responses to dopamine via flow injection analysis

(FIA). We showed electrochemical evidence for glutamate polymerization onto CFMs and characterized this film via scanning electron microscopy (SEM) and atomic force microscopy (AFM). We found that PGA films serve to stabilize or replace Nafion films with prolonged (>2 h) use, an opportune outcome of the *in vivo* environment that facilitates measurements. Finally, we exploited this finding to make a minor modification to our serotonin detection waveform that resulted in a 2-fold increase in response amplitude toward serotonin in the CA2 region of the hippocampus.

Given the analytical and morphological similarities between *in vivo* and PGA electrodes, we conclude that the high levels of ambient brain glutamate play a role in enhancing *in vivo* CFM measurements in the mouse brain. Using this finding, we present a novel treatment protocol to improve the sensitivity of FSCV toward serotonin *in vivo*, which was the original goal of this study. Importantly, this work allows us to suggest that carbon's suitability for neurochemical electroanalysis includes an innate and auspicious interaction of amino acids, like glutamate, with this substrate.

EXPERIMENTAL

General Methods and Materials. Chemicals. Stock solutions were prepared at room temperature and physiological pH (pH = 7.4) by dissolving glutamic acid and dopamine hydrochloride (each prepared to a final concentration of 1 μM) into 1× phosphate buffered saline (PBS) that was diluted from a 10× premixed buffer. Serotonin hydrochloride was prepared similarly in TRIS hydrocholoride buffer, as described elsewhere.22,26 All chemicals were purchased from Sigma Aldrich (St. Louis, MO) unless otherwise specified. Liquion (LQ-1105, 5% by weight Nafion) was purchased from Ion Power Solutions (New Castle, DE, USA).

Electrochemistry. Voltammetry was performed on a two electrode system. CFMs were handmade in-house as previously described.25 Briefly, a single carbon fiber (diameter = 7 μm; Goodfellow Corporation, PA, USA) was aspirated into a glass capillary (1.0 mm external diameter, 0.5 mm internal diameter, A-M Systems, Inc., Sequim, WA, USA). The glass capillary was then pulled with a vertical micropipette puller (Narishige, Tokyo, Japan) to form a carbon-glass seal. The exposed length of the carbon fiber was trimmed to 100 μm under an optical microscope. A Ag wire (A-M systems, WA, USA) was electroplated with Cl^- for 30 s in 0.1 M HCl at 5 V to create a pseudo-Ag/AgCl reference electrode.

Fast-Scan Cyclic Voltammetry (FSCV). Waveforms were generated using a USB-6431DAC/ADC (National Instruments, TX, USA) device. The working electrode was controlled with a waveform (details on waveforms are specific to each experiment, see below). The electrode was cycled at 60 Hz for 10 min and then at 10 Hz for 10 min. This dual frequency strategy speeds up surface preparation but can be achieved with 10 Hz applied for longer.

Fast-Scan Controlled-Adsorption Voltammetry (FSCAV). FSCAV was performed as previously described43,44 using a CMOS precision analog switch, ADG419 (Analog Devices), to control the application of the waveform. The waveform (Dopamine: −0.4 V to +1.3 V to -0.4 V, scan rate = 1200 V/s) was applied at a frequency of 100 Hz for 2 s and then held at a constant potential of −0.4 V for 10 s followed by reapplication of the waveform for the remainder of the total file collection time of 30 s. Cyclic voltammograms

(CVs) were used for dopamine identification. With FSCAV, the first CV after reapplication of the waveform with a signature dopamine peak was integrated to determine charge.

Flow Injection Analysis (FIA). FIA was performed in a system, custom-built in-house. CFMs were inserted into a flangeless short, 1/8 nut (PEEK P-335, IDEX, Middleboro, MA, USA), exposing a small portion of the tip (2 mm) outside of the nut. An HPLC union (Elbow PEEK 3432, IDEX, Middleboro, MA, USA) was modified such that the nut containing the microelectrode was fastened to one end. The out-flowing stream of the FIA buffer was fastened to the other end of the elbow union. Two holes were drilled into the union for the incorporation of the pseudo-Ag/AgCl reference electrode and the "waste" flow stream. A syringe infusion pump (KD Scientific, Model KDS-410, Holliston, MA, USA) was used to maintain the flow at 2 mL min−1. The analyte was introduced into the flow stream for 10 s via a six-port HPLC loop injector (Cheminert Valve, VICI, Houston, TX, USA) resulting in a rectangular plug.

Data Acquisition. FSCV and FSCAV were performed using a Dagan potentiostat, (Dagan Corporation, Minneapolis, MN, USA), National Instruments multifunction IO device USB6341 (National Instruments, Austin, TX, USA), WCCV 3.06 software (Knowmad Technologies LLC, Tucson, AZ, USA), and a Pine Research head stage (Pine Research Instrumentation, Durham, NC, USA). Data filtering (zero phase, Butterworth, 2 kHz low-pass) and signal smoothing were performed within the WCCV software.

Nafion Electrodeposition. Nafion was electrodeposited on the exposed carbon fiber surface by applying a constant potential of 1.0 V vs. a pseudo-Ag/AgCl reference electrode for 30 s. The microelectrode was dried at 70 °C for 10 min and stored for a minimum of 24 h before use.

Animals. Animal use followed NIH guidelines and complied with the University of South Carolina Institutional Animal Care and Use Committee under an approved protocol. *In viv*o animal experiments were performed as described previously.24 To induce anesthesia, 25% w/v urethane (Sigma−Aldrich Co.) dissolved in 0.9% NaCl solution (Hospira) was injected i.p. (7 μL g−1 of body weight). Body temperature was maintained using a heating pad (Braintree Scientific, Braintree, MA, USA), and stereotaxic surgeries (David Kopf Instruments, Tujunga, CA, USA) were performed with coordinates taken in reference to bregma. Specific coordinates used in each experiment can be found below under "Specific Methods." A pseudo-Ag/AgCl reference electrode was placed in the contralateral hemisphere

SPECIFIC METHODS

Figure 2.1. Four-point pre-calibrations were performed before *in vivo* experiments, and postcalibrations were performed within 12 h after *in vivo* experiments where charge (pC for FSCAV measurements) or current (nA for FSCV measurements) was plotted vs. [DA] (nM). If the electrodes were left overnight, they were stored dry in a box at constant temperature. Nafion-coated CFMs were placed in target regions of the mouse brain for *in vivo* exposure times of 2 h, typical of an *in vivo* experiment. For FSCAV data, a Nafion-coated CFM was lowered into the nucleus accumbens core region of the brain (AP: +0.8, ML: +1.3, DV -4.0). CFMs trimmed to 50 μm were cycled using the modified waveform described above. For FSCV data, a CFM was lowered until it was fully immersed in the dorsal striatum (AP: +1.1, ML: +1.7 DV: −2.0) and a triangular waveform was applied (−0.4 V to 1.3 V to −0.4 V, scan rate = 400 V/s) for 10 min at 60 Hz and 10 min at 10 Hz. Dopamine release was electrically evoked via MFB stimulation (AP: -1.8, ML: +1.1, DV:

-4.8). All data were averaged over at least eight electrodes, and the standard error of the mean was calculated (represented by error bars). A one-tailed paired t-test was utilized to determine the significance between two points ($p < 0.05$).

Figure 2.2. The current amplitude and electrode temporal response of various combinations of CFM pretreatments for dopamine analysis with FIA were compared. Dopamine analysis was performed using FSCV with the following triangular waveform: −0.4 V to 1.3 V to −0.4 V at 400 V/s. Each modification protocol was evaluated by averaging the response of five injections of 1 μM dopamine on four electrodes in the bar graph. Additionally, the first 3.5 s of the FIA pulse associated with a dopamine injection is displayed and the slope was calculated by isolating the linear region of the rise curve.

The modification protocols tested were as follows: **1.** Bare: unmodified CFM serving as a control. **2.** Glu: glutamate pretreatment and glutamate in FIA calibration buffer. To deposit PGA, CFMs were dipped in 1 μM glutamate solution (in 1× PBS buffer) and cycled using the same triangular waveform (−0.4 V to 1.3 V to −0.4 V, 400 V/s) applied during analysis for 10 min at 60 Hz and 10 min at 10 Hz. **3.** *In Vivo*: *in vivo* pretreatment. Electrodes were placed into the cortex of a rodent brain (AP: +0.8, ML: +1.7, DV -0.5) for 20 min and dopamine was measured immediately thereafter with FIA in PBS only. **4.** *In Vivo* + Glu: *in vivo* pretreatment and glutamate in FIA calibration buffer. Electrodes underwent the *in vivo* pretreatment as in (3) above and 1 μM glutamate was added to the FIA buffer.

Figure 2.3. Glutamate electropolymerization events were captured on CFMs trimmed to 100 μm using a waveform with a wide potential window: −1.2 V to 1.3 V to −1.2 V at 400 V/ s. With FIA, data from 30 glutamate injections at 0.1 μM were collected followed by 10 injections each of 1, 20, and 100 μM. The peak at 1 V was quantified as the glutamate

electropolymerization event, and the responses of four electrodes were averaged. Error bars were calculated using standard error the mean.

Scanning Electron Microscopy (SEM). Electrodes were prepared for SEM imaging by depositing PGA, employing two triangular waveforms: (1) −0.4 V to 1.3 V to −0.4 V and (2) −0.4 V to 1.0 V to −0.4 V; each at 400 V/s. Electrodes were then transported to the microscope in a closed container. The capillary glass was cracked, and the tip end of the CFM was secured onto a stage with double-sided tape. SEM images were collected using a Zeiss Ultraplus thermal field emission scanning electron microscope. Images in **Figure 2.3Bi−iii** were magnified on the Zeiss software, and the image in **Figure 2.3Biv** was digitally magnified. The edge planes were imaged because significant electrochemistry happens on this plane. The CFM modifications imaged are listed: **1.** PBS, 1.3 V: CFMs were cycled for 20 min total (60 Hz 10 min, 10 Hz 10 min) using triangular waveform 1, with a positive potential limit of 1.3 V, in PBS. **2.** Glutamate in PBS, 1.0 V: CFMs were cycled for 20 min total (60 Hz 10 min, 10 Hz 10 min) using triangular waveform 2, with a positive potential limit of 1.0 V, in 10 mM glutamate. **3.** Glutamate in PBS, 1.3 V: CFMs were cycled for 20 min total (60 Hz 10 min, 10 Hz 10 min) using triangular waveform 1, with a positive potential limit of 1.3 V, in 10 mM glutamate. **4.** *In Vivo*, 1.3 V: The electrode was placed into the cortex of a rodent brain (AP: +0.8, ML: +1.7, DV: -0.5) and cycled for approximately 20 min total (60 Hz 10 min, 10 Hz 10 min) with triangular waveform 1, with a positive potential limit of up to 1.3 V.

Dopamine Analysis. 1 μM DA was measured using FIA either in the presence or absence of 1 μM glutamate within the running buffer (1× PBS). CFMs were cycled for 20 min total (60 Hz 10 min, 10 Hz 10 min) prior to analysis, and the current response of four

CFMs was measured using the triangular waveform: −0.4 V to 1.0 V to −0.4 V at 400 V/s. Cycling was then repeated immediately using a slightly modified triangular waveform: −0.4 V to 1.3 V to −0.4 V at 400 V/s, and the current response of the same four electrodes was reanalyzed. A t-test was used to determine statistical significance.

Atomic Force Microscopy (AFM). Electrodes were prepared for AFM imaging by depositing PGA or Nafion on the day of analysis. Electrodes were transported to the AFM in a closed container and mounted on a glass slide, with the electrode tip flat to the slide surface. AFM images were collected using a Digital Instruments Dimension 3100 AFM (Veeco Metrology Group) with a NanoScope IIIa Controller and a non-contact tip. In **Figure 2.3Ci−iii**, CFMs were imaged immediately following pretreatment. Treatments include (i) cycling a bare electrode in PBS buffer for 20 min (10 min 60 Hz, 10 min 10 Hz), (ii) electroplating Nafion (method described above), and (iii) electropolymerizing PGA with triangular waveform (−0.4 V to 1.3 V to −0.4 V, scan rate of 400 V/s) by cycling for 20 min (10 min 60 Hz, 10 min 10 Hz) in PBS buffer containing 1 μM glutamate. In **Figure 2.3Civ-v**, CFMs were cycled (10 Hz) for 2 h with a triangular waveform (−0.4 V to 1.3 V to −0.4 V, scan rate of 400 V/s) before imaging, to simulate the length of a typical *in vivo* experiment. Treatments include (iv) Nafion electroplating and (v) electropolymerizing PGA on Nafion coated CFMs using the same procedure as (iii) prior to cycling.

Figure 2.4. The "Jackson" waveform was employed to measure serotonin (0.2 V to −0.1 V to 1.0 V to 0.2 V, scan rate: 1000 V/s). In Figure 2.4A, 100 nM serotonin was measured in the presence of 10 μM 5-HIAA in TRIS buffer on electrodes trimmed to 150 μm.

Measurements were collected with FIA every 30 min for 2 h. The serotonin oxidation peak at 0.7 V was quantified, and the current response of three or four electrodes was averaged. Error bars were calculated using standard error of the mean. CFMs that underwent an electrochemical activation pretreatment were cycled using a modified "Jackson" waveform where the positive potential limit was raised to 1.3 V for 10 min at 60 Hz and 10 min at 10 Hz. The electrodes were then cycled again, and analysis was performed using the original "Jackson" waveform (positive potential limit of 1.0 V). In **Figure 2.4B**, a CFM trimmed to 150 μm was placed into the CA2 region of the mouse hippocampus (AP: −2.91 ML: +3.35 DV: −2.5). Serotonin was evoked via electrical stimulation to the MFB (coordinates above), and data was collected and average from four animals for the Jackson waveform (black) and the same after a 10 min treatment period with the extended Jackson waveform (yellow). The maximum amplitude of each current vs. time traces was recorded, averaged, and reported in the inset bar graph. Error bars were calculated using standard error the mean.

RESULTS AND DISCUSSION

Exposure to *In Vivo* Brain Environment Enhances Electrode Sensitivity.

The brain environment is rich in proteins, ligands, and many other redox-active molecules that can interact with analytical probes. Such an interaction is thought to foul or poison the surface. Carbon is generally hydrophobic and more resistant to the fouling effects of biological agents than other common electrode materials.[45,46] Nonetheless, the carbon surface is altered when exposed to brain tissue. Detrimental interactions of biomolecules with carbon can be particularly problematic for low concentration measurements and/or analysis of rapidly fluctuating species, as is the case for *in vivo*

analysis of serotonin neurotransmission. It is known that serotonin metabolites electropolymerize on CFMs and reduce the CFMs' sensitivity to serotonin.[22,31] This is an issue that we tackled in the past by pre-polymerizing a Nafion layer on the CFM under the rationale that Nafion, a cation exchange polymer, would repel negatively charged serotonin metabolites while preconcentrating serotonin cations.[22] The modification enables measurements of extremely low (approx. 10 nM) concentrations of evoked serotonin.[22,28]

While our laboratory routinely makes these measurements, serotonin FSCV has not been adopted widely in the community because these signals are still very low. Thus, we began this work by addressing the Nafion coating since several Nafion (and other polymer) modification procedures have been updated since our first description.[22,35,36,47] We began by seeking to compare and contrast different CFM modification procedures in a bid to improve FSCV sensitivity to serotonin. Since there is a general notion that the sensitivity and/or response time of electrodes declines *in vivo*, as a starting point, we sought to confirm the detrimental effects of the *in vivo* environment on CFMs. We focused this section of the work on dopamine detection since the analysis of this molecule with FSCV is much better understood than serotonin analysis. Four-point calibrations were performed on 16 electrodes (**Figure 2.1A,B**).

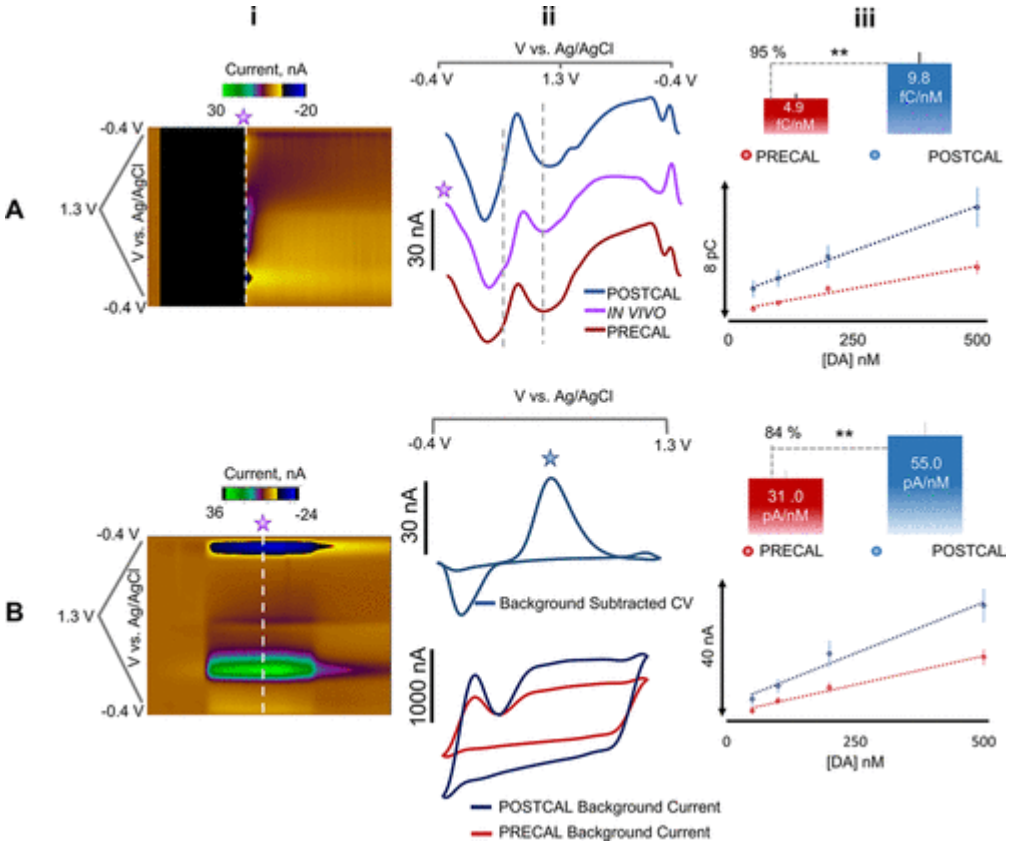

Figure 2.1. CFM sensitivity pre- and post *in vivo* experiments. (A) Pre- and post-calibration data from an *in vivo* experiment measuring dopamine in the mouse nucleus accumbens. (i) Representative *in vivo* FSCAV color plot and (ii) CVs in dopamine (500 nM), before (red), during (purple) and after (blue) *in vivo* measurements. (iii) Pre- (red) and post-calibration (blue). Inset bar graph depicts the increase in the post-calibration slope ($p < 0.01$). (B) Calibration data after an electrode was placed in the mouse dorsal striatum and cycled with the dopamine waveform for 2 h. (i) Representative FSCV color plot and (ii) CV in dopamine (500 nM) collected *via* FIA (above) along with the background signal during pre-calibration and post-calibration (below). (iii) Pre- and post-calibration plot. Inset bar graph depicts the increase in the post-calibration slope ($p < 0.01$). Error bars were calculated using standard error of the mean.

In **Figure 2.1A**, eight electrodes were calibrated in TRIS buffer before implantation into the nucleus accumbens of a mouse brain where extracellular dopamine was monitored for 2 h with FSCAV. Representative color plots and CVs from these experiments are shown in **Figure 2.1Ai,ii**, respectively. Interpretation of color plots can be found elsewhere;48 briefly, these plots convey current vs voltage collected at 10 Hz against collection time, where current is given a false color. The calibration was repeated immediately following

the *in vivo* experiment (calibrations are labeled PRECAL and POSTCAL in **Figure 2.1Aiii**). Contrary to the general view that the *in vivo* environment is detrimental to electrode sensitivity, we found that the electrode sensitivity significantly increased post *in vivo* implantation.

The slope of the calibration curve increased from 4.9 (±0.7) to 9.8 (±1.6) fC/nM ($p = 0.001$, paired t-test). This effect persisted when FSCV was used in a different brain region and calibrated in a different medium. In **Figure 2.1B**, CFMs were precalibrated, placed in the dorsal striatum of a mouse brain for 2 h to measure evoked dopamine release, and re-calibrated immediately thereafter in PBS. A representative color plot and CVs of the Faradaic and background signals are shown in **Figure 2.1Bi,ii**. The background current (mostly comprising capacitative current pre-background subtraction) substantially increases post *in vivo* implantation; an effect that persists with electrodes that have been electrochemically treated with glutamate only (**Figure A.2 in supplemental**), showing that the surface chemistry of the electrode has changed. The pre- and post-calibration curves are in Figure 2.1Biii. In agreement with FSCAV results, the slope increased significantly in the post-calibration from 31.0 (±4.6) to 55.0 (±7.3) pA/nM ($p = 0.004$). These increases in sensitivity were not seen when the electrodes were tested in their respective control experiments in buffer alone (**Figure A.1** in supplemental).

These results contradict the general status quo, which is that electrodes lose sensitivity *in vivo*.[36,49,50] However, a previous study displayed similar results,[29] where the current response to acetaminophen after *in vivo* measurements was larger than before the experiment, and another where the response change to dopamine was insignificant.[51] There may be several factors to explain the contradiction such as experimental conditions, models

and methods. Such differences may include electrode type (disk vs cylinder), waveform (1.0 V vs 1.3 V potential limit), pretreatment before post-calibration (overnight soaking in isopropyl alcohol vs no pretreatment post-calibration),[49] time *in vivo* (several weeks), which results in deterioration of the pseudo-Ag/AgCl reference electrode,[52] and the time after *in vivo* exposure and calibration (our calibration is immediately thereafter). Nonetheless, in our hands this effect is significant and persistent. In sum, our results suggest that an unidentified aspect of the *in vivo* environment contributes to a surface alteration of carbon that improves the sensitivity of the electrode toward dopamine.

Analytical Response to Dopamine Is Improved with Glutamate Pretreatment.

When identifying potential biological molecules that might interact with carbon, we identified glutamate, a neurotransmitter that is ubiquitous across brain regions. While it is generally accepted that glutamate does not offer analytical electroactivity, glutamate electropolymerization is well established in the literature with conventional, slow scan cyclic voltammetry.[40,42,53,54] In fact, electrochemical grafting of amines to carbon surfaces is well demonstrated via a radicalinitiated C−N bond.[55−57] Applying an electrochemical potential not only drives bond formation between amine groups and carbon[56,57] but also facilitates electropolymerization of small amine-containing molecules like amino acids via a chain-like growth mechanism.[55] We thus hypothesized that, *in vivo*, the interaction of glutamate with CFMs may create a polymer layer that facilitates the increase in sensitivity observed in **Figure 2.1**. The rationale here is the structure of a potential PGA film, possessing an overall negative charge, would enhance the preconcentration of cations.

Figure 2.2 shows the first 3.5 s of a flow injection response of dopamine (1 µM) onto CFMs. Bare electrodes (1) served as controls and response to the dopamine injection was rapid, reaching the steady state (34.5 ± 3.8 nA) at 3.5 s (**Figure 2.2A**).

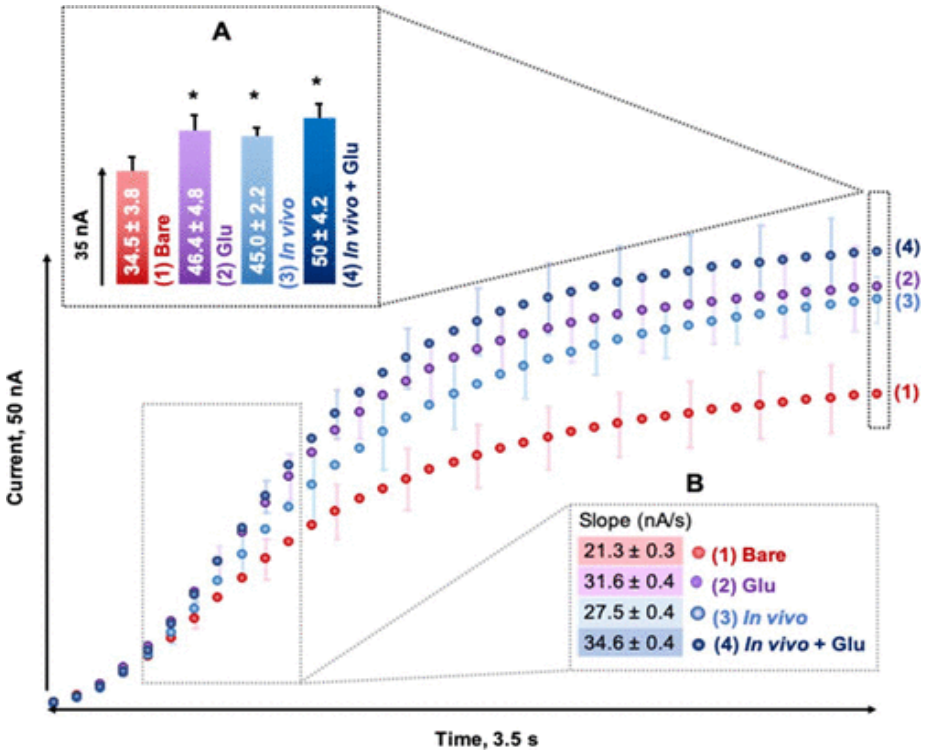

Figure 2.2. Analytical response of glutamate-treated and *in vivo* CFMs. FIA rise curves of the first 3.5 s of a 1 µM DA injection on four different CFMs: bare (1), glutamate in FIA buffer at 1 µM (2), *in vivo* (3), and *in vivo* + glutamate (4). Every third error bar is displayed. (A) Bar graph of the FIA response to 1 µM DA on each pretreated CFM (*$p < 0.05$). (B) Slope of the linear portion of the curve (0.4–1 s, $R2 > 0.99$).

Electrodes pre-treated (via electrochemical cycling) with glutamate (2) prior to and during analysis at a concentration resembling ambient *in vivo* glutamate58 had a significantly higher response than control (46.4 ± 4.8 nA, p = 0.05); the same held for CFMs that had been *in vivo* (3) (45 ± 2.2 nA, p = 0.03). The highest current was from electrodes that had been *in vivo* and were post-analyzed with glutamate in the FIA buffer (50 ± 4.2 nA, p = 0.02). A similar, significant increase in sensitivity is seen with FSCAV for electrodes before and after glutamate treatment.

A concern with modified electrodes is whether a diffusional barrier might induce temporal limitations in the response.[22] We tested whether any of these scenarios slowed down the FSCV response time via FIA in **Figure 2.2B**. In contrast to the expectation that modifications slow the response, we found by estimating the slope of the linear portion of the rise curve that all pre-treatments improved the speed of response ((3) 27.5 ± 0.4, (2) 31.6 ± 0.4, and (4) 34.6 ± 0.4 nA/s) with respect to the bare one ((1) 21.3 ± 0.3 nA/s). Combined, these data show that carbon fibers that have been *in vivo* or have been pretreated with glutamate display improved analytical response toward dopamine. We next explored the interaction of the carbon surface with glutamate.

Glutamate Electropolymerizes onto CFMs with FSCV.

With conventional cyclic voltammetry, applying a high potential (>1.3 V) initiates grafting of the glutamate monomer to carbon followed by chain growth of the polymer.39 Glutamate electropolymerization has not yet been explored with fast voltammetry; thus, we asked, does glutamate electropolymerization occur at the fast scan rates employed with FSCV?

We applied a waveform to the CFM with an intentionally wide potential window (−1.2 V to 1.3 V to −1.2 V at 400 V/s) to best capture any polymerization peaks. Using FIA, a rectangular pulse of glutamate (0.1 μM) was delivered to CFMs and the responses were averaged. A representative color plot and CV are displayed in **Figure 2.3Ai,ii** where the electropolymerization peak occurs at 1 V (denoted by the green arrow in **Figure 2.3Aii**). The first six injections in **Figure 3Aiii** reveal the polymerization peak, with an average current response of 36.7 ± 2.9 nA. Successive injections show that this peak diminishes over time (**Figure 2.3Aii**), decreasing to an average of 11.1 ± 1.0 nA or 30.2% ($p = 0.0002$) of the original amplitude. The polymerization peak is indistinguishable from

the switching peak (an artifact of the FSCV technique) by scan 30. Even when the glutamate concentration was increased to 1, 20, and 100 μM, there was no significant change in amplitude. We believe the disappearance of this peak is due to fewer available sites for PGA attachment and chain length saturation. The structure of PGA on carbon is depicted in **Figure 2.3Aiv**. In previous studies describing PGA electropolymerization with conventional cyclic voltammetry, the free radical-initiated polymerization peak occurred at around +1.5 V.39 Though the high potential is not within the potential window of our FSCV waveform, we hypothesized that adsorption of glutamate to CFMs creates enough thermodynamic favorability to initiate PGA formation. The polymerization peak at 1.0 V suggests that this process is dependent on the application of a positive potential above 1.0 V. PGA formation on CFMs with a fast scan waveform that extends up to 1.3 V is an interesting finding since the application of 1.3 V is known to increase sensitivity to DA.10 This effect has been attributed to overoxidation of the carbon surface, providing a fresh surface for the next analysis and for creating oxygen moieties on the surface that pre-concentrate the dopamine cation before analysis.[10,11] Here, we suggest that 1.3 V also facilitates the signal via PGA formation. Since electrochemical PGA formation onto the carbon surface is covalent, the overoxidation process at 1.3V may be blocked at sites where PGA has grafted to the CFM.

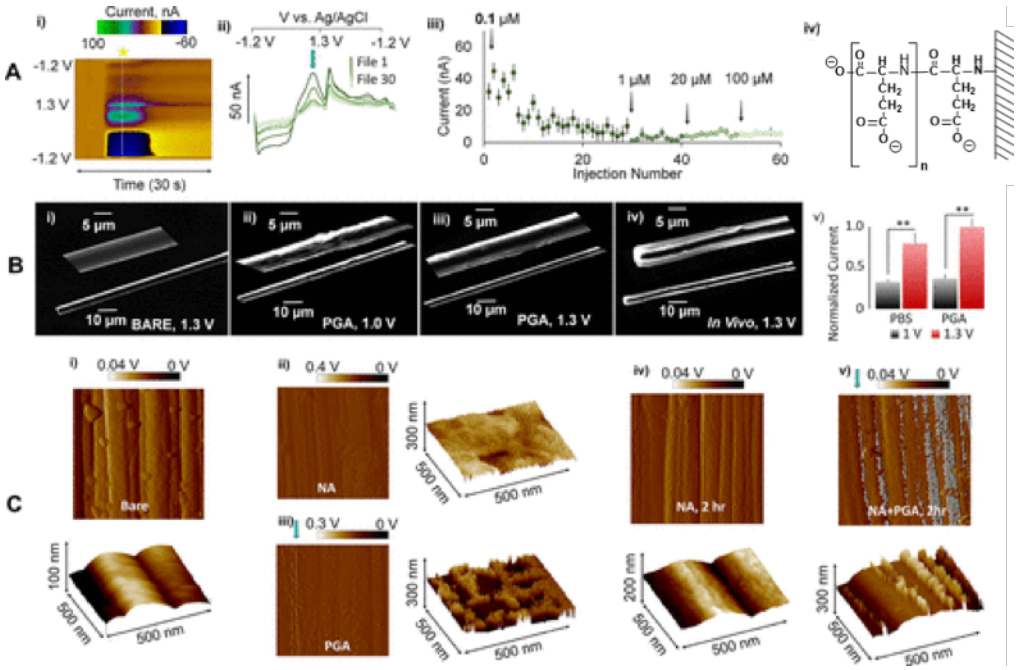

Figure 2.3. PGA electropolymerization and coatings on CFMs. (A) Glutamate electropolymerization at fast scan rates (i) Color plot from FIA injection of 0.1 µM glutamate. (ii) Every fourth CV of 0.1 µM glutamate is displayed. (iii) Varying concentrations (0.1, 1, 20, and 100 µM) of glutamate are measured by 60 successive injections *via* FIA. Error bars: standard error of the mean. (iv) Molecular structure PGA. (B) SEM images of CFMs: (i) bare, (ii) treated for 20 min (10 min 60 Hz, 10 min 10 Hz) in [10 mM] glutamate using the triangular DA waveform (to 1.0 V), (iii) using the extended dopamine waveform (to 1.3 V), and (iv) treated in brain tissue. (v) Bar graph comparing the normalized current response of CFMs to 1 µM DA, cycled at 1.0 V and 1.3 V in PBS and 1 µM glutamate. Statistics: *t*-test (**$p < 0.01$). (C) AFM images of CFMs modified by (i) surface activation with extended dopamine waveform (cycled 10 min 60 Hz, 10 min 10 Hz in PBS), (ii) electrodeposited Nafion and (iii) PGA coated with the extended dopamine waveform (10 min 60 Hz, 10 min 10 Hz in 1 µM glutamate). AFM images following exposure to the extended dopamine waveform for 2 h modified with (iv) electroplated Nafion and (v) Nafion with 1 µM glutamate added to the background buffer.

Given voltammetric evidence of film formation, film deposition was verified and characterized via micro- and nanoimaging. PGA has been imaged on different carbon surfaces including glassy carbon,[40] carbon paste electrodes,[59] carbon nanotubes,[41,60,61] graphite,[62] and reduced graphene oxide[61,63] and other substrates such as Au nanoparticles;[64] however, there have been no reports of PGA deposition on CFMs. Here, we imaged CFM

surfaces with SEM. In particular, we were interested in observing the effects of waveform limits (testing the importance of 1.3 V) on the CFM surface in the presence of glutamate. In **Figure 2.3Bi**, the CFM was cycled in PBS with a 1.3 V positive limit. The carbon surface appeared relatively smooth. In **Figure 2.3Bii**, the CFM was cycled in a glutamate-containing buffer with a positive potential limit of 1.0 V; this waveform is not considered to overoxidize the carbon surface.[11,27,28] When treated in 1 μM glutamate, there were no visible deposits on the CFM (data not shown). This is because SEM does not have the resolving power to visualize the fine deposits of low glutamate concentrations (we visualize these with AFM in **Figure 2.3B** below). With 10 mM glutamate, significant deposits were visualized (**Figure 2.3Bii**). The large deposits indicate the presence of polymers. In **Figure 2.3Biii**, the electrode was in a glutamate-containing buffer and the positive potential limit of the waveform was increased to 1.3 V, a potential limit considered to etch the carbon surface. These electrodes appear to have a thinner deposition layer than the 1.0 V waveform (**Figure 2.3Bii**). In **Figure 2.3Biv**, the electrode was cycled *in vivo* for 20 minutes. There is a visible film on the electrode surface; such deposits have been previously seen after *in vivo* implantation, attributed to debris and biomaterials.[36,65]

The bar chart in **Figure 2.3Bv** compares the response to 1 μM dopamine before and after CFM treatment in 1 μM glutamate between the 1.0 and 1.3 V upper limit dopamine waveforms. In combination with the SEM images collected, the thinner apparent film corresponds to higher sensitivity to dopamine. This implies that having a positive limit of 1.0 V encourages a thicker layer of PGA, potentially creating a kinetic barrier. In contrast, the application of 1.3 V simultaneously etches the carbon as the polymer is deposited, such that the polymer is thin enough to act as a pre-concentration matrix and not as a barrier.

AFM is a useful tool for studying the morphology of conductive coatings on electrodes and could provide insights into how PGA is formed on electrodes *in vivo*. We compared different PGA deposition paradigms to Nafion (abbreviated to NA in **Figure 2.3** and further figures) electrodeposition, which we have previously characterized in detail.[21–25,28] In **Figure 2.3Ci**, the distinct carbon striations are apparent on a bare CFM. After deposition of Nafion (**Figure 2.3Cii**) or PGA (**Figure 2.3Ciii**), the natural carbon striations are shallower and the surface is significantly roughened, as seen previously.[40,63,66,67] Other reports of PGA morphology with AFM on glassy carbon and reduced graphene oxide display similar surface features, however the PGA deposition was more homogeneous than we find.[40,63] When comparing the Nafion coating to the PGA coating, differences in morphology are clear. NA is uniformly deposited while PGA is deposited more sparsely with large patches of the surface devoid of the polymer. This is likely due to the inherent mechanistic differences between Nafion and PGA deposition: Nafion is electrostatically plated while PGA is polymerized from the monomer by covalently grafting to active sites on the carbon surface. In **Figure 2.3Civ**, theNafion-coated electrode was imaged after 2 hrs of electrochemical cycling and it is seen that the coating is degraded with time. Nafion-coated electrodes are commonly employed for biological analysis, and it has been thought that the Nafion-coating enhances the signal stability throughout an *in vivo* experiment,[22,32,35] a phenomenon difficult to reconcile with our finding here. Because at 1.3 V, the underlying carbon is etched away, a large portion of Nafion is removed; thus, it is interesting that Nafion-CFMs are still effective for *in vivo* experiments over several hours. This experiment, however, does not reflect the *in vivo* environment where there is a persistent, innate high concentration of glutamate. Thus, to

better reflect the i*n vivo* matrix, an Nafioncoated CFM was cycled for 2 hrs in the presence of ambient glutamate (**Figure 2.3Cv**). The deposits on this electrode appear more substantial. Of particular interest is the feature denoted by the blue arrow. Here, there appears to be heavy deposition along the vector of a single striation. This behavior implies that Nafion deposition is sparse within these ridges, leaving binding sites available for PGA initiation and that the deeper sections of carbon's striations are a more favorable surface for PGA deposition. We postulate that this is because there are more ridges or imperfection sites where the polymer can nucleate and grow. Nucleation and growth processes are dependent on surface imperfections and are described in great detail for metals.68−70 This finding is not surprising since radicalinitiated polymers are formed via chain growth (vide supra).71−74 From this data, we suggest in vivo that PGA codeposits on electrodes pretreated with Nafion, stabilizing, or even replacing the Nafion throughout an experiment.

PGA Facilitates Serotonin Detection.

The investigations above with dopamine determined that PGA formation on carbon fibers increases electrode sensitivity and stability. We now asked whether these effects are maintained for serotonin. FSCV serotonin detection is fundamentally more challenging because of low evocable serotonin concentrations and high ambient concentrations of 5-HIAA; this metabolite also polymerizes on the electrode but serves to degrade the electrode sensitivity.[22,29−31] This is illustrated in Figure 4A

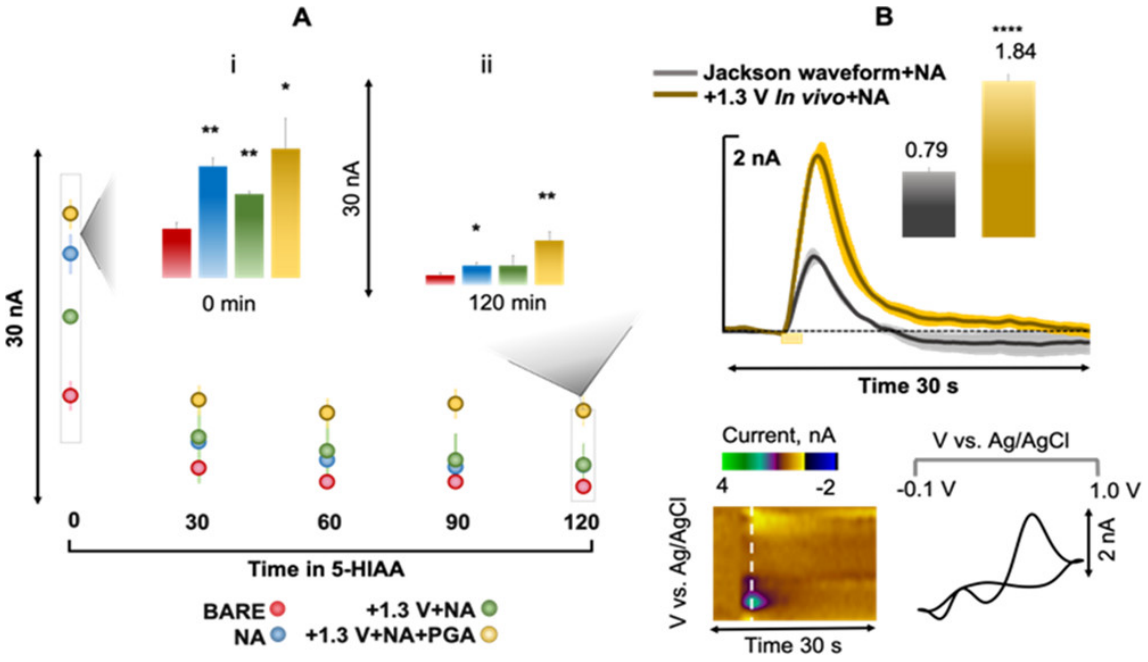

Figure 2.4. Serotonin responses with surface modifications with FIA and *in vivo*. (A) Time of exposure to 10 µM 5-HIAA (every 30 min for 2 h) vs current response (nA) is plotted of 100 nM serotonin, and surface modifications are compared: Bare (red, $n = 3$), NA (blue, $n = 4$), and Nafion-coated carbon fiber activation *via* exposure to an overoxidizing waveform (positive potential limit of 1.3 V, green $n = 3$) and PGA (yellow, $n = 4$). (i) Bar graphs of current response at initial (0 min) and final time point (120 min). (B) Current vs time traces of serotonin collected *in vivo* are averaged ($n = 4$) and compared: extended Jackson waveform pretreatment (yellow) vs. the Jackson waveform on NA electrodes (gray). Inset: bar graphs comparing the average amplitude of each treatment. Representative *in vivo* color plot and CV are shown below, where the oxidation and reduction peaks occur at 0.7 and 0 V, respectively. Statistics: *t*-test with respect to the bare electrode (**$p < 0.01$, *$p < 0.05$).

where bare electrodes (red markers) are utilized to measure serotonin (100 nM) with the standard Jackson waveform75 giving a response of 7.4 ± 0.9 (red bar in the inset bar graph). When this electrode is cycled in a buffer containing 5-HIAA (5 µM), repeated injections of serotonin result in a significant loss of signals (1.3 ± 0.4 nA). While the initial response is greatly improved with Nafion modification (blue markers and blue bar in the bar graph) (16.8 ± 1.2 nA, p = 0.001 compared to bare), after 120 min of repeated serotonin injections in 5-HIAA, the signal is significantly diminished (2.7 ± 0.4 nA, p = 0.03). This is consistent

with the AFM study above that showed severe degradation to the Nafion layer with waveform application. The electrode response and stability can be substantially improved with the application of a pretreatment step whereby the Nafion-coated electrode is cycled in glutamate containing buffer with a 1.3 V upper limit on the Jackson waveform and then analyzed in a buffer that contains both 5-HIAA and glutamate with the 1.0 V waveform (yellow markers and trace; initial: 19.5 ± 4.6 nA, p = 0.04; final 6.4 ± 1.2 nA, p = 0.01). These results are consistent with our hypothesis above that glutamate serves to stabilize or replace Nafion when 1.3 V is applied. To show that this improvement in response is not a simple consequence of the 1.3 V upper limit creating more adsorption sites, the green markers and trace show that Nafion electrodes at cycled at 1.3 V without glutamate pretreatment or glutamate in the buffer do not have a significant effect on the response at the end of the experiment (initial: 12.6 ± 0.3 nA, p = 0.003; final 2.8 ± 1.3 nA, p = ns).

We thus followed the PGA paradigm to complete an *in vivo* experiment to test whether pretreating a Nafion electrode at 1.3 V in the brain would serve to increase sensitivity using the rationale that glutamate (and/or similar amino acids) facilitates the response. In **Figure 2.4B**, we measured serotonin in the CA2 region of the hippocampus of four mice with the Jackson waveform using a Nafion-coated electrode (black). Serotonin concentrations increase upon stimulation of the serotonin axons (denoted by the yellow bar under trace) and then clear rapidly after stimulation. We implemented an *in vivo* activation step (extending the Jackson waveform to a 1.3 V positive potential limit for 10 min at 60 Hz, 10 min at 10 Hz). The original Jackson waveform was restored for measurements. We observed a >2-fold increase in response as seen by the evoked release event (yellow; 0.79

± 0.08 nA to 1.84 ± 0.11 nA, p = 6 × 10−5). A color plot and CV of this event (below) show the relative high integrity of the signal.

We do not believe that glutamate is the sole player here given the abundance of structurally analogous molecules in the brain (aspartate and lysine among others[76−78]). More likely, glutamate is part of an intricate network of molecules that polymerize in complex ways onto carbon and serve to draw equilibria that facilitate and impede the electrode's response. While we have long known about the detrimental effects of these molecules (such as 5-HIAA), here, we provide new evidence that glutamate's interactions with carbon are beneficial for dopamine and, importantly, serotonin detection, which was the initial aim of this project.

CONCLUSIONS

Carbon has been used for decades for biological analyses and is particularly applicable to neurotransmitter analysis in the CFM form. Much of the work with CFMs has been on dopamine detection, but our interests lie in improving serotonin detection at CFMs. We began this work by investigating the carbon surface under the assumption that exposure to the *in vivo* environment is detrimental to electrode sensitivity. In contrast to this assumption, we found that electrodes that had been exposed to the *in vivo* environment for up to 2 h were more sensitive to evoked and ambient dopamine. We postulated that high concentrations of innate glutamate *in vivo* serve to polymerize with a negative charge on CFMs and facilitate response to dopamine. We verified this polymerization electrochemically and characterized the mechanisms of deposition. Critically, we identified that the application of 1.3 V as an upper waveform limit is a key factor for increasing electrode sensitivity to dopamine and experimental stability by augmenting

Nafion film integrity. Finally, we applied the knowledge gained from these dopamine data sets to an *in vivo* serotonin experiment where we were able to induce a 2-fold increase in response to serotonin. We present not only the novel finding that innate aspects of the *in vivo* environment are auspicious for dopamine and serotonin detection via carbon, but also offer an improved FSCV serotonin detection paradigm.

Chapter 3: Novel, User-Friendly Experimental and Analysis Strategies for Fast Voltammetry: 2. Next Generation FSCAV Serotonin Measurement and Analysis[1]

[1] Colby E. Witt‡, Sergio Mena‡, Lauren E. Honan, Marco Visentin, Lauren Batey, Nathan Robins, Yangguang Ou, & Parastoo Hashemi Under peer review. Novel, User-Friendly Experimental and Analysis Strategies for Fast Voltammetry: 2. Next Generation FSCAV Serotonin Measurement. *ACS Measurement Science AU*.

ABSTRACT

Fast voltammetry is an attractive technique to measure neurochemicals in the brain. This technique is biocompatible, causes minimal tissue damage and has real-time temporal resolution. Fast voltammetric techniques have been adapted to measure the ambient or tonic state of neurotransmission (Fast-Scan Controlled Adsorption Voltammetry (FSCAV)) for both serotonin and dopamine. This method is advantageous because of the important biological information in the ambient levels of neurotransmitters: serotonin in the case of our studies. The key to better understanding and treating the disorders in which this modulator is implicated is to decipher the mechanisms that control the tonic extracellular serotonin levels. Since the advent of FSCAV, our lab has developed and employed this niche tool to probe and understand native and pharmacological effects on the serotonin system in mouse models, giving great insight into the role of serotonin in depression. However, some limitations regarding the stability of signals over prolonged periods needs to be evaluated and addressed. Here, we show a robust analytical method to improve the stability of electrodes both *in vitro* and *in vivo*. We reduce FSCAV electrode drift by electrochemically polymerizing amino acids onto the surface of the carbon fiber. This work is intended to provide the research community with improved analytical capabilities of carbon fiber microelectrodes to measure tonic serotonin concentrations in biological environments.

INTRODUCTION

Serotonin plays important roles in brain physiology and disease. Fast-scan cyclic voltammetry (FSCV) can probe *in vitro* and *in vivo* serotonin dynamics at carbon fiber

microelectrodes (CFMs).[1-10] FSCV is only capable of measuring evoked or phasic changes in analytes because it is a background subtracted method. Background subtraction is required to remove a large non-Faradaic charging current consequent with high scan rates (hundreds to thousands of volts per second).[10, 11] While this information has critically advanced the understanding of serotonin in the brain, basal or ambient level serotonin measurements are also critical. There are a number of ways to study ambient analyte levels in the brain such as microdialysis,[12, 13] multiple-cyclic square wave voltammetry (MCSWV)[14] and fast scan controlled adsorption voltammetry (FSCAV).[7]

We have employed FSCAV for ambient serotonin measurements in a variety of studies. We have investigated differences in ambient serotonin in response to antidepressant administration in male vs. female mice,[8], how small differences in regional extracellular serotonin concentration are informative of local tissue architecture[15] and recently we showed rapid modulation of brain serotonin in response to bodily inflammation.[16]

We have encountered an experimental challenge with FSCAV, which is analyzed *via* integration of the Faradaic peak. The issue is a long (average 1.5 hrs) equilibration period after the FSCAV paradigm is applied *in vivo*, which significantly extends experimental time. In this work, we tackle matrix issues to significantly reduce experimental time and improve the ease and reproducibility of FSCAV serotonin analysis. By making use of a newly developed understanding of how the *in vivo* chemical environment interacts with carbon fibers in an auspicious way to improve stability and sensitivity,[17] we are able to dramatically decrease *in vivo* electrode equilibration time. We

thus present new experimental approaches to facilitate efficient and robust serotonin FSCAV data acquisition.

EXPERIMENTAL

Chemicals and Reagents

Mice were anesthetized using urethane. Electrodes were treated with Gamma-aminobutyric Acid (GABA) (2.5 μM), Glycine (Gly) (34 μM), Glutamate (Glu) (21.3 μM), Tyrosine (Tyr) (7.2 μM), Tryptophan (Trp) (11.1 μM), Cysteine (Cys) (1.12 μM), Lysine (Lys) (26 μM), and/or Aspartate (Asp) (0.2 μM) individually or as a combination as dictated above in the manuscript. These Amino Acids (AAs) were dissolved into a 1x phosphate buffered saline (PBS) that was diluted from a 10x premixed buffer. All chemicals were purchased from Sigma Aldrich (St. Louis, MO, USA).

Flow Injection Analysis (FIA)

FIA was performed in a system custom-built in-house. CFMs were inserted into flangeless short 1/8 nuts (PEEK P-335, IDEX, Middleboro, MA, USA), exposing a small portion of the tip (2 mm) outside of the nut. An HPLC union (Elbow PEEK 3432, IDEX, Middleboro, MA, USA) was modified such that the nut containing the microelectrode was fastened to one end. The out-flowing stream of the FIA buffer was fastened to the other end of the elbow union. Two holes were drilled into the union for the incorporation of the pseudo-Ag/AgCl reference electrode and the "waste" flow stream. A syringe infusion pump (KD Scientific, Model KDS-410, Holliston, MA, USA) was used to maintain the flow at 2 mL min^{-1}. The analyte was introduced into the flow stream for 10 s via a six-port HPLC loop injector (Cheminert Valve, VICI, Houston, TX, USA) as a rectangular plug.

Animals and Surgical Procedure

Mice (C57BL/6J) (Jackson Laboratory, Bar Harbor, ME, USA) were injected with a 25% urethane solution based on a calculation that is dependent on their weight (7 μL/g). Following anesthetic administration, the mouse was placed into a stereotaxic system (David Kopf Instruments, Tujunga, CA, USA) where body temperature was maintained *via* heating pad (Braintree Scientific, Braintree, MA, USA) Three holes were drilled into the skull of the mouse based on coordinates from the mouse brain atlas. The working electrode was placed in the CA2 region of the hippocampus (CA2: -2.91, +3.35, -2.50) the stimulating electrode (insulated stainless-steel, diameter 0.2 mm, untwisted, Plastics One, Roanoke, VA, USA) was placed in the medial forebrain bundle (MFB: -1.58, +1.00, -4.80), and the pseudo-Ag|AgCl reference electrode was placed in the opposite hemisphere of the brain as the working and stimulating electrodes. Animal use followed NIH guidelines and complied with the University of South Carolina Institutional Animal Care and Use Committee under an approved protocol.

Microelectrodes Fabrication

Carbon Fiber Microelectrodes (CFMs) were made individually by aspirating a single carbon fiber (Goodfellow Corporation, PA, USA) into a 0.6 mm x 0.4 mm glass capillary (A-M Systems, Inc., Sequim, WA, USA). The capillary was then pulled by a vertical puller (Narishige, Tokyo, Japan) to create a carbon-glass seal. The carbon fiber was then trimmed to 150 ± 5 μm for serotonin electrodes. Liquion (LQ-1105, 5% by weight Nafion^{TM}) (New Castle, DE, USA) was electrodeposited onto the surface of the carbon fiber by dipping and

applying a constant potential of +1.0 V for 30 s. The electrode was then dried at 70 °C for 10 minutes and used after 24 hours.

Hardware

FSCAV was performed using a Dagan Potentiostat, (Dagan Corporation, Minneapolis, MN, USA), National Instruments multifunction device USB-6341 (National Instruments, Austin, TX, USA), WCCV 4.0 software (Knowmad Technologies LLC, Tucson, AZ, USA) and a Pine Research headstage (Pine Research Instrumentation, Durham, NC, USA). Data filtering (zero phase, Butterworth, 2 kHz low-pass) and signal smoothing were done within the WCCV software.

Data Collection

FSCV

A selective waveform for serotonin was applied to the electrode (Serotonin: +0.2 V to +1.0 V to -0.1 V to +0.2 V, 1000 V s^{-1}) at the frequency of 10 Hz. The output of this technique was a colorplot generated using custom software. From this, a cyclic voltammogram was collected every 100 ms with a signature serotonin redox peak that appears at 0.7 V. A current vs. time plot was also extrapolated from this color plot showing the change in serotonin concentration over time. Current vs time will then be turned into concentration vs. time by using a predetermined calibration factor. This method is a background subtracted method due to the very fast scan rate generating a large nonfaradaic current. A change must be induced to visualize serotonin's redox processes: this is accomplished *in vivo via* electrical stimulation.

FSCAV

FSCAV was performed in three steps: (1) the serotonin waveform was applied at 100 Hz to minimize adsorption of serotonin to the electrode surface; (2) a fixed potential (0.2 V)

was applied for 10 s, allowing for maximized adsorption; (3) the waveform was then reapplied and the first signature cyclic voltammogram collected was used to measure ambient serotonin concentration. The concentration was found *via* a post-calibration process (*vide infra*). An electronic relay was employed to switch between the serotonin specific waveform described above and a constant potential for a controlled adsorption period.

Computational Methods

FSCAV Measurement Methods

Limits of integration to estimate the charge of the faradaic peak and maximum amplitude from FSCAV serotonin cyclic voltammograms are obtained using custom-designed automatic local minima and local maxima algorithms implemented in *The Analysis Kid*.[18] Charge of the faradaic peak is calculated using the Simpson's rule. The first integration point is normalized to have a current value of zero to avoid subtraction of area between the negative and positive currents of the CVs. A linear regression is obtained between the two integration points to obtain the baseline used to measure the faradaic charge. This minimizes the interference from the capacitive peak. Linear regression models from postcalibrations are obtained using linear least squares between concentration labels and estimated charge of the serotonin faradaic peak. The coefficient of determination (R^2) and the standard error of the estimate are used as parameters to assess the goodness of fit. FSCAV experimental drifts (*vide infra*) are modeled with a shifted negative exponential function shown in eq.1

$$Q(t) = - Q0\ e\text{-}kt + Qf \qquad (1)$$

where Q(t) is the charge of the faradaic serotonin peak at time t, Q0 and Qf determine the position of the exponential function in the Cartesian axes, and k is the exponential constant

that determines the speed of growth. The time constant of the exponential function, t63% = 1/k, is used to characterize the speed of the sensor to achieve stability. The sensor response time (this was defined as the time it takes the sensor to reach 95% stability), was set as three times the time constant, since t95% ≈ 3t63%. The nonlinear fitting is performed using the Levenberg-Marquardt algorithm.[19] Subtraction of the exponential fit is performed by adding to the experimental trace an exponential decay function (Q0 e-kt) with the fitted parameters.

Statistical Analyses

Statistical significance is defined as $p < 0.05$. All statistical tests are performed using Python 3.6 SciPy library[20] and Matlab 2020b. Distribution of samples are shown as mean ± SEM if not stated otherwise. Error of model predictions is shown as the RMSE between true and predicted concentrations. FSCAV post-calibrations and *in vivo* predictions of serotonin were tested for significance using analysis of variance (ANOVA) and *Tukey-Kramer post-hoc* multiple comparisons. See the Supplementary Information for a full description of the statistical analyses.

RESULTS AND DISCUSSION

A New Technique to Improve FSCAV Equilibration Time

As with most i*n vivo* methods, electrochemical methods for in vivo analysis can be characterized by an equilibration time. We define this equilibration time for FSCAV as the time it takes for the electrode surface to come to 63% of equilibrium in the complex system. This equilibration time is in part due to the high acquisition rate of the technique as well as the scan rate/frequency at which the waveform is applied, but mostly it is dependent on the environmental matrix itself: *e.g.* protein redox behavior, biofouling, *etc.*[21-25] During this

time, the electrode itself has not consistently met a steady state, thereby making these electrochemical measurements unreliable. It is essential to reach a steady state before beginning experimental analysis.

Specifically, with FSCAV data analysis has a baseline drift associated with the equilibrium has been found to be challenging. In **Figure 3.1**, representative examples of this drift are given for *in vitro* and *in vivo* recordings. The *in vitro* trace in **panel A** was obtained by measuring the electrode response to 75 nM serotonin in PBS for 120 minutes. This *in vitro* signal decays over time and reaches steady state after about 30 minutes. It can be modeled with the shifted negative exponential function shown in **eq.1**, which allows us to obtain an estimation of the response time of the electrode. We hypothesized that this drift is a direct result of stripping of the Nafion layer from the electrode surface *in vitro*, which is supported in **Chapter 2** where we showed that the Nafion layer is unstable in a beaker (but not *in vivo*).

The *in vivo* trace in **Figure 3.1 panel B** was obtained by measuring the electrode response to serotonin in the CA2 region of a mouse hippocampus for 120 minutes. The highlight feature of this *in vivo* drift is that the baseline shows a logarithmic *growth* rather than the decay seen in the *in vitro* signal.

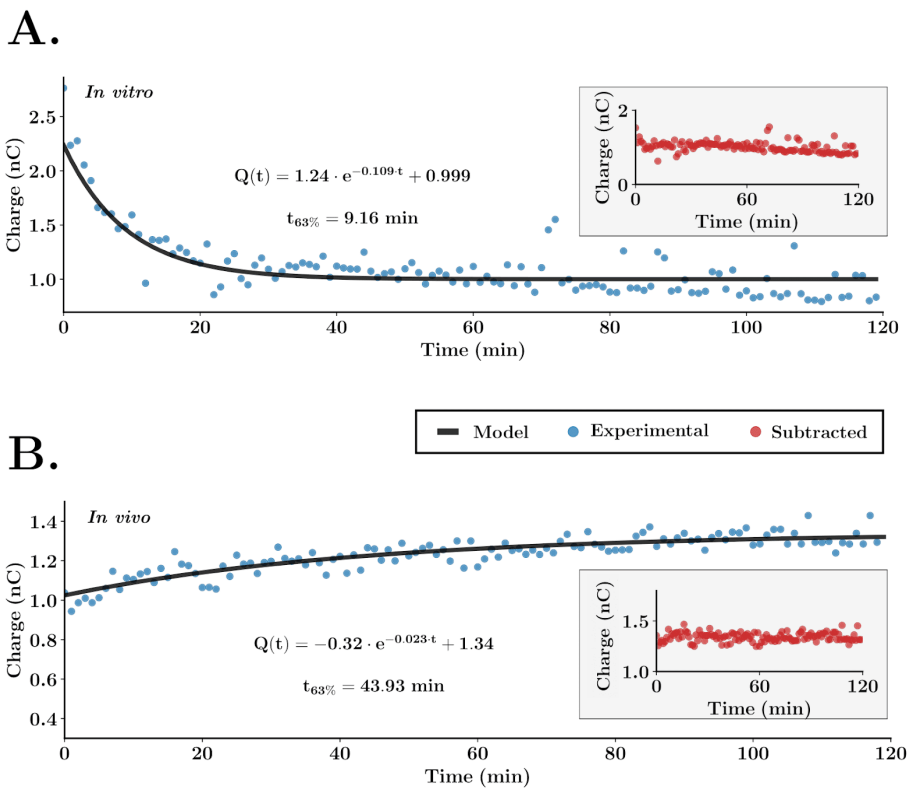

Figure 3.1: *In vitro* and *in vivo* representative examples of FSCAV acquisition for 120 min. (A) *In vitro* FSCAV acquisition in PBS-buffered 75 nM serotonin solution. From the fitted curve mode, the time constant is estimated to be 9.16 min. (B) *In vivo* FSCAV acquisition from the CA2 region of a mouse hippocampus. From the fitted curve model, the time constant is estimated to be 43.93 min. Part A and Part B show similar trends and comparable stability times. Interlaid in red, the experimental data is shown for both acquisitions after the exponential model subtraction (*vide supra*)

The drift in each case must be derived from different sources. Presently the exponential trace model can be used to eliminate the excess time for stability to be reached by subtracting the drift from the experimental trace. **Figure 3.1** shows this in practice on the *in vivo* and *in vitro* examples of the experimental traces together with the exponential model fit and the experimental trace after subtraction (see red). This estimation of the drift takes place on the section of the trace where we assume that the drift estimation is not influenced by evoked physiological changes, which would undermine the drift subtraction process. To remove this assumption, it is better to wait until the electrode has reached

equilibrium; however, such a long wait period (over 2 hrs) may come at the expense of experiment failure (*i.e.* animal death). We thus ask 2 questions here: 1) what causes the *in vivo* drift and 2) how do we improve equilibration time?

In **Chapter 2**[17], we showed that after *in vivo* implantation of the CFM there was a robust increase in sensitivity toward serotonin and dopamine. One contributing factor to this finding is high extracellular glutamate levels resulting in polyglutamate electropolymerization on the electrode surface facilitating the preconcentration of serotonin and dopamine.[17, 26] In this work, such a layer may also stabilize the Nafion coating *in vivo* and eliminate the exponential decay drift observed *in vivo* in **Figure 3.1**. However, polyglutamate may not be the only contributor to this phenomenon. We hypothesized that other amino acids in the *in vivo* environment may be contributing to the formation of complex polymer layers on the electrode surface, taking over 120 minutes to reach an equilibrated state and serving to increase electrode sensitivity. Here, we investigated a variety of amino acid pretreatments and their effects on equilibration time.

We first set out to determine which AAs contribute to a robust change in sensitivity toward serotonin *via* flow injection analysis using FSCV in **Figure 3.2**. Using FIA, the initial electrode response to 1 μM serotonin was recorded in PBS buffer. Then, the electrode was modified to polymerize one of eight AAs chosen based off of their similarity in size and charge to glutamate, abundance in the CA2 region of the hippocampus or involvement in serotonin and DA synthesis pathways.[27-32] To polymerize the AAs onto the CFM surface, the following steps were employed: 1) the electrode was placed in biologically relevant concentration of the specific AA in a PBS matrix. 2) we the applied a wide potential window, as previously noted in **chapter 2**, from -1.2 V to 1.3 V to -1.2 V

for 10 mins at 60 Hz. 3) the electrodes were then cycled on the serotonin waveform in PBS at 60 Hz for 10 mins and 10 Hz for 10 mins. Then, the electrode response to 1 μM serotonin in PBS buffer was recorded again and sensitivity shifts were attributed to the AA modification. In **Figure 3.2**, it was determined from this experiment that Cys (blue), Glu (purple), Gly (violet), and GABA (pink) electrode modifications (students t-test, $p < 0.005$) are major contributors to sensitivity shifts toward serotonin using FSCV. Each contributes to a ~ 50% change in sensitivity toward serotonin compared to control waveform experiments (brown).

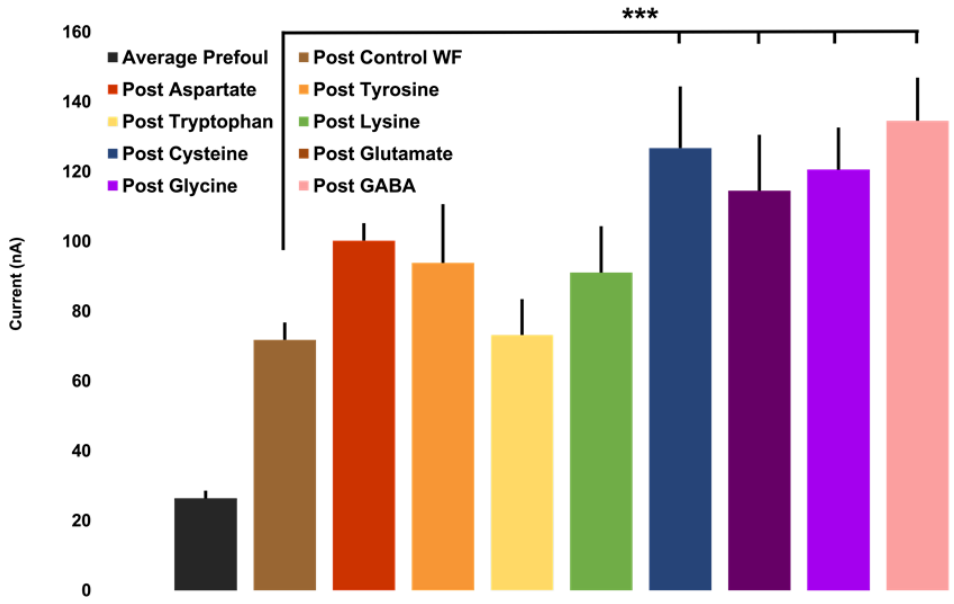

Figure 3.2: Surface Modifications Towards Serotonin Sensitivity. All electrodes in this data set are Nafioned. The polymer waveform (-1.2 V to 1.3 V to -1.2 V) was applied and each AA modification was compared to this control (brown). Of the 8 AAs studied, Cys, Gly, Glut and GABA were shown to have the significant effects on sensitivity compared to control. Response and error bars show the mean ± SEM across 5 electrodes.

Next, we set out to determine whether these four AAs affected the FSCAV signal in **Figure 3.3**. Using FSCAV, the electrode response to 75 nM serotonin in PBS buffer was recorded over a period of 60 minutes. Then, the same electrode was modified (see

Figure 3.2 description for methods) with one of the four AAs. Then, the electrode response to 75 nM serotonin in PBS buffer was recorded for another 60 minutes, and significant sensitivity shifts were determined to be a result of AA electrode modification. From this experiment, it was determined that glycine, glutamate, and GABA ($p < 0.01$) electrode modifications are major contributors to robust sensitivity shifts toward serotonin using FSCAV. Of note, there was no effect of applying the polymerization waveform in the absence of AA (one-way ANOVA, $F = 1.1650$, $p = 0.3558$) (see Supporting Information).

Next, we concentrated on the effect of these three AAs in a matrix more complicated than PBS (comprising all 8 amino acids, to better mimic the brain) and found the same trends. In **Figure 3.3**, electrodes modified with AAs appeared to reach a point of stability at a quicker rate than simply Nafioned electrodes in this matrix. Thus, a time constant ($t_{63\%}$) was calculated in addition to the sensitivity (pC/μM) and both were plotted in panel B. It was observed that modification with glutamate, glycine, and a combination of glutamate, glycine, and GABA resulted in a significant decrease in time to stability compared to no polymerization (one-way ANOVA and post-hoc test on the $t_{63\%}$ differences pre and post polymerization, glutamate: $\Delta t_{63\%} = 34.49 \pm 4.07$ min vs. -16.75 ± 3.76 min, $p = 0.0005$; Glycine: $\Delta t_{63\%} = 27.02 \pm 13.24$ min vs. -16.75 ± 3.76 min, $p = 0.0028$; 3 AAs: $\Delta t_{63\%} = 28.46 \pm 6.26$ min vs. -16.75 ± 3.76 min, $p = 0.0021$). GABA polymerization alone decreases the time constant, but this decrease is not significant (GABA: $\Delta t_{63\%} = 12.48 \pm 3.14$ min vs. -16.75 ± 3.76 min, $p = 0.0636$). However, the sensitivity of the electrode does increase (N.S.) after the application of the extended waveform. This is most likely due to the etching of the CFM surface and the additional oxygen moieties that would be formed on the electrodes surface at this high potential.[33]

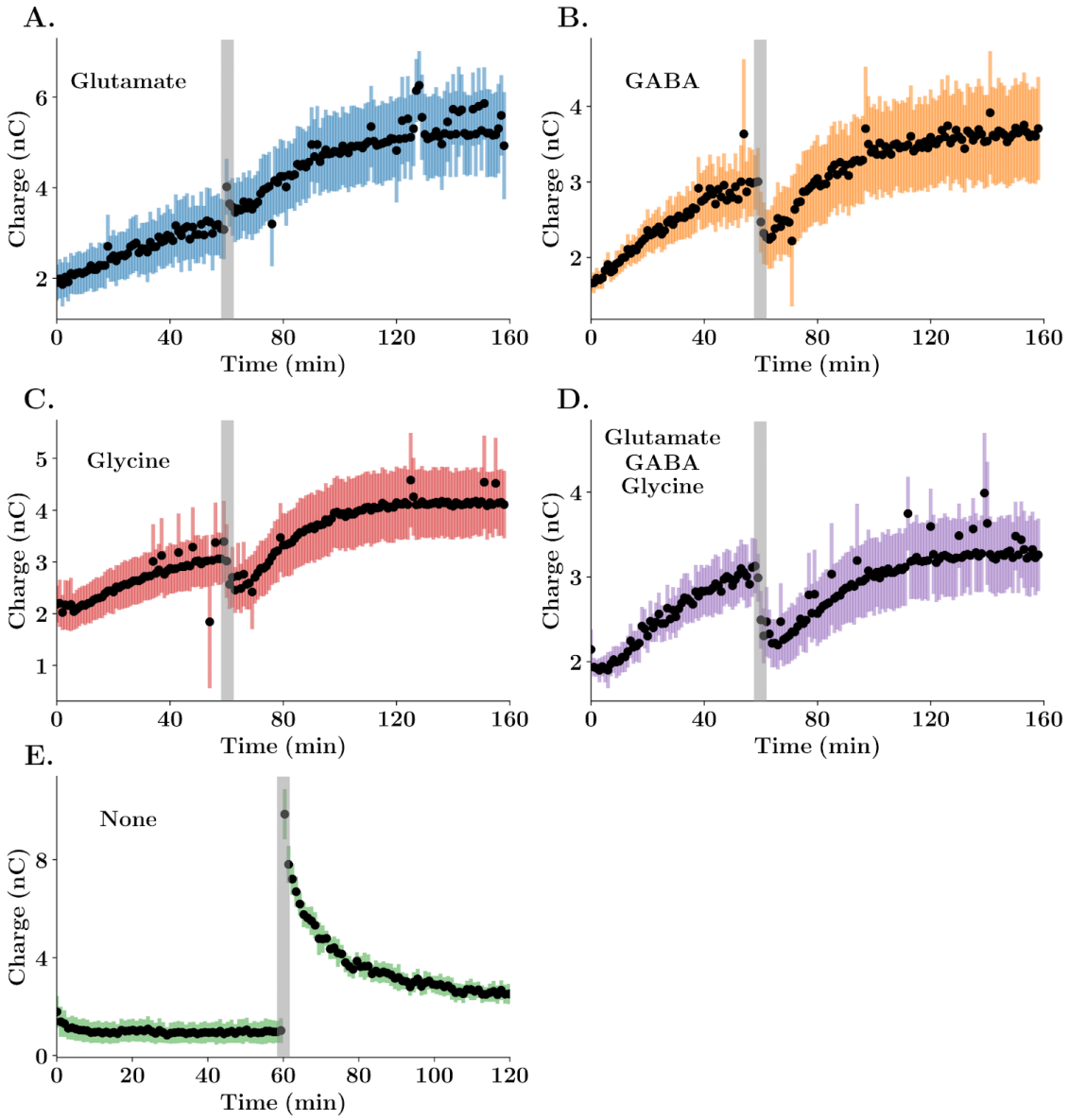

Figure 3.3: FSVAV Beaker Matrix Effects. (A, B, C, D) *In vitro* FSCAV acquisitions in AA-PBS-buffered 75 nM serotonin solution together with the polymerization of the amino acid stated in the graph of each panel. Scatter points and error bars show the mean ± SEM across 5 electrodes. The gray bar shows the time at which the polymerization waveform is applied. (E) *In vitro* FSCAV acquisitions in PBS-buffered 75 nM serotonin solution with Nafion only. Scatter points and error bars show the mean ± SEM across 5 electrodes. The gray bar shows the time at which the polymerization waveform is applied.

Based on the results from the *in vitro* studies above, a series of experiments were performed in order to even better subside the baseline drift while utilizing this new polymer

coating (see Supporting Information **Figure B.2**). In brief, the combination of AA modifications determined in **Figure 3.3** was investigated with various time periods of holding at 0.2 V, the holding potential of the Jackson waveform. It was found that the combination of modification with the three AAs and holding at 0.2 V for 10 min best alleviated the baseline drift. This new analysis paradigm was finally employed *in vivo* in **Figure 3.4.**

Figure 3.4, shows Nafioned electrodes (red, n = 8), the standard pretreatment for our electrodes for *in vivo* analysis, in the CA2 region of the hippocampus measuring ambient serotonin. The normalized baseline drift again was fit to determine the $t_{63\%,}$ which was found to be 38.84 ± 5.85 min. This was directly compared to the proposed GABA, glutamate and glycine modified electrode. This was then compared to that of the proposed analysis paradigm of the three AA combination electrode modification and holding at 0.2 V for 10 minutes (blue, n = 5). These experimental traces were fit to estimate a $t_{63\%}$ = 20.22 ± 3.04 min. As evident in **Figure 3.4A**, AA polymer electrodes have a faster response time compared to electrodes treated only with Nafion polymer (**Figure 3.4B**, Student's *t*-test, p = 0.0376).

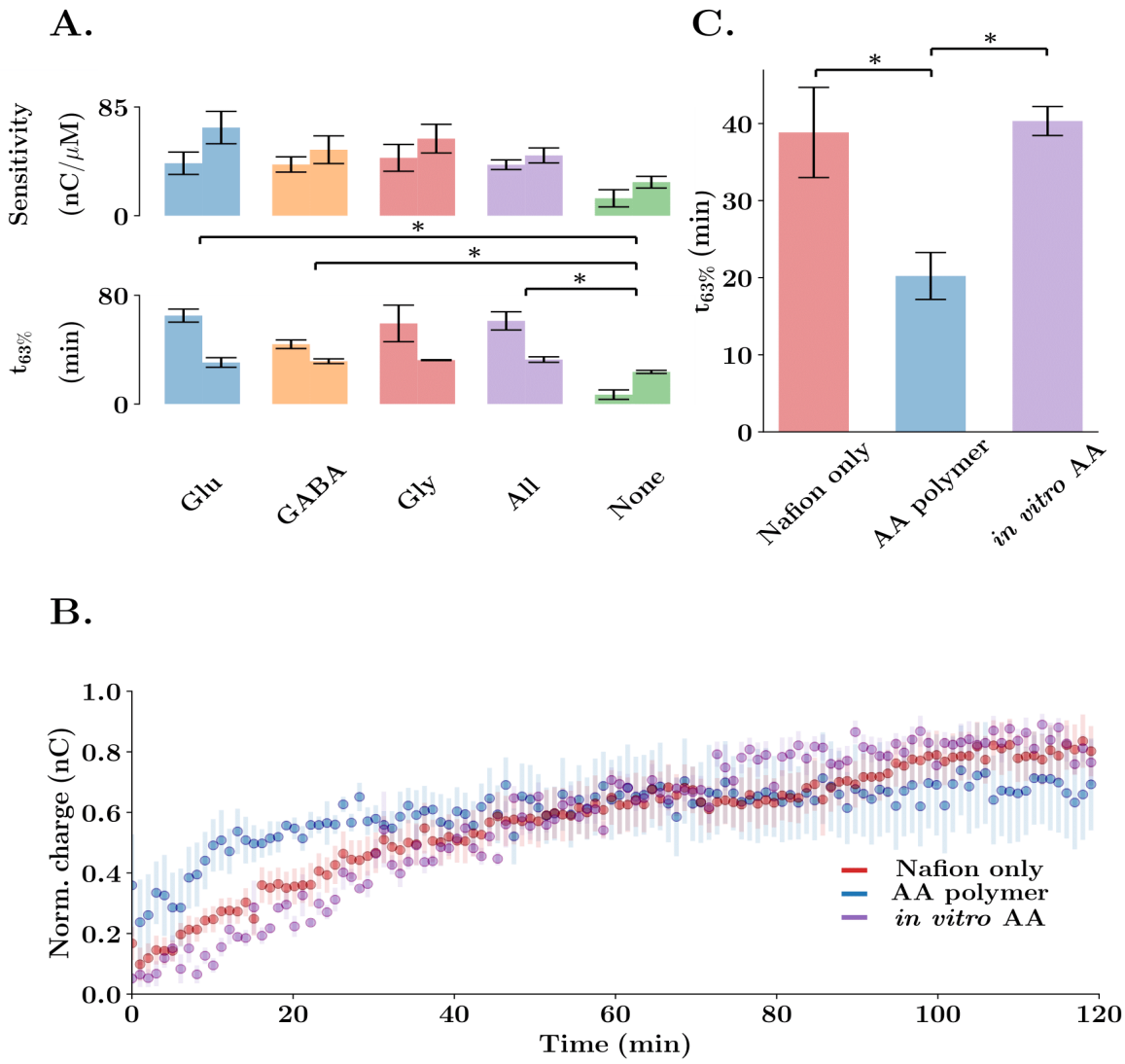

Figure 3.4: Surface treatments of the carbon fiber with polymerized amino acids. (A) Mean ± SEM (n = 5 electrodes) of sensitivity at the end of the experiment and time constant of the drift model. Statistical significance ($p < 0.05$) of the differences is shown with an asterisk (one-way ANOVA and *post-hoc* test of differences in sensitivity and time constant pre and post polymerization). For each treatment, the left bar shows the statistics measured pre polymerization, while the right bar corresponds to the same parameters measured post polymerization. (B) Mean ± SEM *in vivo* traces of the Nafion-only electrode acquisitions (red, n = 8 animals) and AA-polymerized electrodes (blue, n = 5 animals). AA polymerization was performed by the application of the extended polymer waveform (-1.2 V to 1.3 V to -1.2 V) prior to data acquisition. (C) Mean ± SEM of drift time constant for both datasets. The drift model was fit to each of the experimental traces. Nafion electrodes in the in vivo matrix, take a longer stability time compared to Nafion/AA treated electrodes (Student's unpaired t-test t63% = 38.84 ± 5.85 min vs. 20.25 ± 3.04 min, $p = 0.0376$).

CONCLUSIONS

FSCAV has given great insights in the study of serotonin tonic concentrations *in vivo*, but despite these achievements, some challenges regarding the calibration and stability of signals had to be addressed. In this work, we have shown robust methods to correct and improve the stability of electrodes and the prediction capabilities of FSCAV calibration models. First, we have shown a method to mathematically correct electrode drift FSCAV experiments. After that, we developed an experimental approach to minimize the FSCAV electrode drift taking advantage of the complexation of AAs to carbon surfaces. The novel treatment of the CFM surface, which included the electrodeposition of Nafion and 3 AAs (glycine, GABA and glutamate) has been shown to be advantageous both *in vitro* and *in vivo.* We believe that this work will make serotonin ambient detection more user-friendly and accessible to other research groups.

Chapter 4: Voltammetric Assessment of the Effects of Different Antidepressant Types on *In Vivo* Serotonin[1]

[1] Witt, C. E., Mena, S., Berger, S. N., Parke, B., Hersey, M., Ou, Y., Honan, L. E., Fadel, J. and Hashemi, P. Voltammetric Assessment of the Effects of Different Antidepressants Types on *In Vivo* Serotonin. In Preparation. *Cells*.

ABSTRACT

Depression is the leading cause of disability in the world, yet this disorder is notoriously difficult to treat. Over the last few decades there have been several classes of antidepressant therapies that have precipitated from different theories outlining mechanisms of depression However, because the neurochemical underpinnings of depression are not well defined, these therapies suffer poor efficacy rates and new therapies are difficult to develop. In this chapter, we outline the application of fast scanning electrochemical techniques to directly detect serotonin dynamics in response to several classes of antidepressants. We review the major classes of antidepressants and assess their effects, utilizing novel analytical tools, on serotonin dynamics in the brain to correlate this chemistry to clinical efficacy. Thus, we highlight the critical role for electrochemical techniques in the assessment of current antidepressants and the development of new pharmacological treatments.

INTRODUCTION

Neuropsychiatric diseases, like depression, affect an already large and growing number of individuals. Depression in now classified as the primary contributor to the global burden of disease.[1] This is due, in large, to the currently limited understanding of this debilitating disease. Though years of research have gone into understanding the pathology of depression, there are still more questions than there are answers. Clinically, patients have been treated with an array of pharmaceutical agents all classified under the umbrella of "antidepressants". Antidepressants (ADs) are classified into groups based on time of discovery, mechanism of action and pharmacological targets.[2, 3] Key AD groups include tricyclic amines (TCAs), monoamine oxidase inhibitors (MAOIs), selective serotonin reuptake inhibitors (SSRIs), norepinephrine reuptake inhibitors (NRIs) and modern/novel

ADs (including ketamine). Unfortunately, the reason so many ADs and so many classes of ADs are available on the market is that most ADs have low efficacy[4, 5] and a delay of therapeutic effects that greatly mar their ability to act to improve depression symptoms[6, 7], per their intended use. Importantly, improving the efficacy of ADs has been the focus of pharmaceutical companies for decades and thus many new ADs have emerged on the market. These ADs' mode of action ranges from the glutamatergic system all the way to primarily acting on serotonin, dopamine or norepinephrine respectively. All have shown varying clinical efficacies, however, there are no screening tools for these drugs.

Screening and analysis techniques for ADs are essential to improving drug discovery. Researchers have employed microdialysis, electrophysiology and PET imaging to probe depression neurochemistry and screen ADs. The golden standard for understanding pharmacological dynamics *in vivo* has been microdialysis. Microdialysis can quantitatively analyze the direct and downstream effects of each AD to increase extracellular serotonin following acute/chronic administration limited only by its temporal resolution and large probe size.[10, 11] For example, David *et al.* showed a dose response and potency/efficacy analysis of serotonin efflux with the SSRIs paroxetine, citalopram, and venlafaxine.[12] Electrophysiology overcomes the large probe size and minimal temporal resolution; however, it is limited to the measurement of the electrical activity of single neurons. Czachura *et al.* employed electrophysiology study doses, and routes of administration of the SSRI fluoxetine on firing activity of serotonergic neurons in the dorsal raphe nucleus.[13] PET imaging is minimally invasive and can be used to determine receptor or transporter populations, however, it is not capable of determining neurotransmitter concentrations. Riad *et al.* determined that fluoxetine

administration resulted in increased internalization of $5HT_{1A}$ autoreceptors in the dorsal raphe nucleus using PET studies. This autoreceptor internalization is predicted to be essential to SSRI/fluoxetine efficacy.[14] These analytical techniques have separately made great strides in characterizing antidepressant mechanisms'.

Analytical chemistry provides a unique opportunity to improve screening and analysis techniques for ADs. We present how fast electrochemical techniques can also be used as a screening tool and for novel analysis. Fast-scan cyclic voltammetry (FSCV) and its adapted sister technique fast-scan controlled adsorption voltammetry (FSCAV) are analytical techniques that employ a microscopic (7 μm diameter) carbon fiber electrode to probe the *in vivo* neurochemistry in rodent models. These voltammetric techniques work by applying an analyte-specific waveform traditionally used to study central nervous system (CNS) dopamine. However, this technique was later adapted to probe and understand the serotonergic system of the CNS.[15, 16] Since their adaptations, FSCV and FSCAV has been used to study real-time evoked serotonin as well as reuptake dynamics *in vivo*.[15, 17-22]

Serotonin is a biomarker of interest because it is an essential neurotransmitter that has long been highlighted for its importance in the regulation of mood. Therefore, it has been postulated that the dysregulation of this transporter could result in mood disorders like depression. Specifically, the monoamine hypothesis of depression has long been acknowledged serotonin as a primary suspect in depression pathology.[23, 24] Serotonin (and its precursors and metabolites) have been shown to be decreased in the cerebrospinal fluid[25] (CSF) and blood of depressed patients.[26] However, this is not always reproducible[27] suggesting it is not a good biomarker for depression. Arguably, the best support of the

monoamine hypothesis is that many of the most efficacious ADs prescribed today target these monoamine systems.[28, 29] Fast voltammetry also offers the capability to look at and understand pharmacodynamics from multiple vantage points including phasic release, ambient dynamics. This work sets out to utilize/establish fast-voltammetry as a clinical screening tool to look at the efficacy of commonly prescribed and atypical ADs as well as to highlight the versatility and power of this technique. In this work, we compare multiple classes of ADs to understand their effects on the serotonergic system, our biomarker of choice. We utilize stimulated data to analyze reuptake dynamics (Amp_{max} and $t_{1/2}$) as well as ambient analysis to understand how these drugs change extracellular serotonin over time. This unique combination of efforts/techniques has never been achieved, and we show that although serotonin may not be affected in phasic stimulation dynamics, *most* of these treatments show capacity to increase extracellular serotonin levels. Thus, placing serotonin to the forefront, once more, as a main pharmacological target for treating depression.

MATERIALS AND METHODS

Chemicals and Reagents

Ketamine hydrochloride (Vet One, MWI Animal Health, Boise, ID, USA), escitalopram oxalate (Sigma Aldrich, St. Louis, MO, USA), pargyline hydrochloride (Sigma Aldrich, St. Louis, MO, USA), fluoxetine hydrochloride (Sigma Aldrich, St. Louis, MO, USA) and reboxetine mesylate hydrate (Sigma Aldrich, St. Louis, MO, USA), were individually dissolved in sterile saline (0.9% NaCl solution, Hospira, Mountainside Medical Equipment, Marcy, NY, USA) and administered *via* intraperitoneal injection (*i.p.*) at 10 mg kg^{-1} and a volume of 5 mL kg^{-1} body weight. Urethane (Sigma Aldrich, St. Louis,

MO, USA) was dissolved in sterile saline at 25% w/v and administered at 7 µL/g mouse body weight for surgical anesthesia.

Electrode Fabrication

Carbon Fiber Microelectrodes (CFMs) were made individually by aspirating a single carbon fiber (Goodfellow Corporation, PA, USA) into a 0.6 mm x 0.4 mm glass capillary (A-M Systems, Inc., Sequim, WA). The capillary was then pulled in a vertical puller (Narishige, Tokyo, Japan) to create a carbon-glass seal. The exposed carbon fiber was then trimmed to 150 ± 5 μm. Liquion (LQ-1105, 5% by weight Nafion^{TM}, New Castle, DE, USA) was electrodeposited onto the surface of the carbon fiber by submerging the fiber in Nafion and applying a constant potential of +1.0 V for 30 s. The electrode was then dried at 70°C for 10 minutes and used after 24 hours.

Animal and Surgical Procedures

Mice (C57BL/6J) (Jackson Laboratory, Bar Harbor, ME, USA) were injected with a 25% urethane solution based on a calculation that is dependent on their weight (7µL/g). Following anesthetic administration, the mouse was placed into a stereotaxic system (David Kopf Instruments, Tujunga, CA, USA) where body temperature was maintained *via* heating pad (Braintree Scientific, Braintree, MA, USA). Three holes were drilled into the skull of the mouse based off of coordinates from the mouse brain atlas. The working electrode was placed in the CA2 region of the hippocampus (CA2: -2.91, +3.35, -2.50) the stimulating electrode (insulated stainless-steel, diameter 0.2 mm, untwisted, Platistics One, Roanoke, VA, USA) was placed in the medial forebrain bundle (MFB: -1.58, +1.00, -4.80) and the pseudo-Ag|AgCl reference electrode (made by chloritizing a silver wire in a solution of 1 M HCl for 30 secs at 5 V) was placed in the

opposite hemisphere of the brain as the working and stimulating electrodes. Stimulation was accomplished via linear constant current stimulus isolator (NL800A Neurolog, Medical Systems Corp, Great Neck, NY, USA) with the following parameters: 60 Hz, 360 μA each, 2 ms in width and 2 s in length. Animal use followed NIH guidelines and complied with the University of South Carolina Institutional Animal Care and Use Committee under an approved protocol.

Hardware for Data Collection and Analysis

FSCV and FSCAV were performed using a Dagan Potentiostat, (Dagan Corporation, Minneapolis, MN, USA), National Instruments multifunction device USB-6341 (National Instruments, Austin, TX, USA), WCCV 4.0 software (Knowmad Technologies LLC, Tucson, AZ, USA) and a Pine Research headstage (Pine Research Instrumentation, Durham, NC, USA). Data filtering (zero phase, Butterworth, 2 kHz low-pass) and signal smoothing were done within the WCCV software. The "Jackson" waveform was applied to elicit the redox properties of serotonin (+0.2V to +1.0V to -0.1V to +0.2V, 1000 V s^{-1}). For FSCV data collection, this was applied at 10 Hz. For FSCAV data collection, this was applied at 100 Hz. A more detailed account for FSCAV data acquisition can be found in **Chapter 2 and 3**.

Statistical Analyses

Control files were averaged (4) per animal found in black for each drug. Animals that were excluded were outliers based on a Grubbs test and animals that did not survive to the 100 min mark after drug administration. Standard error of the mean was propagated to show error among the groups based on the n-count of the animals per drug. Significance between

two groups were found via a 2-tailed paired t-test ($p < 0.05$). FSCAV estimations of basal concentration of serotonin were analyzed *via* two-way analysis of variance (ANOVA) with effects of mouse and pharmacological treatment (control, saline and drug separated by time). Analysis of covariance (ANCOVA) was used with basal estimations of serotonin to identify significant changes in the rates of change of concentrations. *Tukey-Kramer post-hoc* tests were used to compare all the individual groups once significant effects on the ambient levels of serotonin were found. Exclusion criteria were based on outliers (*via* Grubbs test) and animals that did not survive the experimental paradigm.

RESULTS AND DISCUSSION

Voltammetric serotonin analysis can be used to probe the response of brain serotonin to ADs. In Fig. 4.1 we show the histograms of the ambient level responses of extracellular hippocampal serotonin in anesthetized mice to a variety of common AD treatments in terms of their increase from baseline as well as the rapidity of the response (slope). We find that *most* of the commonly prescribed ADs effectively target hippocampal serotonin and administration of these agents rapidly increases extracellular serotonin after equivalent acute doses. Though these ADs act *via* different modes of action, they still all show a robust change in the ambient release from control data. Following, each data set will be analyzed to further probe this robust increase in basal serotonin. The following is part review / part data and will proceed chronologically, from the first synthesized ADs (TCAs) and will end with atypical ADs (ketamine). Of particular note, we will investigate the properties of new pharmacological agent as well as describe a rationale for the robust ambient changes upon

ketamine administration. Both of these mechanisms center on the inflammatory system and serotonin connection.

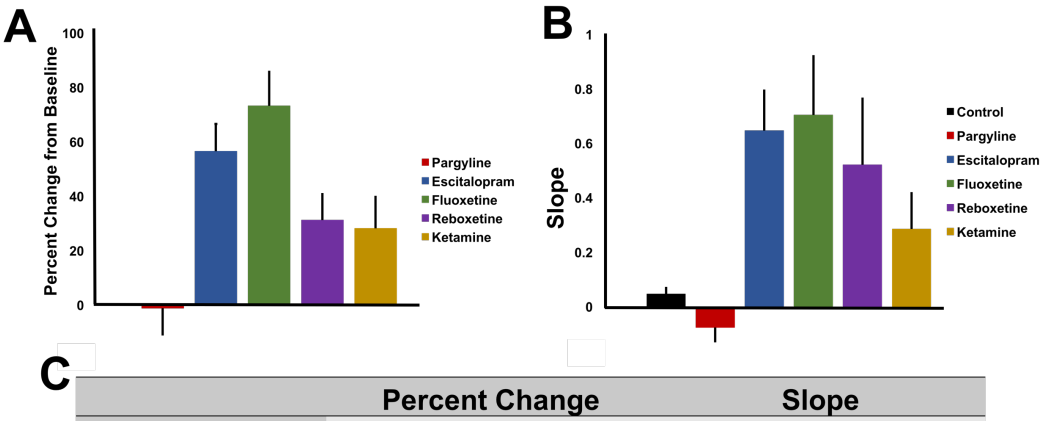

C

	Percent Change	Slope
Pargyline	-1.12 ± 14.18	0.0610 ± 0.05
Escitalopram	56.55 ± 11.99 *	0.6469 ± 0.15 *
Fluoxetine	73.29 ± 12.18 *	0.7042 ± 0.22 *
Reboxetine	31.31 ± 10.01 *	0.5211 ± 0.21 *
Ketamine	28.18 ± 13.18 *	0.2847 ± 0.14 *

Figure 4.1: Ambient Pharmacological Changes to the Serotonergic System Summary (**A**) Percent change from extracellular hippocampal serotonin baseline was calculated for each drug. (**B**) Slope changes were compared across each drug, to show the effects on ambient release of serotonin. (**C**) Table summary of figures 4.1A and 4.1B with statistical significance denoted by * (p-value ≤ 0.05).

Tricyclic Antidepressants (TCAs)

Imipramine, the first TCA, was synthesized in 1951 and was approved for medical use in1957.[30] Imipramine strongly binds to SERT (1.3-1.4 nM K_m), NET (20-37 nM K_m) and histamine H1R (7.6-37 nM).[31] TCAs were initially prescribed as an antihistamine, then an antipsychotic and finally for the treatment of anxiety and depression.[32] Due to TCA's harsh side-effects (including tachycardia, hypothermia) and its high toxicity, they were quickly phased out of clinical use.[28] However, TCAs, like imipramine, are still used as second-line treatments and for the treatment of major

depression cases. Over the years, SSRIs have been shown to be more tolerable than TCAs; withdrawal rates for SSRIs was 13.9% and for TCAs 18.8% (4.9% difference statistically significant).[28] There have been reported cases of TCA toxicity over the years and more patients find themselves taking themselves off the TCA opposed to continue using it as a treatment.[33] This discounted used of the TCA is primarily due to the lack of alleviated symptoms but also due to the adverse side effects.

Our analysis of TCAs is limited due to a combination of factors. We attempted to use 3 TCAs (imipramine, desipramine and amitriptyline) and, at several doses, and they all lead to death of our anesthetized mice. We have attributed this issue to two things: 1) the harsh side effects of this class of ADs and 2) a serotonin syndrome pathway that was shown in our basal data—this in conjuncture of the combination of the drug itself with our anesthetic that we give our mice: urethane. This hypothesis is based on the immediate elevation of serotonin followed by a "dip" below baseline ending in the mice's death.

Monoamine Oxidase Inhibitors (MAOIs)

MAOIs are a class of ADs that pharmacologically target the intracellular degradation of monoamines *via* inhibition of the enzyme MAO-A, MAO-B or a combination of the two.[34, 35] This class of ADs hit the market in the 1960s and later fell out of the commonly prescribed ADs due to other, more effective lines of treatment coming to the forefront (i.e. SSRIs and NRIs).[36] One of the most common MAOI that was, and still is, prescribed in some cases is pargyline. Pargyline acts primarily on MAO-B and has been shown in the literature to robustly increase serotonin ambient levels *via* microdialysis experiments.[37] MAOIs were found to be effective in treating treatment-resistant depression and major depressive disorder—however they were discontinued due

to hypertensive effects due to the adverse side effects, MAOIs are recommended as third- or fourth-line treatments; although some doctors will recommend it earlier for treatment-resistant or atypical depressive patients.[37] However, there are newer MAOIs that are administered transdermally and do not require the same dietary restrictions that have been seen to increase the severity of side effects.[38]

Voltammetric analysis of serotonin was used to further study the effects of pargyline on the serotonergic system. In all experimental paradigms (**figures 4.2-4.4, 4.6 & 4.7**), we employee both FSCV and FSCAV to understand reuptake dynamics pre- and post-drug administration and ambient changes due to the drugs effect on the CNS. In these experiments, a carbon fiber microelectrode is placed into a mouse hippocampus to monitor serotonin. First, serotonin is confirmed *via* four stimulated control files, averaged in every dataset in black (error is standard error of the mean in the lighter shade around the line). We then employ FSCAV analysis and monitor the ambient serotonin for 30 min as a control, then administer saline to the animal and see no statistically significant changes. We then administer our pharmacological agent and monitor ambient changes over an hour of data collection. Then, we switched back to stimulated analysis to look at the changes in phasic/stimulated release of serotonin due to each drug. In each experiment that follows, we explore the effects that are imparted on serotonin from administration of these commonly prescribed and emerging ADs. Serotonin remains an important molecule in the context of depression, therefore, our goal was to expand the understanding of serotonin's effects on the CNS by monitoring how hippocampal serotonin responded to a sub-anesthetic dose of pargyline (10 mg kg^{-1}). We find that the phasic levels of serotonin do

not statistically change, but contrary to the literature, we see an immediate dip in ambient serotonin upon pargyline administration.

Figure 4.2.A highlights a key finding that acute pargyline has effect on serotonins stimulated or phasic release we see this twofold: 1) $t_{1/2}$ and 2) Amp_{max} pre- and post-pargyline. The $t_{1/2}$ went from 2.1 ± 0.5 s to 2.9 ± 0.4 s (NS), there is a trend towards an increase here. The Amp_{max} went from 29.5 ± 6.0 nM to 42.1± 13.6 nM (NS), showing a similar trend towards an increase. **Figure 4.2.B** indicates that there is a no change in ambient serotonin levels after drug administration from control to 60 min after pargyline administration (*post-hoc* test, 40.72 ± 1.90 vs. 37.08 ± 19.09 nM, p = 1.000). Additionally, the slopes of the time series for the control, saline and post pargyline acquisition do not differ significantly (ANCOVA test, F = 0.3604, p = 0.7859). This is no robust ambient change and differs from the literature associated with this drug. One thought here is that the microdialysis literature saw these increase in ambient serotonin at a much slower sampling rate; however, data acquisition of our technique is begins within 30 secs of drug administration. We do see at the end of the hour-long ambient experiment, that levels slowly increase. Though this is not significant, we plan to explore this instantaneous drop in serotonin levels to evaluate and tease out this stark difference from the literature values.

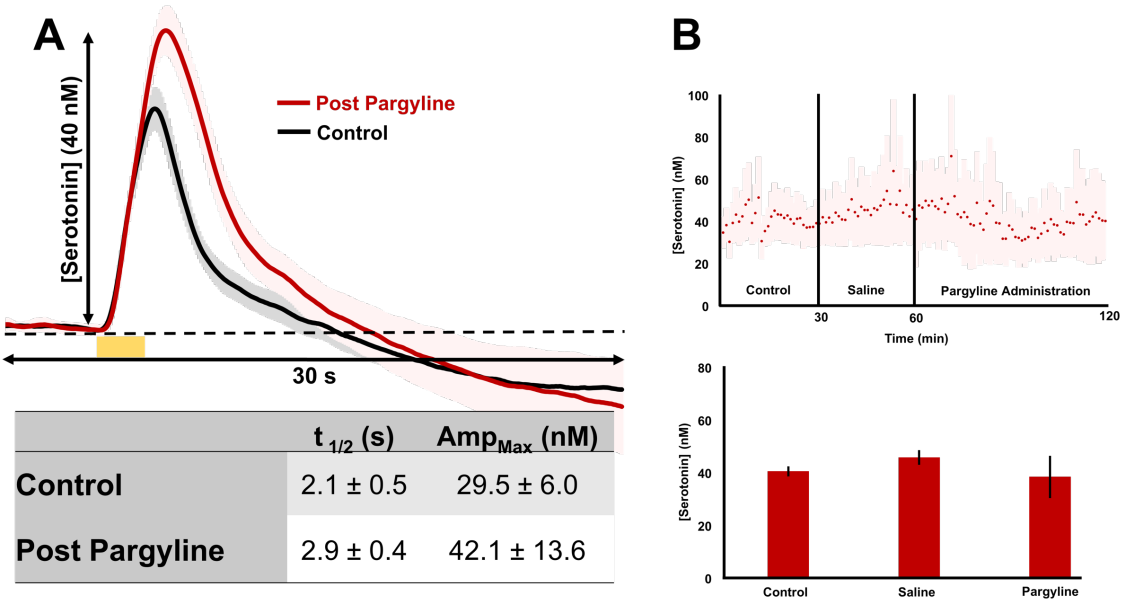

	$t_{1/2}$ (s)	Amp_{Max} (nM)
Control	2.1 ± 0.5	29.5 ± 6.0
Post Pargyline	2.9 ± 0.4	42.1 ± 13.6

Figure 4.2: Pargyline-induced changes in serotonin. (**A**) Extracellular hippocampal serotonin at baseline (black), post saline injection (grey), and post pargyline (*i.p.* 10 mg kg^{-1}, red) (n=5, male + female mice). (**B**) Evoked hippocampal serotonin at baseline (black) and 70+ min post pargyline (red). Stimulation is marked by a yellow box at 5-7 s. Statistical significance is marked by an * ($p < 0.05$).

Selective Serotonin Reuptake Inhibitors (SSRIs)

SSRIs have been used as the frontline treatment for depression since the rollout of fluoxetine in 1987.[39] This class of drugs are small organic molecules, structurally resembling serotonin, that inhibit the serotonin transporter (SERT), a protein tasked with clearing the monoamine after synaptic release.[40] However, the therapeutic mechanism of action of SSRIs remains unknown since the effects of these drugs on *in vivo* serotonin chemistry in the brain is hard to assess. However, generally, it is accepted that the pharmacological pathway of SSRIs works by selectively targeting and blocking the

SERTS, thereby increasing the concentration of serotonin in the synaptic cleft and the spill over into the extracellular space.[41]

SSRIs are the most commonly prescribed AD and this is due to the efficacious rate of these drugs as well as their less harmful side effects than other classes of ADs.[42] As a patient continues their treatment, the overall levels of serotonin have been hypothesized to reach a homeostatic maximum and the depressed patient begins to feel symptom alleviation. This efficacy is thought to be due to, but not limited to, desensitization of the serotonin autoreceptors and SERTs over the prolonged SSRI administration.[43, 44]

For this portion of this work, we focused on the first SSRI come to market and the most clinically efficacious: fluoxetine and escitalopram, respectively. Again, we focus on the reuptake dynamics via FSCV analysis and ambient changes via FSCAV analysis. We explored the role that serotonin plays in this emerging depression from effects of these commonly prescribed ADs. We wanted to investigate effects to hippocampal serotonin in response to a sub-anesthetic dose of fluoxetine (20 mg kg^{-1}) and escitalopram (10 mg kg^{-1}). We find that serotonin phasic release is changed upon both drug administration as well as an increase in basal levels.

Figure 4.3.A highlights a key finding that acute fluoxetine has effect on the stimulated release of serotonin, and we see this twofold: 1) $t_{1/2}$ and 2) Amp_{max} pre- and post-fluoxetine. The $t_{1/2}$ went from 2.3 ± 0.3 s to 4.9 ± 0.5 s ($p < 0.05$), this shows a significant increase and therefore is evidence that fluoxetine has an effect on blocking SERTs, and may illustrate the reason fluoxetine is an efficacious treatment for depression. The Amp_{max} significantly increased from 31.5 ± 7.7 nM to 53.4 ± 11.5 nM, this shows a statistical change and therefore shows evidence of that fluoxetine does have an effect on

blocking transporters and increasing the amout of serotonin present, this is again probably due to the blocking and binding of the drug to SERTs, further illustrating the reason fluoxetine is an efficacious drug for depression treatment. However, **Figure 4.3.B** indicates that there is a robust change in ambient release of serotonin from the control state to 60 min after drug administration (*post-hoc* test, 48.89 ± 1.86 vs. 73.31 ± 11.82 nM, p = 0.0150). This represents a 49% increase respect to the initial basal levels. Additionally, using an ANCOVA test and *post-hoc* multiple comparisons, the slopes of the time series for control and after fluoxetine administration were found to be significantly different (*post-hoc* test, slope = -0.02 vs. 0.22 nM/min, p < 0.0001). robust ambient change is on par with the literature trends for this commonly prescribed AD.

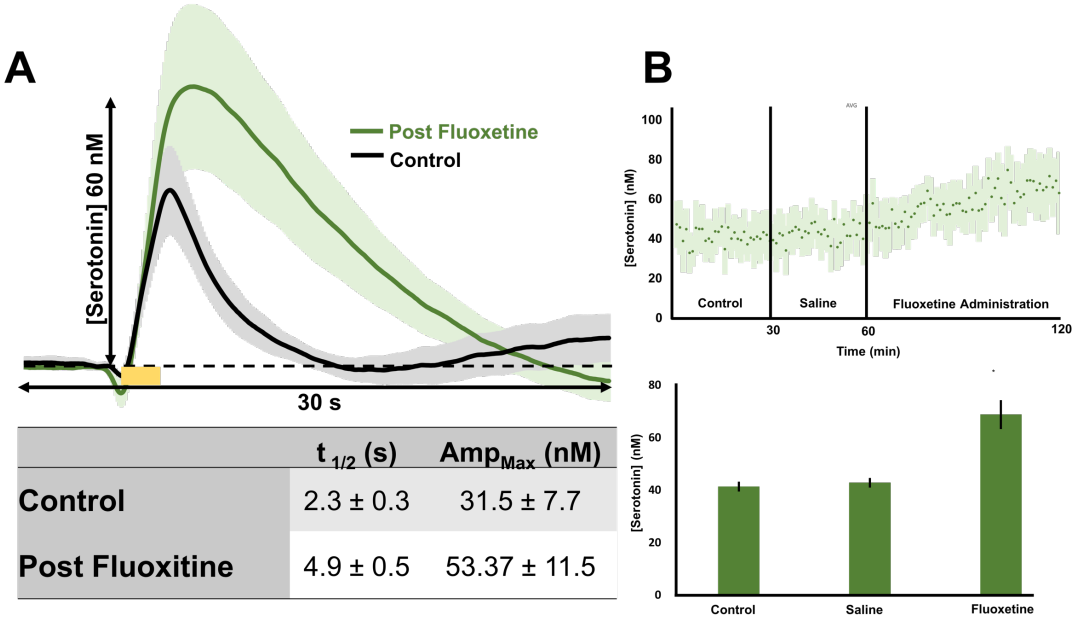

	$t_{1/2}$ (s)	Amp_{Max} (nM)
Control	2.3 ± 0.3	31.5 ± 7.7
Post Fluoxitine	4.9 ± 0.5	53.37 ± 11.5

Figure 4.3: Fluoxetine-induced changes in serotonin. (**A**) Extracellular hippocampal serotonin at baseline (black), post saline injection (grey), and post fluoxetine (*i.p.* 20 mg kg^{-1}, green) (n=5, male + female mice). (**B**) Evoked hippocampal serotonin at baseline (black) and 70+ min post fluoxetine (green). Stimulation is marked by a yellow box from 5-7 s. Statistical significance is marked by an * (p < 0.05).

Figure 4.4.A highlights a key finding that acute administration of escitalopram affects the stimulated release of serotonin in two ways: 1) $t_{1/2}$ and 2) Amp_{max} pre- and post-escitalopram. The $t_{1/2}$ significantly increased from 1.7 ± 0.1 s to 9.1 ± 1.6 s ($p < 0.05$) over 30 minutes. The Amp_{max} significantly increased from 17.4 ± 4.4 nM to 35.5 ± 10.3 nM. The combined increase in t1/2 and Amp_{max} shows that escitalopram effectively blocks SERTs to increase the extracellular levels of serotonin in the brain. However, **Figure 4.4.B** indicates that there is a robust change in ambient release of serotonin from control acquisition to 60 min after drug administration (*post-hoc* test, 48.89 ± 1.86 vs. 73.31 ± 11.82 nM 10.86 nM, $p = 0.0108$). This represents an 87% increase respect to the initial basal estimations of serotonin. Additionally, using an ANCOVA test and *post-hoc* multiple comparisons, the slopes of the time series for control and after escitalopram administration were found to be significantly different (*post-hoc* test, slope = 0.01 vs. 0.40 nM/min, $p < 0.0027$). This robust ambient change is on par with the literature trends for this commonly prescribed AD.

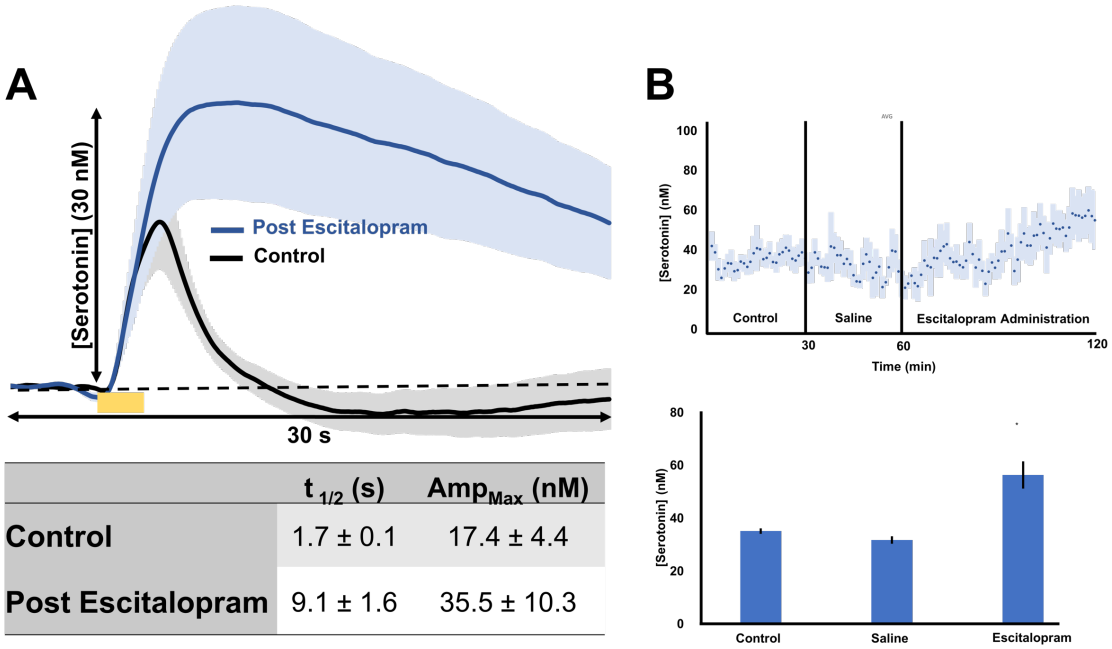

	$t_{1/2}$ (s)	Amp_{Max} (nM)
Control	1.7 ± 0.1	17.4 ± 4.4
Post Escitalopram	9.1 ± 1.6	35.5 ± 10.3

Figure 4.4: Escitalopram-induced changes in serotonin. (**A**) Extracellular hippocampal serotonin at baseline (black), post-saline injection (grey), and post-escitalopram (*i.p.* 10 mg kg^{-1}, blue) (n=10, male + female mice). (**B**) Evoked hippocampal serotonin at baseline (black) and 70+ min post escitalopram (blue). Stimulation is marked by a yellow box from 5-7 s. Statistical significance is marked by an * ($p < 0.05$).

These SSRIs show similar mechanisms on both the reuptake and ambient levels *via* our analysis of the serotonergic system. This illustrates further that most SSRIs do act similarly on a pathway. It should be noted that these two SSRIs are currently the most common ADs prescribed to depressed patients today.[45] We have shown here that these drugs are both robustly increase extracellular serotonin levels in mice models and that escitalopram is more effective at increasing basal levels, which is in line with its better clinical efficacy.

Though the frontline pharmacological therapy for depression are SSRIs they do not bring clinical relief to the majority of patients who take them. Up to 60% of the depressed population do not respond to SSRI treatments, forcing patients to either try the few atypical

ADs available or go without medication. There is no explanation for the variable efficacy of SSRIs and has led to a lull in drug discovery for alternative ADs because there is no new data to help navigate these efforts. There is now a growing body of evidence that inflammation plays an important role in this diminished clinical response[46-48]. Inflammation is a blanket term to describe a state of immune-activation[49] where immune cells prompt a biochemical cascade (e.g. cytokines) to identify and remove the source of inflammation (such as infection). An important, but largely damaging aspect of inflammation is oxidative stress[50] which is hallmarked by generation of reactive oxygen species (ROS)[50]. Oxidative stress causes significant acute and chronic macromolecular and cellular damage[50]. While this process is the subject of investigation in many chronic illnesses, oxidative stress caused by inflammation co-morbid with depression is only recently being appreciated[51].

The damaging effects of oxidative stress can be easily curtailed *via* antioxidant therapies that scavenge ROS. Therefore, there may be therapeutic potential in combining SSRI and antioxidant therapy. In conjunction with another research group, our lab has recently developed a novel antidepressant-antioxidant agent in a selenium-modified fluoxetine molecule[52]. Such drug-like chimeric compounds are designed with the aim of combining the SSRI effect of fluoxetine with the enhanced antioxidant, ROS-scavenging activity granted by selenium. We aimed to understand and evaluate the selenofluoxetine fluorinated-derivative's ability to inhibit *in vivo* serotonin reuptake in mice. We therefore present an exciting new strategy to target both serotonin and oxidative stress as the next generation of antidepressant. We do this by comparing the analogous model fluoxetine to this newly synthesized drug.

A control serotonin signal was isolated in 5 mice in the CA2 region of the hippocampus in a mixed sex cohort (**Fig. 4.5.A: blue**). After 4 control files were collected, the F-Se-derivative was administered *via i.p.* injection at 50 mg kg^{-1}. After 30 minutes, the signal was taken and averaged between the mice (**Fig. 4.5.A: orange**). Serotonin release amplitude increased from 22.73 ± 4.07 nM to 25.84 ± 3.41 nM (N.S.) and the $t_{1/2}$ of reuptake was found to significantly increase from 1.93 ± 0.30 s to 3.38 ± 0.41 s ($p < 0.05$). A further set of experiments in a separate mouse cohort was performed in the same way, however this time classic fluoxetine was administered at 20 mg kg^{-1} (**Fig 4.5.B: orange**). We found a significant amplitude increase from 35.75 ± 10.16 nM to 56.05 ± 13.40 nM and a significant $t_{1/2}$ increase from 1.90 ± 0.46 s to 4.01 ± 0.70 s ($p < 0.05$).

Fluoxetine has a more pronounced effect on the serotonin signal than the F-Se-derivative, despite the lower dose. We believe this is a consequence of two effects. Firstly, the electronegativity conferred by the oxygen group in fluoxetine plays an important role in the way the SSRI binds to the SERTs[41] Secondly, the Se-C bond could be more easily hydrolyzed than the O-C bond because the valence electrons in the Se-C bond are more shielded from the nucleus because of its size of the Se atom.[17] Nevertheless, this new agent *does* have ability to inhibit serotonin reuptake, and therefore positions this drug up as a possible therapeutic for depression. Further evidence to support the effects on serotonin reuptake of this newly developed compound is our Michaelis-Menten analysis. For both fluoxetine and the new analog, we see that the V_{max} (maximum rate of reuptake) decreases upon the administration of the agent. For fluoxetine, the V_{max} trends from 17.69 to 15.21

nM/s and for the F-Se-derivative the V_{max} trends from 15.60 to 13.46 nM/s. Thus, our new compounds show promising chemical efficacy for slowing serotonin reuptake.

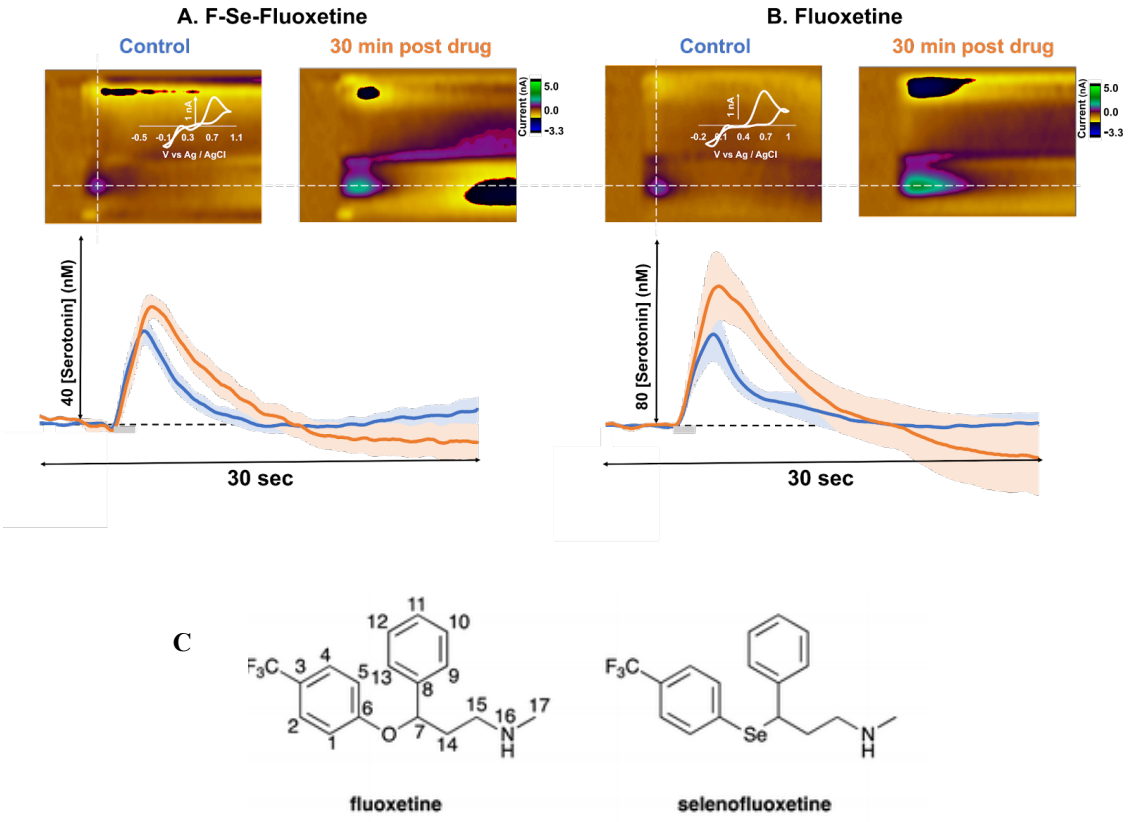

Figure 4.5. ***In Vivo*** **Stimulated Serotonin Release in the CA2 region of the hippocampus.** (A) Representative color plots for this experimental paradigm, before and 30 mins into drug analysis, are found above the representative IT curves. The averaged control evoked serotonin in mixed sex cohort can be found in blue (n = 5) with SEM calculated and outlined in the lighter shade of blue. The averaged drug files (F-Se-Fluoxetine, 50 mg kg^{-1}) at 30 mins for serotonin in mixed sex cohort is plotted in orange (n = 5) with SEM calculated and outlined in the lighter shade of orange. Stimulation is indicated via the gray bar. (B) Representative color plots for this experimental paradigm, before and 30 mins into drug analysis, are found above the representative IT curves. The averaged control evoked serotonin in mixed sex cohort can be found in blue (n = 5) with SEM calculated and outlined in the lighter shade of blue. The averaged drug files (Fluoxetine, 20 mg kg^{-1}) at 30 mins for serotonin in mixed sex cohort is plotted in orange (n = 5) with SEM calculated and outlined in the lighter shade of orange. Stimulation is indicated via the gray bar. Statistical analysis can be found for each data set in *table 4.1*. (C) Shows the molecular structure of both drugs used during this experimental procedure.

Table 4.2 Features of *in vivo* Experimental Curves

	Maximum Release (nM)	**$t_{1/2}$ of Clearance (s)**	**V_{max} (nM/s)**
Control Pre-Fluoxetine	35.75 ± 10.16	1.90 ± 0.46	17.69
30 min Post-Fluoxetine	56.05 ± 13.40*	4.01 ± 0.70*	15.21
Control Pre-1F Se-Fluoxetine	22.73 ± 4.07	1.93 ± 0.30	15.60
30 min Post-1F Se-Fluoxetine	25.84 ± 3.41	3.38 ± 0.41*	13.46

Mean ± SEM (n = 5 animals) of the maximum evoked serotonin amplitude ($Ampmax$) and clearance rate ($t_{1/2}$). Each parameter was tested for significant difference between control and drug treatment (paired samples t-test). Significance (*) was defined as $p < 0.05$. Michaelis-Menten reuptake kinetics model for serotonin was fitted to the signal. K_m was set to 5 nM, while V_{max} was optimized to fit the average experimental trace.

Norepinephrine Reuptake Inhibitors (NRIs)

NRIs are subclass of ADs that primarily inhibit norepinephrine transporter (NETs), effectively increasing extracellular concentrations norepinephrine and epinephrine. The first widely prescribed NRI was reboxetine, introduced to market in 1997: reboxetine.[53] Reboxetine has high affinity for NETs (K_m = 13.4 nM) comparted to its affinity for SERTs (K_m = 273.5), which is about 20-fold selectivity.[54] Despite this stark affinity difference, reboxetine has been shown to inhibit the serotonin reuptake.[55]

For this portion of the work, we focused on studying the direct effects of reboxetine on the serotoninergic system by, again, focusing on the reuptake dynamics *via* FSCV analysis and ambient changes *via* FSCAV analysis. We find that phasic serotonin release is altered upon administration of a sub-anesthetic dose of reboxetine (20 mg kg^{-1}), expanding the understanding of serotonin dynamics in response to a non-serotonin targeting AD.

Figure 4.6.A highlights the effect of an acute dose of reboxetine on the stimulated release of serotonin via analysis of: 1) $t_{1/2}$ and 2) Amp_{max} pre- and post-reboxetine. The $t_{1/2}$ significantly increased from 2.9 ± 0.2 s to 5.9 ± 1.5 s ($p < 0.05$). The Amp_{max} significantly increased from 44.8 ± 7.1nM to 53.4 ± 1.5 nM. This begins to illustrate the power of downstream effects on increasing serotonin in neuronal space. Additionally, **Figure 4.6.B** indicates a robust change in ambient release of serotonin from control acquisition to 60 min after drug administration (*post-hoc* test, 34.43 ± 1.08 vs. 62.43 ± 19.79 nM, $p = 0.0302$). This represents a 79% increase respect to the initial basal estimations of serotonin. Using an ANCOVA test and *post-hoc* multiple comparisons, the slopes of the time series for control and after escitalopram administration were found to be significantly different (*post-hoc* test, slope = 0.04 vs. 0.15 nM/min, $p = 0.0014$). This is on par with literature trends.

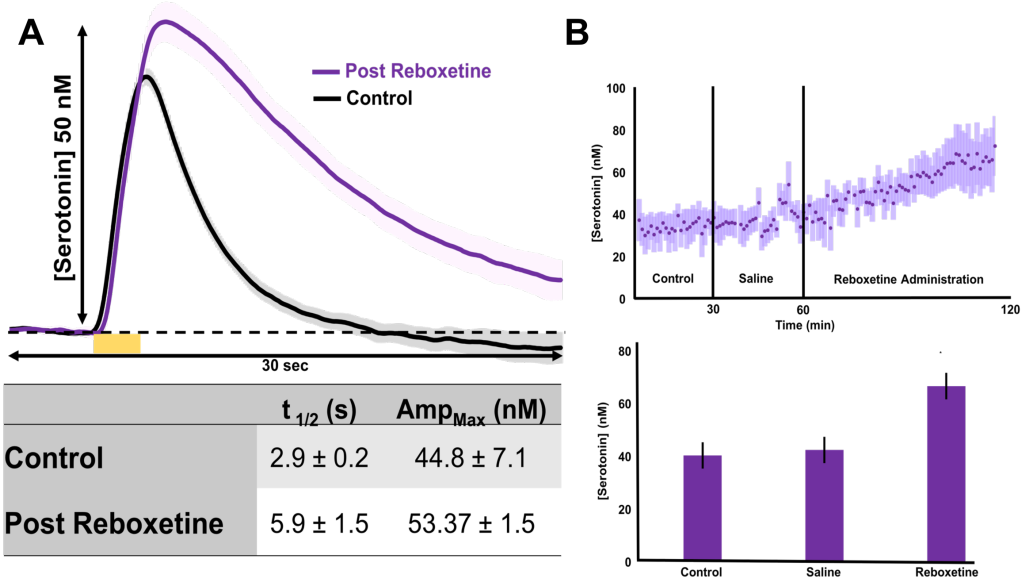

	$t_{1/2}$ (s)	Amp_{Max} (nM)
Control	2.9 ± 0.2	44.8 ± 7.1
Post Reboxetine	5.9 ± 1.5	53.37 ± 1.5

Figure 4.6: Reboxetine-induced changes in serotonin. (**A**) Extracellular hippocampal serotonin at baseline (black), post-saline injection (grey), and post-reboxetine (*i.p.* 20 mg kg^{-1}, purple) (n=5, male + female mice). (**B**) Evoked hippocampal serotonin at baseline and 70+ min post reboxitine. Stimulation is marked by yellow box from 5-7 s. Statistical significance is marked by an * ($p < 0.05$).

Modern ADs: Ketamine

Ketamine, an anesthetic, has recently been proposed to be used as an AD for patients with major depressive disorder. This drug is not used as a frontline treatment for depression, but it has been shown to be efficacious for patients that do not respond to traditional antidepressants.[56] Though ketamine has shown promise as an AD, over time its effects become less and require higher doses.[57-60] The exact mechanism in which ketamine acts as an antidepressant is not well-defined, but ketamine is a known *N*-methyl-D-aspartate (NMDA) receptor antagonist.[61] Therefore, ketamine doesn't function the same as "classical" ADs, i.e. it does not act directly on monoaminergic systems. Ketamine is known to act primarily on glutamatergic and GABAergic pathways.[62] The metabolic

products of this drug from (*R*/*S*)-ketamine to (2*R*,6*R*;2*S*,6*S*)-hydroxynorketamine has been shown to be a key feature of ketamine's effects as an AD; with the *S* enantiomer having stronger affinity for the long-lasting AD effects.[63, 64]

Most work to understand ketamine's AD effects has centered on GABA, glutamate and serotonin. So again, we investigate what an acute dose of ketamine (10 mg kg $^{-1}$) does to hippocampal serotonin both in its stimulated and ambient release. **Figure 4.7.A** highlights a key finding that after an acute dose of ketamine the $t_{1/2}$ increased from 1.8 ± 0.2 s (control, black) to 2.5 ± 0.3 s (post-drug, yellow) (NS). Since there is no significant change in uptake time pre- and post-ketamine, there is no alteration in the reuptake of serotonin back into the presynaptic neuron. Similarly, there was no significant change in the Amp_{max} from the control at 32.3 ± 10.9 nM to our post drug signal at 32.2 ± 10.2 nM, showing no change in the release of serotonin *via* electrical stimulation. However, **Figure 4.7.B** indicates there is a significant change in ambient release of serotonin from control acquisition to 60 mins after ketamine administration (*post-hoc* test 27.91 ± 0.95 vs 40.82 ± 6.97 nM, $p = 0.0001$). This represents a 46% increase with respect to the initial basal estimation of serotonin. Using an ANCOVA test and *post-hoc* multiple comparisons, the slopes of the time series for control and after ketamine administration were found to be significantly different (post-hoc test, slope = -0.05 vs. 0.26 nM/min, $p < 0.0001$). This robust increase in ambient serotonin is consistent with microdialysis work for this atypical antidepressant. Further work needs to be done to investigate the discrepancy between the stimulated and basal levels of serotonin in response to ketamine.

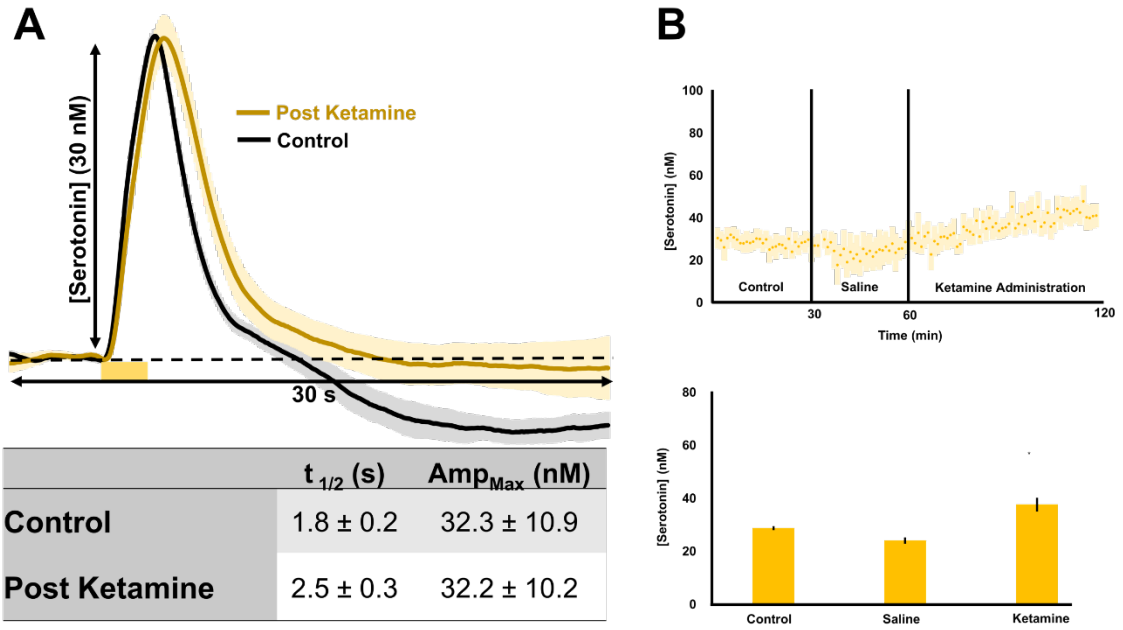

	$t_{1/2}$ (s)	Amp_{Max} (nM)
Control	1.8 ± 0.2	32.3 ± 10.9
Post Ketamine	2.5 ± 0.3	32.2 ± 10.2

Figure 4.7: Ketamine-induced changes in serotonin. (**A**) Extracellular hippocampal serotonin at baseline (black), post saline injection (grey), and post ketamine (*i.p.* 10 mg kg^{-1}, gold) (n=5, male + female mice). (**B**) Evoked hippocampal serotonin at baseline (black) and 70+ min post ketamine.

As previously stated, ketamine does not act directly on the serotonergic system and is thought to be mediated via the glutamatergic or GABAergic systems. In the following section, we explore an alternative pathway of depression via histaminergic mediation. Depression is highly comorbid with inflammation, and we have recently shown that histamine directly mediates serotonin signaling in the brain.[65, 66] Therefore, we will examine the downstream effects of ketamine on the histaminergic system in order to understand this discrepancy between stimulated and ambient hippocampal serotonin levels. In this data set, we found that systemic administration of ketamine causes rapid and sustained inhibition of hypothalamic histamine and attenuates histaminergic inhibition of serotonin. As such ketamine increases the ambient levels of serotonin in a manner

synonymous to standard SSRIs. Our results thereby help to uncover ketamine's rapid AD effects on the ambient system.

Histamine is a neurotransmitter that is thought to be related to the antithesis of serotonin. Therefore, if histamine levels increase, serotonin levels concomitantly decrease. So, it is of interest to study histaminergic changes due to the administration of ketamine. In this experimental paradigm, we again administer the same acute dose of ketamine *via* the *i.p.* cavity and monitor the changes in histamine dynamics over two hours. We saw that ketamine caused a robust and persistent decrease in evoked histamine seen in **Figure 4.8.A-C**. We saw a significant change in amplitude in control files vs drug files from 8.92 ± 1.80 μM to 6.09 ± 1.61 μM ($p = 0.005$). However, there was no significant effect on clearance rate from a control of 4.1 ± 1.1 s to a drug response of 3.3 ± 0.8 s ($p = 0.23$)**.** Overall, we saw an inhibition of evoked serotonin peak amplitude from controls: 44.70 ± 7.91 nM to post-drug files: 20.12 ± 4.88 μM ($p = 0.013$). There was a rapid and prolonged suppression of histamine all throughout data collection (100 min), and subsequent relief of the serotonin inhibition. This is indicative that ketamine indirectly inhibits the release of histamine and therefore rapidly imparts change on ambient serotonin levels.

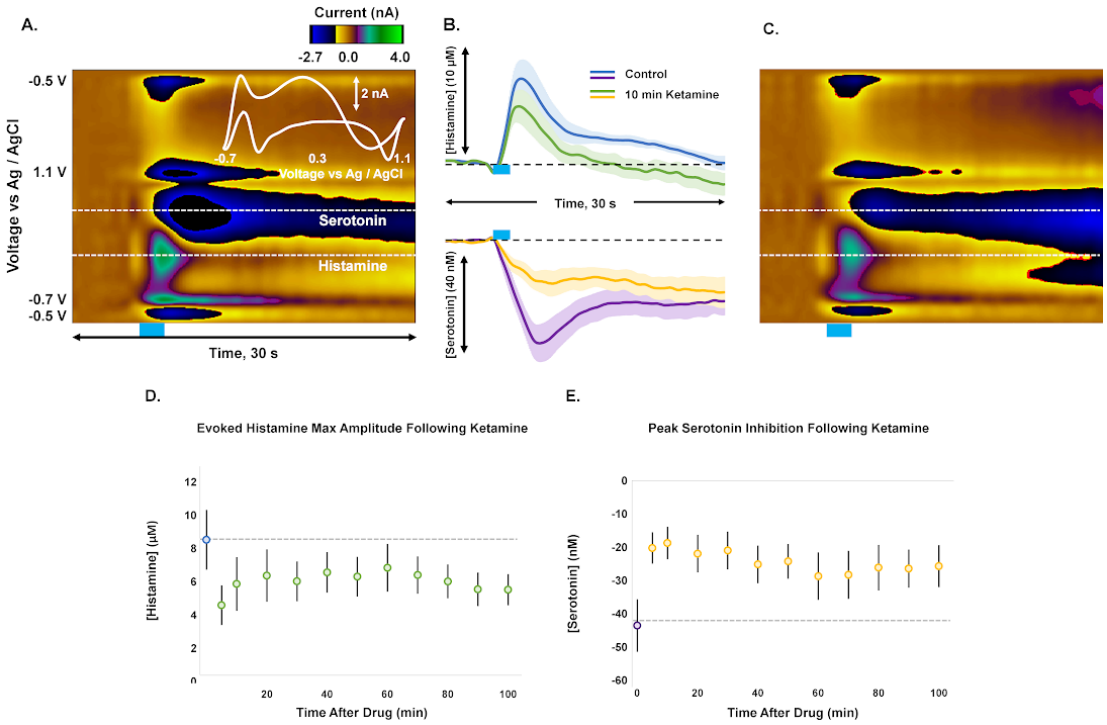

Figure 4.8. Histamine Response to Ketamine. Panel A is a representative color plot for simultaneous histamine and serotonin monitoring with the associated colorplot interlayed. **Panel B** depicts the IT curves for histamine (top) and serotonin (bottom) pre- and post-ketamine. **Panel C** shows the change in the colorplot 10 mins after drug administration. **Panel D** depicts the evoked histamine amplitude over time where **Panel E** shows the inhibition of serotonin amplitude over time.

Overall, we have shown how ketamine, at a low acute dose, has the ability to indirectly and rapidly increase serotonin. These advantageous effects of serotonin increase are thought to stem from glutamate activated Alpha-amino-3-hydroxy-5-methyl-4-isoxazole propionic acid (AMPA) receptors, increased abrineurin, activation of mammalian target of rapamycin (mTOR), inhibition of glycogen synthase kinase-3; however, it is most likely a likely a combination of all the previously mentioned.[67-69] These have all been studied and ultimately show effect to increase serotonin levels.[70] This in combination with the evidence that ketamine acts in an anti-inflammatory manner and

decreases pro-inflammatory cytokines[71] and the data presented sets ketamine as true AD agent toward serotonin.

CONCLUSIONS

In this chapter, we have given a brief history, analyzed stimulated releases and ambient changes of four classes of antidepressants effects on the serotonergic system. We have shown that these drugs all act differently on stimulated release of serotonin. But the stark takeaway is though these drugs act *via* different pathways and systems, escitalopram, fluoxetine, reboxetine and ketamine have all been shown to robustly increase concentration of basal serotonin. We have also shown the promise for a new emerging AD as well as offer a mechanism for the rapidly increase of serotonin upon ketamine administration. In **chapter 5**, we will revisit the drug's basal data sets and analyze it through a new lens. Thus, further cementing FSCAV as a versatile tool for neurochemical analysis.

Chapter 5: FSCAV Parameter Optimization for Improved Definition and Temporal Resolution of Ambient Serotonin Oscillations[1]

[1] Witt, C.E., Islam, F., Honan, L. E., Mena, S., Ou, Y., Cook, J. & Hashemi, P. FSCAV Parameter Optimization for Improved Definition and Temporal Resolution of Ambient Serotonin Oscillations. In preparation. *Analytical Methods.*

ABSTRACT

The behavior of serotonin in the brain is extensively studied because of its implication in many mood disorders, including depression. The evoked release and reuptake of this neuromodulator is well-understood, but the ambient levels of serotonin also reveal functionality and are of benefit to study and understand. Experiments using fast-scan cyclic voltammetry have shown that serotonin is more tightly regulated compared to other neurochemicals such as dopamine. The ambient concentration levels of serotonin in the extracellular space offer additional insight on their regulatory behavior and can be studied using fast-scan cyclic adsorption voltammetry (FSCAV). Preliminary *in vivo* data revealed that the ambient concentration of serotonin demonstrates distinct oscillatory patterns. A series of *in vitro* experiments where the time parameters of FSCAV were systematically adjusted were performed to improve the temporal resolution and ultimately isolate these *in vivo* oscillations from technical noise. With the aid of mathematical modeling, mechanism of oscillatory behavior is explored. Ultimately, optimized parameters of FSCAV aim to further surpass the Nyquist Limit and improve the technical noise filtering paradigm used to help further define the *in vivo* ambient regulatory patterns of serotonin.

INTRODUCTION

Mood disorders are a class of psychiatric illnesses that disrupt emotion, motivation and wellbeing over prolonged periods.[1] The most common mood disorders include the spectrum of major depressive and bipolar disorders.[1 2] The symptoms of depression are comprised of a range of emotional and physiological changes that negatively impact an individual's ability to function and complete daily activities.[1 2]

21.4% of U.S. adults have experienced depression over their lifetime and the prevalence of depression is growing.[2]

To date, diagnostics of depression is *via* a questionnaire that bases the symptomology off the defined criterion found in the DSM-5 and ultimately diagnosis is based off the discretion of a physisician.[1] There is no *current* chemical diagnostic test, unlike for many diseases of the periphery, which makes it difficult to chemically identify depression in patients.[1, 2] Diagnosed depressed patients are prescribed antidepressant therapies and often cycle through *several* antidepressants at various doses before depression symptoms are alleviated. This process often takes several months and thus the risk for harsh side effects are prolonged.[1]

To develop a diagnostic test and an improved treatment process, chemical biomarkers of depression in the brain must be investigated. However, these chemical biomarkers are difficult to identify due to the isolated and protective nature of the brain and neurotransmission.[2] Neurotransmitters act as chemical messengers when they are released by neurons at the synapse after an action potential.[3] The monoamine hypothesis of depression theorizes that an imbalance of specific neurotransmitters contributes to the pathophysiology of depression. A deficiency or excess in levels of serotonin, dopamine (DA), and/or norepinephrine (NE) can cause dysregulation in the brain and lead to the onset of depression.[3]

Serotonin is a neuromodulator, a specific type of neurotransmitter, that is released at a high volume.[2] The high-volume transmission causes spill over beyond the synaptic cleft into the extracellular space. This allows for neuromodulators to exert control over and modify several cells at one time.[2] Serotonin and DA are electroactive neuromodulators

which allows for the concentrations of serotonin and DA at the synapse and in the extracellular space to be detected using electroanalytical techniques.[2, 4, 5] Specifically, serotonin has been isolated as a possible biomarker of depression due to its efficacious nature as a pharmaceutical target.[4, 5]

The electroanalytical techniques actively used to study serotonin are Fast-Scan Cyclic Voltammetry (FSCV) and Fast-Scan Controlled Adsorption Voltammetry (FSCAV).[4, 5] Both techniques utilize the redox properties of serotonin to monitor the real-time dynamics *in vivo* and *in vitro*. A carbon-fiber microelectrode (CFM) is the niche tool in which these techniques are applied to elucidate the precarious nature of this neurochemical. FSCV is used to measure the evoked response of neurotransmitters, while FSCAV is used to measure the ambient state of neurotransmitters typically present in the extracellular space.[4, 5]

As shown in **Chapter 4**, we can employ FSCAV to monitor ambient serotonin levels after antidepressant administration. Due to the nature of the data presented, we hypothesized that these data sets may also contain oscillatory patterns that have been noted in the literature[6, 7]. Specifically, if we are to take individual electrodes, we notice individual patterns in these "oscillations" (**Figure 5.1A.**).

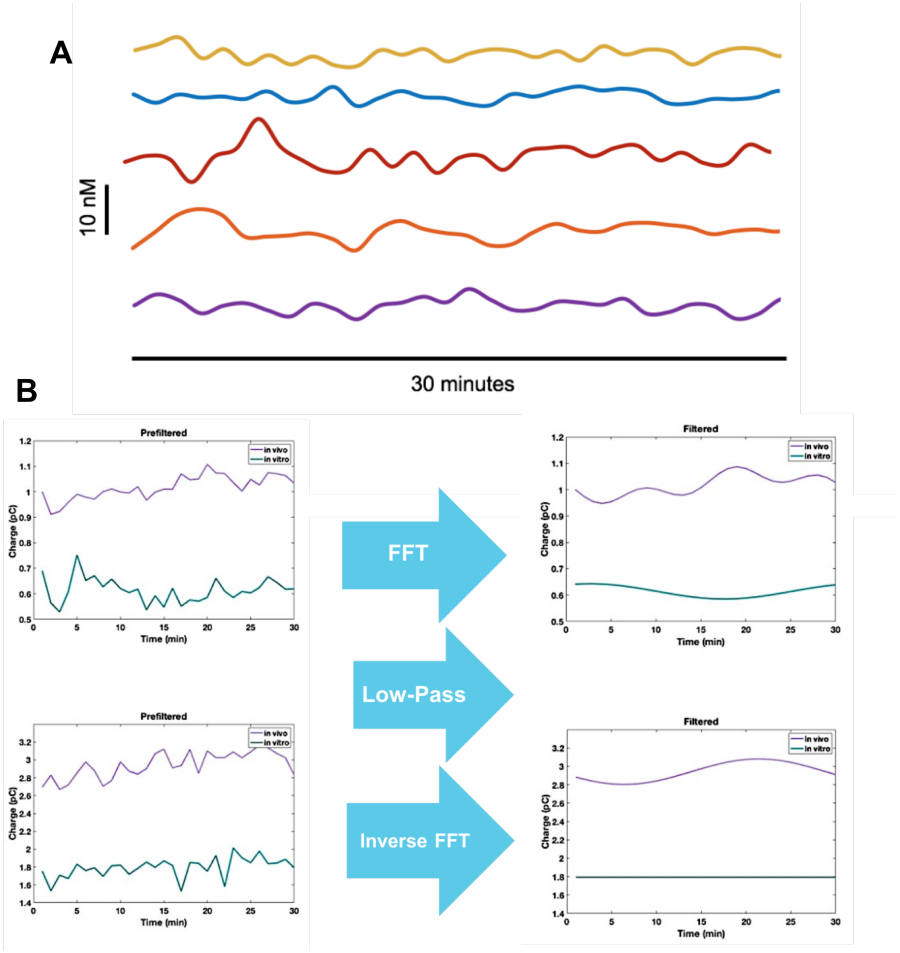

Figure 5.1: *In Vivo* FSCAV Response and Filtering (A) 5 individual serotonin responses and oscillations over time in male control mice. (B) Two separate experiments comparing the response of the same CFM in vitro in a 75 nM solution of serotonin (blue) and in vivo (purple). The plots are filtered using a low-pass filter in MATLAB *via* a fast-Fourier Transform.

In each of these cases, we conducted an FSCAV experiment to observe subtle oscillations in the ambient serotonin levels in the extracellular space. An electrode was placed in the CA2 region of the hippocampus in control mice (n = 5) and the data was collected during the mouse's light cycle; the data is displayed in **Figure 5.1.A**. This shows that there are oscillations in serotonin concentration and that these oscillations are unique for each individual mouse. We believe these oscillations are biologically relevant and hypothesize that they represent a feedback mechanism that serves to control extracellular

mechanisms. However, we need to take these experiments a step further to further confirm that we are looking at oscillations that are not an artifact of the technique. To establish the nature of the oscillations, the following experimental procedure was employed: an electrode was placed in beaker of 75 nM serotonin solution and files taken over an hour time period. This data was then analyzed and plotted in blue in **Figure 5.1.B** (pC). After the *in vitro* experiment, the same electrodes were placed into the hippocampus of an anesthetized mouse and FSCAV data of serotonin was taken *in vivo* on that animal. The *in vivo* and *in vitro* data obtained from the oscillation curves underwent a fast-Fourier transform using a low pass filter from MATLAB (see **figure 5.1**). *In vitro* the signal is relatively unchanging (blue), whereas *in vivo* (purple) we see oscillations on a ~20-minute time scale. We believe that these oscillations are due to a feedback loop defined by reuptake mechanisms and properties for serotonin. In this work, we apply this analysis to *in vivo* experiments before after antidepressant administration, we find interesting shifts that speak to feedback loops *in vivo*. However, we conclude that to find significance in our work, it would be in best interest to increase the temporal resolution of FSCAV itself.

Thus, the FSCAV technical parameters were optimized to measure ambient serotonin. To generate a more robust filtering paradigm, the technical noise of FSCAV must become more distinct. The technical noise can be characterized by its frequency and amplitude. By systematically adjusting the time parameters of FSCAV we can manipulate the frequency and amplitude of the technical noise. High frequency noise is filtered out by the low pass filter since the *in vivo* signal maintains a low frequency. Technical noise that bypasses the low-pass filter should maintain a low amplitude so that the *in vivo* signal is not obscured. This work aims to optimize the FSCAV temporal parameters by

systematically adjusting each time parameter in biologically relevant concentrations of serotonin *in vitro* to maximize the frequency and minimize the amplitude of the technical noise. The optimized FSCAV temporal parameters will allow for faster data collection in order to surpass the Nyquist Limit and define the *in vivo* ambient regulatory patterns of serotonin.

METHODOLOGY

Solutions

Dopamine hydrochloride and serotonin hydrochloride were purchased from Sigma-Aldrich (St. Louis, MO, USA). Liquion (LQ-1105, 5% by weight Nafion) was purchased from Ion Power Solutions (New Castle, DE, USA). Tris buffer solution was composed of 15 mM Tris, 140 mM NaCl, 3.25 mM KCl, 1.25 mM NaH_2PO_4, 2.0 mM Na_2SO_4, 1.2 mM $CaCl_2$, and 1.2 mM $MgCl_2$, then adjusted to pH 7.4 (all purchased from Sigma-Aldrich (St. Louis, MO, USA)). Serotonin solutions were made using serotonin hydrochloride powderand 1XTris Buffer.

CFM Fabrication

CFMs were assembled in-house by aspirating a single 7-10 μm diameter carbon fiber (T-650, Goodfellow, Coraopolis, PA, USA) into cylindrical glass capillaries (internal diameter: 0.4 mm, external diameter: 0.6 mm, A-M Systems, Carlsborg, WA, USA). The carbon-filled capillaries were positioned vertically in a micropipette puller (Narishige Group, Setagaya-Ku, Tokyo, Japan) to form a carbon−glass seal under gravity. The exposed length of the carbon fibers was then cut approximately to 150 (± 5) μm for

serotonin under an optical microscope. An electrical connection was forged to a connection pin using silver paint and a connecting wire.

Nafion Electrodepoistion: Nafion™ was electrodeposited onto the exposed carbon surface using a constant potential of +1.0 V vs Ag/AgCl applied for 30 s. The CFMs were dried at 70 °C for 10 minutes and stored for 24 hours prior to use.

FSCAV

FSCAV data collection and analyses were performed using WCCV 3.06 software (Knowmad Technologies, LLC, Tucson, AZ, USA), a Dagan potentiostat (Dagan Corporation, Minneapolis, MN, USA), and a Pine Research headstage (Pine Research Instrumentation, Durham, NC, USA). The serotonin waveform was applied scanning from 0.2 to 1.0 to -0.1 to 0.2 V at a scan rate of 1000 V/s and frequency of 100 Hz.[8, 9] The holding potential for serotonin was 0.2 V.[8, 10] The signals collected from solutions of 75 nM serotonin were processed by the same software to perform signal deconvolution, filtering, and smoothing.

Parameter Adjustments

The original FSCAV time was systematically adjusted based on the background time, controlled adsorption time, redox time and wait time. A sample size of 5 microelectrodes for each adjustment was collected for serotonin, respectively. Background time was adjusted from the original 2 s to 1 s. Controlled adsorption time was adjusted from the original 10 s to 5 s or 1 s. Redox time was adjusted from the original 18 s to 12 s or 6 s. Wait time was adjusted from the original 30 s to 15 s and 0 s. An example total file time for the adjusted 15 s Redox time parameter is 45 s (2 s + 10 s + 15 s + 30 s). Each microelectrode was used *in vitro* for 30 minutes.

Statistical Analysis: Among the electrode cohorts (n=5) for each time parameter, a two-tailed paired t-test was employed to reveal statistical significance of the data. P-values are denoted as follows: * = $p<0.05$, ** = $p<0.025$, *** = $p<0.001$

Data Processing

All data processing and analysis was performed using a custom-designed Python 3.6 code. For FSCAV signals, intervals of integration of the faradaic peak were automatically found using a local minima detection algorithm. Each interval of integration was visually inspected and corrected when the program fails to detect the faradaic peak of interest. The numerical integral between the faradaic peak and a linear baseline is calculated using the Simpson's rule.

Charge vs. time traces were filtered using a 3rd order bandpass Butterworth filter with a designed passband between 0.0008 Hz and 0.005 Hz. The low cutoff frequency was chosen to remove from consideration the low frequency drug effects on serotonin absolute concentration. The high cutoff frequency removes the noise component of the signal. Autocorrelation and sliding window correlation (SWC) using Pearson's coefficient were used to study the relationships between observations in the time series as a function of delay. The autocorrelation function, expressed in **Equation 1**, was used to calculate the correlation between pairs of samples distanced by a lag (p), where X denotes the mean value across the time series of length N. [CITE Time Series Analysis: Forecast and Control]

$$r_p = \frac{\sum_{i=1}^{N-P}(X_i-\overline{X})(X_{i+p}-\overline{X})}{\sum_{i=1}^{N}(X_i-\overline{X})^2} \qquad (1)$$

Similarly, SWC was used to study the association of fixed-length windows. **Equation 2** shows the general formulation of the correlation function between a window of length l starting at time t and another window of the same size distanced by a lag p.[11]

$$r_{t,p} = \frac{\sum_{s=t}^{t+l-1}(X_s - \overline{X_s})(X_{s+p} - \overline{X_{s+p}})}{\sqrt{(\sum_{s=t}^{t+l-1}(X_s - \overline{X_s})^2)(\sum_{s=t}^{t+l-1}(X_{s+p} - \overline{X_{s+p}})^2}} \qquad (2)$$

Autocorrelation and SWC were calculated for all possible delays to study the presence of oscillatory patterns in the time series. Correlation scores are tested for a significant difference from 0 and the highest autocorrelation obtained from random white noise and *in vitro* time series.

White noise was generated by drawing pseudo-randomized samples from a Gaussian distribution of mean 0 and standard deviation matching the mean standard deviation of all *in vivo* experiments presented in this study. The power spectral density (PSD) of time series was calculated from the fast Fourier transform spectrum using the Welch method.[12] Analysis of oscillatory patterns pre- and post-drug administration were performed by comparison of the PSD peak that corresponds to the largest oscillation pattern established with the correlation measurements.

Statistical Analyses

Statistical significance is defined as $p < 0.005$. All statistical tests are performed using Python 3.6 SciPy library[13] and MATLAB 2020b. Distribution of samples are shown as mean ± SEM. Correlation coefficients are tested to be significantly different from zero using Student's t-test and assuming time series to be non-stationary. Statistical significance of changes in the power spectrum peak was tested using Student's paired t-test.

RESULTS AND DISCUSSION

Oscillatory Changes in Response to Pharmacological Manipulations

In **Chapter 4**, we investigated the effects of antidepressants on tonic concentrations of serotonin. Above, we analyzed the oscillations in the ambient levels of serotonin to understand what might be responsible for changes in this tightly regulated system by using autocorrelation and sliding window correlation to certify that the oscillations are indeed present *in vivo*, but not *in vitro*, after filtering. Rather, the filtered *in vitro* trace is nearly identical to that observed for random white noise. Thus, this confirms that the pseudo-oscillatory pattern prior to filtering *in vitro* data can be directly equated to random white noise. However, the oscillatory pattern that remains *in vivo* following the filtering is the result of a biological phenomenon. This filtering method is detailed above in the methods section under "data processing". A representative example of this process is found in **Figure 5.2** below.

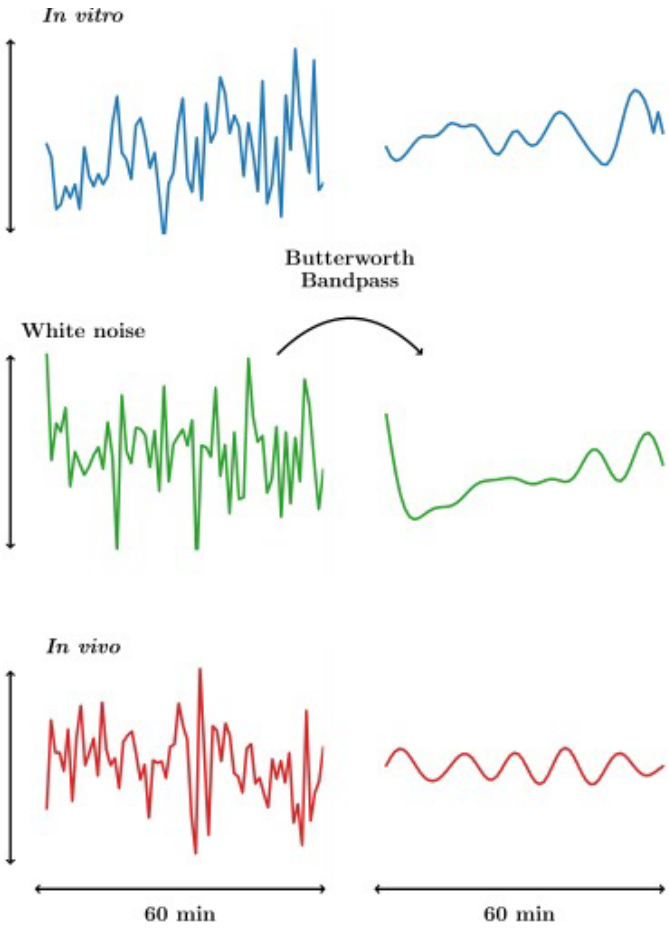

Figure 5.2: Filtering Paradigm Expanded. Blue is an example *in vitro* experiment; an electrode is placed in 75 nM of serotonin and the noise is plotted on the left. The data is then placed through a Butterworth bandpass filter and the outcome is found on the right. The same is done for random white noise (green) and in vivo data (red). After the filter is applied, the *in vitro* data has similar features to the random white noise. Whereas, the in vivo data shows distinct oscillations.

After the mathematical confirmation, we performed a power spectral analysis of the charge vs. time traces to compare the spectrum of traces pre- and post-administration of drug to see spectral changes in the oscillations. The frequency with a higher power in the spectrum was taken as the representative oscillatory frequency of the acquisition. Prior to drug administration, the serotonin oscillations are measured to have a period of 0.069 ± 0.005 min. Acquisitions following escitalopram and fluoxetine administration present a period of 0.079 ± 0.005 min, 0.085 ± 0.005 min, respectively ($F = 1.16$, $P = 0.3399$).

Following ketamine and pargyline administration the period changes to 0.071 ± 0.006 min and 0.070 ± 0.005 min respectively (F = 1.16, P = 0.3399). Finally, following reboxetine administration, the period changes to 0.066 ± 0.005 min (F = 1.16, P = 0.3399). In sum, ketamine and pargyline have a negligible effect on the frequency of serotonin oscillations, fluoxetine and escitalopram increased the frequency, and lastly, reboxetine slowed the frequency of these oscillatory patterns. Though this data set in **figure 5.7** is not statistically significant, it begins to illustrate our hypothesis for why these frequency shifts happen.

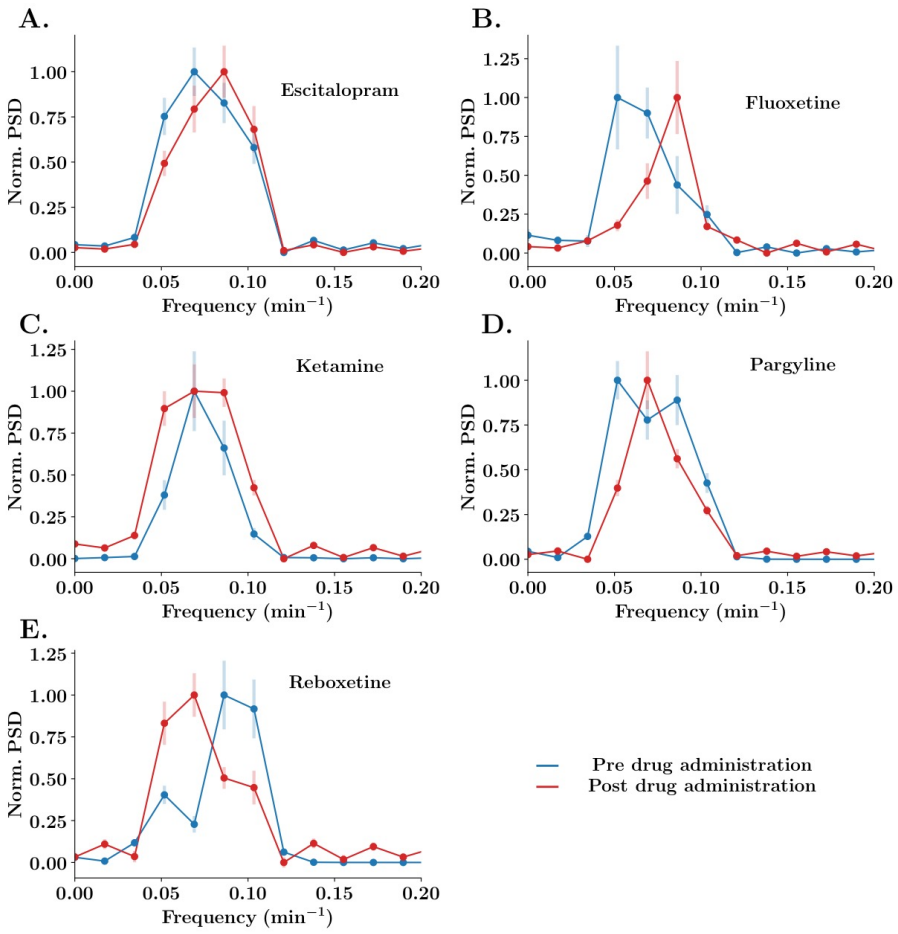

Figure 3: Oscillation Shifts to AD Administration. Shows the average ± SEM power spectra density pre- and post-acquisition for all the drug treatments stated above (n = 5 mice). A and B shows two SSRIs' effects to speed up frequency of oscillatory patterns. C and D shows two drugs that do not directly act on transporters and show no change in oscillatory patterns. E shows an NRIs' effect to slow down oscillatory patterns. Rational for these changes in patterns can be found in the sections that follow.

Briefly, biogenic amines such as serotonin are transported from the extracellular space by a variety of transporters.[14] The serotonin transporter (SERT) is a high affinity, low capacity ($uptake_1$) transporter of extracellular serotonin. Other molecules, such as the dopamine transporter (DAT), the norepinephrine transporter (NET), the plasma monoamine transporter (PMAT) and organic cation transporters (OCTs), can transport serotonin in a low affinity, high-capacity fashion ($uptake_2$). Both classes of transporters are involved in the reuptake of extracellular serotonin into the cell for degradation and recycling. In the ambient state, these transporters are acting in a delicate balance to perform this function.

As an atypical antidepressant, ketamine acts primarily through the inhibition of N-methyl-D-aspartate (NMDA) receptors and pargyline inhibits intracellular monoamine oxidase[20]. Considering that the effects of these two antidepressants do not alter the balance between the $uptake_1$ and $uptake_2$ transporters, it follows that they, in turn, do not alter the frequency of oscillation in ambient serotonin levels. This is consistent with the data set above, in **figure 3.7C & 3.7D**, which shows that there is no change in frequency pre- and post-administration of ketamine and pargyline.

However, the other drugs administered in this study, escitalopram, fluoxetine and reboxetine, directly impart their effects on these $uptake_1$ and $uptake_2$ transporters. escitalopram[21, 22] and fluoxetine[23] are SERT antagonists, meaning they are inhibiting the action of $uptake_1$ transporters. To restore balance in this environment, compensatory action is taken *via* the $uptake_2$ transporters. Considering the fact that this class of $uptake_2$ transporters functions in a high capacity, low affinity fashion, it suitably follows that the

frequency of ambient serotonin oscillations is enhanced. This is consistent with the data above, in **figure 3.7A & 3.7B**, in which these two antidepressants increased the oscillatory frequency following administration.

Finally, reboxetine is a NET antagonist that imparts its action on this uptake$_2$ transporter.[24, 25] Because this is inhibiting the activity of this low affinity, high capacity transporter class, compensatory actions of the high affinity, low capacity SERT likely occurs. It follows, then, that the frequency of oscillation would decrease with an upregulation of high affinity, low-capacity transporter activity. This is confirmed in the data in which the oscillations of ambient serotonin are slowed following administration of reboxetine in **figure 3.7E**.

In sum, these two classes of transporters are in a delicate balance in the homeostatic system, and pharmacological disruption of this balance results in subsequent alterations in serotonin steady state dynamics. In the present study, we assessed various classes of antidepressant effects on serotonin oscillations. Clinically, SSRIs are often prescribed on a "trial-and-error" basis before a pharmaceutical agent proves efficacious in alleviating symptoms.[26] This period of trial-and-error can span months before patients see any improvement in phenotypic symptoms.[27] Imbalances in extracellular serotonin are hypothesized to cause the adverse symptoms seen in depression, but the origin of this imbalance is unknown.[28] It makes sense, then, that some classes of antidepressants are particularly efficacious in some cases of depression while virtually ineffective in others because the origin of the imbalance is not identical in all cases. Thus, this data explicitly confirms that these antidepressants are variable even in their effects on ambient serotonin dynamics. Pertinent consideration of these differing effects is necessary in understanding

the clinical efficacy or inefficacy of antidepressant compounds. In addition, this phenomenon should be evaluated in screening compounds during the drug discovery process.

Ultimately, we have shown that FSCAV is powerful, versatile and able to visualize fine changes in extracellular ambient serotonin levels. Though these frequency changes are not *statistically* significant, they are *promising* for future studies. By combining the efforts to speed up the data acquisition rate we will further surpass the Nyquist limit, and thus our new sample rate will allow us to enhance the definition of oscillatory patterns in the ambient state. Proof of principle studies for speeding up the acquisition are below.

For each adjusted FSCAV time parameter, the *in vitro* signals of serotonin were plotted against time to visualize oscillations associated with the technical noise. The average frequency and amplitude were quantified from the concentration vs. time graphs for each parameter. A two-tailed t-test was conducted to determine statistical significance at p-values of 0.05, 0.025, and 0.001. The optimized FSCAV time parameter was defined as the shortest time at which frequency was maximized and amplitude was minimized when compared to the original FSCAV time parameter.

Background Time

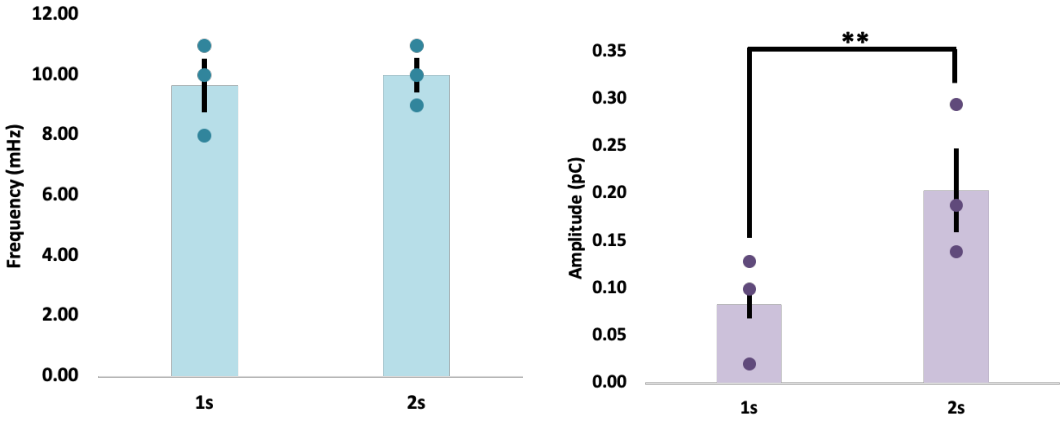

Figure 5.4: Background Time. Average technical noise frequency (blue) and amplitude (purple) for background time adjusted from 2 s to 1 s

The average frequency (blue) for 2 s background time is 10.00 ± 1.0 mHz (**Figure 5.4**). The average frequency for 1 s background time is 9.67 ± 0.9 mHz (**Figure 5.4**). The average technical noise frequency does not significantly increase or decrease when the background time is adjusted from 2 s to 1 s for serotonin. Since frequency does not change, the background time parameter may be adjusted to 1 s depending on the amplitude effects of the time adjustment. The average amplitude (purple) for 2 s background time is 0.20 ± 0.05 pC (**Figure 5.4**). The average amplitude for 1 s background time is 0.08 ± 0.03 pC (**Figure 5.4**). The amplitude of the technical noise significantly decreases when the background time is adjusted to 1 s. Because amplitude is minimized and frequency is maintained at a maximum, the FSCAV background time for serotonin can definitively be reduced to 1 s.

Controlled Adsorption Time

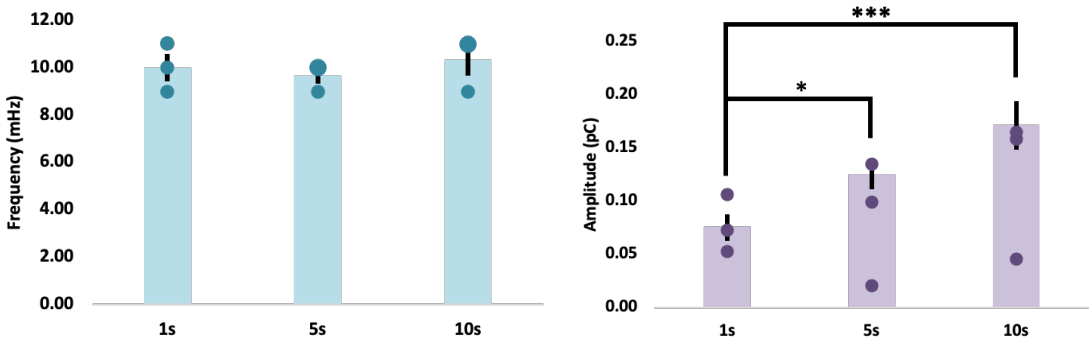

Figure 5.5: Controlled Adsorption Time. Average technical noise frequency (blue) and amplitude (purple) for controlled adsorption time adjusted from 10 s to 5 s and 1 s

The average frequency (blue) for 10 s controlled adsorption time is 10.33 ± 1.1 mHz. The average frequency for 5 s controlled adsorption time is 9.67 ± 0.9 mHz, the average frequency for 1 s controlled adsorption time is 10.00 ± 1.0 mHz (**Figure 5.5**). The average technical noise frequency does not significantly change when the controlled adsorption time is adjusted from 10 s to 1 s for serotonin. Since frequency is not significantly affected, the controlled adsorption time parameter may be adjusted to 1 s depending on the amplitude effects of the time adjustment. The average amplitude (purple) for 10 s controlled adsorption time is 0.17 ± 0.09 pC, the average amplitude for 5 s controlled adsorption time is 0.13 ± 0.09 pC, the average amplitude for 1 s controlled adsorption time is 0.08 ± 0.03 pC (**Figure 5.5**). The amplitude of the technical noise significantly decreases when the controlled adsorption time is adjusted to 1 s. Because amplitude is minimized and frequency is maintained at a maximum, the FSCAV controlled adsorption time for serotonin can be reduced to 1 s. It is important to note that during controlled adsorption time, serotonin must reach an equilibrium concentration when adsorbed onto the surface of the microelectrode. A series of flow injection analysis

experiments must be conducted *in vitro* to verify that maximum adsorption can be reached within 1 s before the time parameter is modified for *in vivo* experiments.

Redox Time

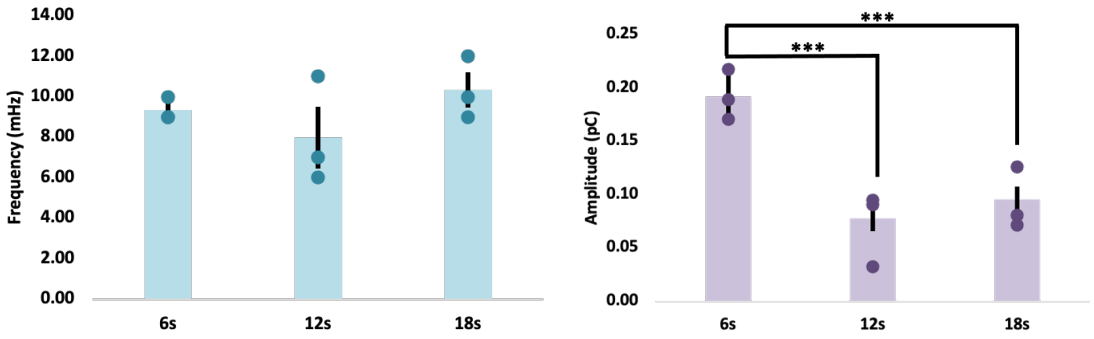

Figure 5.6: REDOX Time. Average technical noise frequency (blue) and amplitude (purple) for redox time adjusted from 18 s to 12 s and 6 s

The average frequency (blue) for 18 s redox time is 10.33 ± 1.5 mHz, average frequency for 12 s redox time is 8.00 ± 3.6 mHz and for 6 s redox time is 9.33 ± 0.8 mHz (**Figure 5.6**). The average technical noise frequency does not significantly change when the redox time is adjusted from 18 s to 12s or 6 s for serotonin. Since frequency is not significantly affected, the controlled adsorption time parameter may be adjusted depending on the amplitude effects of the time adjustment. The average amplitude (purple) for 18 s redox time is 0.10 ± 0.01 pC, for 12 s redox time is 0.9 ± 0.02 pC and for 6 s redox time is 0.19 ± 0.04 pC (**Figure 5.6**). The amplitude of the technical noise is significantly increased when the redox time is adjusted to 6 s. The amplitude does not significantly change when the redox time is adjusted to 12 s. Because amplitude is minimized and frequency is maintained at a maximum at 12 s redox time, the FSCAV redox time for serotonin can be reduced to 12 s.

Wait Time

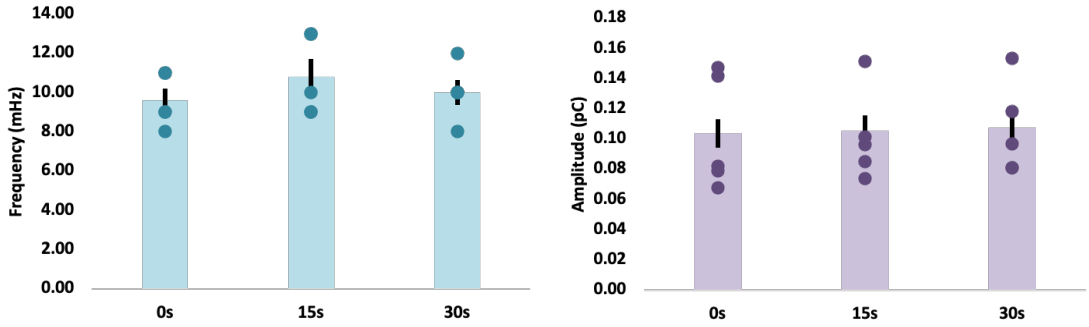

Figure 5.7: Wait Time. Average technical noise frequency (blue) and amplitude (purple) for wait time adjusted from 30 s to 15 s and 0 s

The average frequency (blue) for 30 s wait time is 10.00 ± 1.9 mHz (**Figure 5.7**). The average frequency for 15 s wait time is 10.80 ± 2.1 mHz (**Figure 5.7**). The average frequency for 0 s wait time is 9.60 ± 1.7 mHz (**Figure 5.7**). The average technical noise frequency does not significantly change when the wait time is adjusted from 30 s to 15 s or 0 s for serotonin. Since frequency is not significantly altered, so the wait time parameter may be adjusted depending on the amplitude effects of the time adjustment. The average amplitude for 30 s wait time is 0.11 ± 0.04 pC (**Figure 5.7**). The average amplitude for 15 s wait time is 0.10 ± 0.04 pC (**Figure 5.7**). The average amplitude (purple) for 0 s wait time is 0.10 ± 0.03 pC (**Figure 5.7**). The amplitude of the technical noise is maintained at a minimum across all time adjustments. The amplitude does not significantly change when the wait is adjusted to 0 s. Because amplitude is minimized and frequency is maintained at a maximum at 30 s, the FSCAV wait time for serotonin can be eliminated.

Optimized File Times for Serotonin

A total optimized FSCAV file time was determined for serotonin. The background time was reduced to 1 s, the controlled adsorption time was reduced to 1 s, the redox time was reduced to 12 s and the wait time was reduced to 0 s.

CONCLUSIONS

We can tease out fundamental differences in serotonin patterns—thus alluding to transporter class mediation of steady state serotonin. The temporal resolution of FSCAV can be increased for serotonin through the optimization of background, controlled adsorption, redox and wait time parameters. Compared to the original FSCAV file time of 60 seconds our new optimized time is 14 secs, trimming over 3/4ths of the time of the original data acquisition time. Ultimately, the optimized file times will allow for faster data collection and will improve definition of the ambient regulatory patterns for serotonin by further surpassing the Nyquist limit.

.

Chapter 6: Conclusions and Outlook

FSCV and FSCAV are advantageous platforms for understanding neuronal communication and to aid in answering fundamental questions about the brain. These techniques have shown promise to probe discrete changes in neurochemicals due to their biocompatibility, rapid data acquisition, selectivity and sensitivity. Over the years, most of the information about neuronal commutation has centered on monitoring the rapid-fire, phasic changes in neurotransmission. Recently, tools like FSCAV have been developed to probe the delicate homeostatic state of the central nervous system to eavesdrop on the natural tonic state. In this dissertation, we have positioned fast-voltammetry as a unique technique to understand ambient dynamics of the serotonergic system.

In **Chapter 2**, we confirmed the formation of an auspicious gluatmate layer formed on our electrodes surface due to the i*n vivo* environment. We confirmed this voltammetrically, spectrally and microscopically. We then applied this new, confirmed coating in order to get a two-fold increase in our serotonin stimulated detection. Ultimately, we have shown that these improvements to sensitivity our due to the complex extracellular matrix. However, we note that glutamate contributes to this robust change, however this neuromodulator is *most likely* not the only contributor. This is explored further **chapter 3**.

In **Chapter 3**, we describe novel and robust amino acid surface treatment and alleviate shortcomings of serotonin detection with FSCAV. In short, we show that by electrochemically pre-treating the electrode surface in a biologically relevant matrix, we improve upon the equilibrium time before ambient data acquisition. Ultimately, this has

made FSCAV to be more user-friendly, giving it the opportunity for it to be more widely used.

In **Chapter 4**, we investigated classical, modern and novel antidepressant treatments on the serotonergic system. We compared stimulated and basal data upon drug administration and saw that no matter the pathway of action, there are direct or downstream effects on serotonin We also explored the downstream effects of ketamine administration on the histaminergic system. Finally, we showed the promise for a novel drug, selenium-fluoxetine, as an alternative antidepressant treatment *via* phasic release.

In **Chapter 5**, we utilized FSCAV to understand the regulatory mechanisms of ambient serotonin oscillations. We introduce FSCAV as a tool to understand the tight regulatory processes of serotonin oscillations. We first verified that FSCAV does indeed detect small fluctuations in ambient serotonin levels. We proposed a rationale for these tight fluctuations in ambient serotonin *via* pharmacological and mathematical manipulations and show that ambient levels are heavily regulated by reuptake transporters. Upon confirmation, we set to improve our data acquisition time to better define these changes. We systemically confirmed that we can improve the temporal resolution of FSCAV from 60 s to 14 s files.

Our future plans for the continuation of this work are three-fold:

1. Continue efforts to improve FSCAV data collection with further surface modification to the CFMs s and applying them to *in vivo* analysis.
2. Understand the fundamental changes to ambient serotonin upon the administration of pargyline.

3. Verify and utilize optimized FSCAV data acquisition time and apply *in vivo* to better understand and probe biological oscillations of serotonin.

Overall, this dissertation has setup FSCAV as a powerful and versatile method for ambient analysis of the serotonin system. We have improved this technique *via* surface modification and acquisition time, and have probed and pharmacologically manipulated the serotonergic pathway to understand underlying mechanisms of control. These fundamental studies have ultimately improved analysis of ambient serotonin, and in doing so, we have laid the groundwork to answer fundamental biological questions in the future.

Bibliography

Chapter 1 References

1. Artigas, F.; Martínez, E.; Camón, L.; Rodríguez Farré, E., Synthesis and Utilization of Neurotransmitters: Actions of Subconvulsant Doses of Hexachlorocyclohexane Isomers on Brain Monoamines. *Toxicology* **1988,** *49* (1), 49-55.
2. Südhof, T. C., Calcium Control of Neurotransmitter Release. *Cold Spring Harb Perspect Biol* **2012,** *4* (1), a011353-a011353.
3. Battezzati, A.; Riso, P., Amino Acids: Fuel, Building Blocks for Proteins, and Signals. *Nutrition (Burbank, Los Angeles County, Calif.)* **2002,** *18* (9), 773-4.
4. Dalangin, R.; Kim, A.; Campbell, R. E., The Role of Amino Acids in Neurotransmission and Fluorescent Tools for Their Detection. *Int J Mol Sci* **2020,** *21* (17), 6197.
5. Meldrum, B., Amino Acid Neurotransmitters and New Approaches to Anticonvulsant Drug Action. *Epilepsia* **1984,** *25 Suppl 2*, S140-9.
6. Kress, G. J.; Mennerick, S., Action Potential Initiation and Propagation: Upstream Influences on Neurotransmission. *Neuroscience* **2009,** *158* (1), 211-222.
7. Wu, Y. W.; Grebenyuk, S.; McHugh, T. J.; Rusakov, D. A.; Semyanov, A., Backpropagating Action Potentials Enable Detection of Extrasynaptic Glutamate by NMDA Receptors. *Cell Reports* **2012,** *1* (5), 495-505.
8. Nam, H. W.; McIver, S. R.; Hinton, D. J.; Thakkar, M. M.; Sari, Y.; Parkinson, F. E.; Haydon, P. G.; Choi, D. S., Adenosine and Glutamate Signaling in Neuron-glial Interactions: Implications in Alcoholism and Sleep Disorders. *Alcoholism, Clinical and Experimental Research* **2012,** *36* (7), 1117-25.
9. Somogyi, J., Differences in Ratios of GABA, Glycine and Glutamate Immunoreactivities in Nerve Terminals on Rat Hindlimb Motoneurons: A Possible Source of Post-synaptic Variability. *Brain Research Bulletin* **2002,** *59* (2), 151-61.
10. Burger, P. M.; Hell, J.; Mehl, E.; Krasel, C.; Lottspeich, F.; Jahn, R., GABA and Glycine in Synaptic Vesicles: Storage and Transport Characteristics. *Neuron* **1991,** *7* (2), 287-293.
11. Fagg, G. E., l-Glutamate, Excitatory Amino Acid Receptors and Brain Function. *Trends in Neurosciences* **1985,** *8*, 207-210.
12. Purkayastha, P.; Malapati, A.; Yogeeswari, P.; Sriram, D., A Review on GABA/Glutamate Pathway for Therapeutic Intervention of ASD and ADHD. *Current Medicinal Chemistry* **2015,** *22* (15), 1850 - 59.
13. Schousboe, A.; Scafidi, S.; Bak, L. K.; Waagepetersen, H. S.; McKenna, M. C., Glutamate Metabolism in the Brain Focusing on Astrocytes. *Springer International Publishing*: Cham, 2014; pp 13-30.
14. Kinoshita, P. F.; Leite, J. A.; Orellana, A. M. M.; Vasconcelos, A. R.; Quintas, L. E. M.; Kawamoto, E. M.; Scavone, C., The Influence of Na(+), K(+)-ATPase on

Glutamate Signaling in Neurodegenerative Diseases and Senescence. *Frontiers Physiology* **2016,** *7*, 195-195.
15. Stuart, G.; Spruston, N.; Sakmann, B.; Häusser, M., Action potential initiation and backpropagation in neurons of the mammalian CNS. *Trends Neuroscience* **1997,** *20* (3), 125-31.
16. Vreeland, R. F.; Atcherley, C. W.; Russell, W. S.; Xie, J. Y.; Lu, D.; Laude, N. D.; Porreca, F.; Heien, M. L., Biocompatible PEDOT:Nafion Composite Electrode Coatings for Selective Detection of Neurotransmitters In Vivo. *Analytical Chemistry* **2015,** *87* (5), 2600-2607.
17. Roberts, J. G.; Toups, J. V.; Eyualem, E.; McCarty, G. S.; Sombers, L. A., In Situ Electrode Calibration Strategy for Voltammetric Measurements In Vivo. *Analytical Chemistry* **2013,** *85* (23), 11568-75.
18. Ewing, A. G.; Dayton, M. A.; Wightman, R. M., Pulse Voltammetry with Microvoltammetric Electrodes. *Analytical Chemistry* **1981,** *53* (12), 1842-1847.
19. Harreither, W.; Trouillon, R.; Poulin, P.; Neri, W.; Ewing, A. G.; Safina, G., Carbon Nanotube Fiber Microelectrodes Show a Higher Resistance to Dopamine Fouling. *Analytical Chemistry* **2013,** *85* (15), 7447-53.
20. Logman, M. J.; Budygin, E. A.; Gainetdinov, R. R.; Wightman, R. M., Quantitation of In Vivo Measurements with Carbon Fiber Microelectrodes. *Journal of Neuroscience Methods* **2000,** *95* (2), 95-102.
21. Jackson, B. P.; Dietz, S. M.; Wightman, R. M., Fast-Scan Cyclic Voltammetry of 5-hydroxytryptamine. *Analytical Chemistry* **1995,** *67* (6), 1115-1120.
22. Schildkraut, J. J., The Catecholamine Hypothesis of Affective Disorders: A Review of Supporting Evidence. *The American Journal of Psychiatry* **1965,** *122* (5), 509-22.
23. Ferguson, J. M., SSRI Antidepressant Medications: Adverse Effects and Tolerability. *Primary Care Companion Journal of Clinical Psychiatry* **2001,** *3* (1), 22-27.
24. Hillhouse, T. M.; Porter, J. H., A Brief History of the Development of Antidepressant Drugs: From Monoamines to Glutamate. *Experimental and Clinical Psychopharmacology* **2015,** *23* (1), 1-21.
25. Walker, F. R., A Critical Review of the Mechanism of Action for the Selective Serotonin Reuptake Inhibitors: Do These Drugs Possess Anti-inflammatory Properties and How Relevant is this in the Treatment of Depression? *Neuropharmacology* **2013,** *67*, 304-17.
26. Schmidt, F. M.; Sander, C.; Dietz, M. E.; Nowak, C.; Schröder, T.; Mergl, R.; Schönknecht, P.; Himmerich, H.; Hegerl, U., Brain Arousal Regulation as Response Predictor for Antidepressant Therapy in Major Depression. *Scientific Reports* **2017,** *7*, 45187.
27. Anderson, I. M., SSRIS Versus Tricyclic Antidepressants in Depressed Inpatients: a Meta-Analysis of Efficacy and Tolerability. *Depression and Anxiety* **1998,** 11-7.
28. Sangare, A.; Dubourget, R.; Geoffroy, H.; Gallopin, T.; Rancillac, A., Serotonin Differentially Modulates Excitatory and Inhibitory Synaptic Inputs to Putative Sleep-Promoting Neurons of the Ventrolateral Preoptic Nucleus. *Neuropharmacology* **2016,** *109*, 29-40.
29. Liu, C.; Meng, Z.; Wiggin, T. D.; Yu, J.; Reed, M. L.; Guo, F.; Zhang, Y.; Rosbash, M.; Griffith, L. C., A Serotonin-Modulated Circuit Controls Sleep Architecture

to Regulate Cognitive Function Independent of Total Sleep in Drosophila. *Current Trends in Biology* **2019,** *29* (21), 3635-3646.e5.
30. Nakamaru-Ogiso, E.; Miyamoto, H.; Hamada, K.; Tsukada, K.; Takai, K., Novel Biochemical Manipulation of Brain Serotonin Reveals a Role of Serotonin in the Circadian Rhythm of Sleep-wake Cycles. *The European Journal of Neuroscience* **2012,** *35* (11), 1762-70.
31. Karayol, R.; Medrihan, L.; Warner-Schmidt, J. L.; Fait, B. W.; Rao, M. N.; Holzner, E. B.; Greengard, P.; Heintz, N.; Schmidt, E. F., Serotonin Receptor 4 in the Hippocampus Modulates Mood and Anxiety. *Molecular Psychiatry* **2021**.
32. Gillihan, S. J.; Rao, H.; Wang, J.; Detre, J. A.; Breland, J.; Sankoorikal, G. M. V.; Brodkin, E. S.; Farah, M. J., Serotonin Transporter Genotype Modulates Amygdala Activity During Mood Regulation. *Social Cognitive and Affective Neuroscience* **2010,** *5* (1), 1-10.
33. Bari, A.; Theobald, D. E.; Caprioli, D.; Mar, A. C.; Aidoo-Micah, A.; Dalley, J. W.; Robbins, T. W., Serotonin Modulates Sensitivity to Reward and Negative Feedback in a Probabilistic Reversal Learning Task in Rats. *Neuropsychopharmacology* **2010,** *35* (6), 1290-1301.
34. Wargent, E. T.; Martin-Gronert, M. S.; Cripps, R. L.; Heisler, L. K.; Yeo, G. S. H.; Ozanne, S. E.; Arch, J. R. S.; Stocker, C. J., Developmental Programming of Appetite and Growth in Male Rats Increases Hypothalamic Serotonin (5-HT)5A Receptor Expression and Sensitivity. *International Journal of Obesity* **2020,** *44* (9), 1946-1957.
35. Kinney, M. P.; Panting, N. D.; Clark, T. M., Modulation of Appetite and Feeding Behavior of the Larval Mosquito Aedes aegypti by the Serotonin-selective Reuptake Inhibitor Paroxetine. *Journal of Experimental Biology* **2014,** *217* (6), 935-943.
36. Halford, J. C. G.; Harrold, J. A., 5-HT2C Receptor Agonists and the Control of Appetite. *Appetite Control*, Joost, H.-G., Ed. Springer Berlin Heidelberg: Berlin, Heidelberg, 2012; pp 349-356.
37. Nichols, D. E.; Nichols, C. D., Serotonin Receptors. *Chemical Reviews* **2008,** *108* (5), 1614-1641.
38. Wood, K. M.; Zeqja, A.; Nijhout, H. F.; Reed, M. C.; Best, J.; Hashemi, P., Voltammetric and Mathematical Evidence for Dual Transport Mediation of Serotonin Clearance In Vivo. *Journal of Neurochemistry* **2014,** *130* (3), 351-359.
39. Shaskan, E. G.; Snyder, S. H., Kinetics of Serotonin Accumulation Into Slices from Rat Brain: Relationship to Catecholamine Uptake. *The Journal of Pharmacology and Experimental Therapeutics* **1970,** *175* (2), 404-18.
40. Horton, R. E.; Apple, D. M.; Owens, W. A.; Baganz, N. L.; Cano, S.; Mitchell, N. C.; Vitela, M.; Gould, G. G.; Koek, W.; Daws, L. C., Decynium-22 Enhances SSRI-induced Antidepressant-like Effects in Mice: Uncovering Novel Targets to Treat Depression. *The Journal of Neuroscience* **2013,** *33* (25), 10534-43.
41. Daws, L. C.; Koek, W.; Mitchell, N. C., Revisiting Serotonin Reuptake Inhibitors and the Therapeutic Potential of "Uptake-2" in Psychiatric Disorders. *ACS Chemical Neuroscience* **2013,** *4* (1), 16-21.
42. Prah, A.; Purg, M.; Stare, J.; Vianello, R.; Mavri, J., How Monoamine Oxidase A Decomposes Serotonin: An Empirical Valence Bond Simulation of the Reactive Step. *The Journal of Physical Chemistry B* **2020,** *124* (38), 8259-8265.

43. Cakir, K.; Erdem, S. S.; Atalay, V. E., ONIOM Calculations on Serotonin Degradation by Monoamine Oxidase B: Insight into the Oxidation Mechanism and Covalent Reversible Inhibition. *Organic & Biomolecular Chemistry* **2016,** *14* (39), 9239-9252.
44. Hashemi, P.; Dankoski, E. C.; Lama, R.; Wood, K. M.; Takmakov, P.; Wightman, R. M., Brain Dopamine and Serotonin Differ in Regulation and Its Consequences. *Proceedings of the National Academy of Sciences of the United States of America* **2012,** *109* (29), 11510-5.
45. Bel, N.; Artigas, F., Modulation of the Extracellular 5-Hydroxytryptamine Brain Concentrations by the Serotonin and Noradrenaline Reuptake Inhibitor, Milnacipran Microdialysis Studies in Rats. *Neuropsychopharmacology* **1999,** *21* (6), 745-754.
46. Gardier, A. M., Antidepressant Activity: Contribution of Brain Microdialysis in Knock-out Mice to the Understanding of BDNF/5-HT Transporter/5-HT Autoreceptor Interactions. *Frontiers in pharmacology* **2013,** *4*, 98.
47. Ruda-Kucerova, J.; Amchova, P.; Havlickova, T.; Jerabek, P.; Babinska, Z.; Kacer, P.; Syslova, K.; Sulcova, A.; Sustkova-Fiserova, M., Reward Related Neurotransmitter Changes in a Model of Depression: An In Vivo Microdialysis Study. *The World Journal of Biological Psychiatry* **2015,** *16* (7), 521-35.
48. Jacobsen, J. P. R.; Siesser, W. B.; Sachs, B. D.; Peterson, S.; Cools, M. J.; Setola, V.; Folgering, J. H. A.; Flik, G.; Caron, M. G., Deficient Serotonin Neurotransmission and Depression-like Serotonin Biomarker Alterations in Tryptophan Hydroxylase 2 (Tph2) Loss-of-function Mice. *Molecular Psychiatry* **2012,** *17* (7), 694-704.
49. Wiedholz, L. M.; Owens, W. A.; Horton, R. E.; Feyder, M.; Karlsson, R. M.; Hefner, K.; Sprengel, R.; Celikel, T.; Daws, L. C.; Holmes, A., Mice Lacking the AMPA GluR1 Receptor Exhibit Striatal Hyperdopaminergia and 'Schizophrenia-related' Behaviors. *Molecular Psychiatry* **2008,** *13* (6), 631-40.
50. Koek, W.; Sandoval, T. L.; Daws, L. C., Effects of the Antidepressants Desipramine and Fluvoxamine on Latency to Immobility and Duration of Immobility in the Forced Swim Test in Adult Male C57BL/6J Mice. *Behavavioral Pharmacology* **2018,** *29* (5), 453-456.
51. Bowman, M. A.; Vitela, M.; Clarke, K. M.; Koek, W.; Daws, L. C., Serotonin Transporter and Plasma Membrane Monoamine Transporter Are Necessary for the Antidepressant-Like Effects of Ketamine in Mice. *International Journal of Molecular Science* **2020,** *21* (20), 7581.
52. Hashemi, P.; Dankoski, E. C.; Petrovic, J.; Keithley, R. B.; Wightman, R. M., Voltammetric Detection of 5-Hydroxytryptamine Release in the Rat Brain. *Analytical Chemistry* **2009,** *81* (22), 9462-9471.
53. Lama, R. D.; Charlson, K.; Anantharam, A.; Hashemi, P., Ultrafast Detection and Quantification of Brain Signaling Molecules with Carbon Fiber Microelectrodes. *Analytical Chemistry* **2012,** *84* (19), 8096-8101.
54. Wood, K. M.; Hashemi, P., Fast-Scan Cyclic Voltammetry Analysis of Dynamic Serotonin Reponses to Acute Escitalopram. *ACS Chemical Neuroscience* **2013,** *4* (5), 715-720.

55. Atcherley, C. W.; Wood, K. M.; Parent, K. L.; Hashemi, P.; Heien, M. L., The Coaction of Tonic and Phasic Dopamine Dynamics. *Chemical Communications (Camb)* **2015,** *51* (12), 2235-2238.
56. Abdalla, A.; Atcherley, C. W.; Pathirathna, P.; Samaranayake, S.; Qiang, B.; Peña, E.; Morgan, S. L.; Heien, M. L.; Hashemi, P., In Vivo Ambient Serotonin Measurements at Carbon-Fiber Microelectrodes. *Analytical Chemistry* **2017,** *89* (18), 9703-9711.
57. Saylor, R. A.; Hersey, M.; West, A.; Buchanan, A. M.; Berger, S. N.; Nijhout, H. F.; Reed, M. C.; Best, J.; Hashemi, P., Corrigendum: In Vivo Hippocampal Serotonin Dynamics in Male and Female Mice: Determining Effects of Acute Escitalopram Using Fast Scan Cyclic Voltammetry. *Frontiers in Neuroscience* **2019,** *13*, 726-726.
58. Abdalla, A.; West, A.; Jin, Y.; Saylor, R. A.; Qiang, B.; Peña, E.; Linden, D. J.; Nijhout, H. F.; Reed, M. C.; Best, J.; Hashemi, P., Fast Serotonin Voltammetry as a Versatile Tool for Mapping Dynamic Tissue Architecture: I. Responses at Carbon Fibers Describe Local Tissue Physiology. *Journal of Neurochemistry* **2020,** *153* (1), 33-50.
59. Yang, H.; Sampson, M. M.; Senturk, D.; Andrews, A. M., Sex- and SERT-Mediated Differences in Stimulated Serotonin Revealed by Fast Microdialysis. *ACS Chemical Neuroscience* **2015,** *6* (8), 1487-1501.
60. Yang, H.; Thompson, A. B.; McIntosh, B. J.; Altieri, S. C.; Andrews, A. M., Physiologically Relevant Changes in Serotonin Resolved by Fast Microdialysis. *ACS Chemical Neuroscience* **2013,** *4* (5), 790-8.
61. Cowen, P. J.; Browning, M., What Has Serotonin to do with Depression? *World Psychiatry* **2015,** *14* (2), 158-160.
62. Albert, P. R.; Benkelfat, C., The Neurobiology of Depression--Revisiting the Serotonin Hypothesis. II. Genetic, Epigenetic and Clinical Studies. *Philoslophy Translantic Royal Society of Lond B Biological Sciences* **2013,** *368* (1615), 20120535-20120535.
63. Simon, L. V.; Keenaghan, M., Serotonin Syndrome. In *StatPearls*, StatPearls Publishing Copyright © 2021, StatPearls Publishing LLC.: Treasure Island (FL), 2021.
64. Francescangeli, J.; Karamchandani, K.; Powell, M.; Bonavia, A., The Serotonin Syndrome: From Molecular Mechanisms to Clinical Practice. *International Journal Molecular Science* **2019,** *20* (9), 2288.
65. Berg, K. A.; Clarke, W. P.; Cunningham, K. A.; Spampinato, U., Fine-tuning Serotonin2c Receptor Function in the Brain: Molecular and Functional Implications. *Neuropharmacology* **2008,** *55* (6), 969-976.
66. Moreau, A. W.; Amar, M.; Le Roux, N.; Morel, N.; Fossier, P., Serotoninergic Fine-tuning of the Excitation-inhibition Balance in Rat Bisual Cortical Networks. *Cerebral Cortex (New York, N.Y. : 1991)* **2010,** *20* (2), 456-67.
67. McDevitt, R. A.; Neumaier, J. F., Regulation of Dorsal Raphe Nucleus Function by Serotonin Autoreceptors: A Behavioral Perspective. *Journal of Chemical Neuroanatomy* **2011,** *41* (4), 234-46.
68. Lee, S.; Jeong, J.; Kwak, Y.; Park, S. K., Depression Research: Where Are We Now? *Molecular Brain* **2010,** *3* (1), 8.
69. Mitchell, A. J.; Vaze, A.; Rao, S., Clinical Diagnosis of Depression in Primary Care: a Meta-analysis. *Lancet* **2009,** *374* (9690), 609-19.

70. Pereira, V. S.; Hiroaki-Sato, V. A., A Brief History of Antidepressant Drug Development: From Tricyclics to Beyond Ketamine. *Acta Neuropsychiatrica* **2018,** *30* (6), 307-322.
71. Skolnick, P.; Popik, P.; Trullas, R., Glutamate-based Antidepressants: 20 Years On. *Trends in Pharmacological Sciences* **2009,** *30* (11), 563-569.
72. Corriger, A.; Pickering, G., Ketamine and Depression: A Narrative Review. *Drug Design, Development and Therapy* **2019,** *13*, 3051-3067.
73. Carreno, F. R.; Lodge, D. J.; Frazer, A., Ketamine: Leading Us Into the Future for Development of Antidepressants. *Behavioural Brain Research* **2020,** *383*, 112532.
74. Clapp-Lilly, K. L.; Roberts, R. C.; Duffy, L. K.; Irons, K. P.; Hu, Y.; Drew, K. L., An Ultrastructural Analysis of Tissue Surrounding a Microdialysis Probe. *Journal of Neuroscience Methods* **1999,** *90* (2), 129-142.
75. Khan, A. S.; Michael, A. C., Invasive Consequences of Using Micro-electrodes and Microdialysis Probes in the Brain. *Trends in Analytical Chemistry* **2003,** *22* (8), 503-508.
76. Silvani, A.; Bojic, T.; Cianci, T.; Franzini, C.; Lenzi, P.; Lucchi, M. L.; Zoccoli, G., Brain Capillary Perfusion in the Spontaneously Hypertensive Rat During the Wake-sleep Cycle. *Experimental Brain Research* **2004,** *154* (1), 44-9.
77. Stamford, J. A.; Kruk, Z. L.; Millar, J.; Wightman, R. M., Striatal Dopamine Uptake in the Rat: In Vivo Analysis by Fast Cyclic Voltammetry. *Neuroscience Letters* **1984,** *51* (1), 133-8.
78. Kurbanoglu, S.; Ozkan, S. A., Electrochemical Carbon Based Nanosensors: A Promising Tool in Pharmaceutical and Biomedical Analysis. *Journal of Pharmaceutical and Biomedical Analysis* **2018,** *147*, 439-457.
79. Noked, M.; Soffer, A.; Aurbach, D., The Electrochemistry of Activated Carbonaceous Materials: Past, Present, and Future. *Journal of Solid State Electrochemistry* **2011,** *15* (7), 1563.
80. Hiremath, N.; Mays, J.; Bhat, G., Recent Developments in Carbon Fibers and Carbon Nanotube-Based Fibers: A Review. *Polymer Reviews* **2017,** *57* (2), 339-368.
81. Yang, C.; Denno, M. E.; Pyakurel, P.; Venton, B. J., Recent Trends in Carbon Nanomaterial-based Electrochemical Sensors for Biomolecules: A Review. *Analytica Chimica Acta* **2015,** *887*, 17-37.
82. Venton, B. J.; Cao, Q., Fundamentals of Fast-scan Cyclic Voltammetry for Dopamine Detection. *Analyst* **2020,** *145* (4), 1158-1168.
83. Atcherley, C. W.; Laude, N. D.; Parent, K. L.; Heien, M. L., Fast-Scan Controlled-Adsorption Voltammetry for the Quantification of Absolute Concentrations and Adsorption Dynamics. *Langmuir* **2013,** *29* (48), 14885-92.
84. Guiard, B. P.; Lanfumey, L.; Gardier, A. M., Microdialysis Approach to Study Serotonin Outflow in Mice Following Selective Serotonin Reuptake Inhibitors and Substance P (Neurokinin 1) Receptor Antagonist Administration: A Review. *Current Drug Targets* **2006,** *7* (2), 187-201.
85. Liu, Y.; Zhang, J.; Xu, X.; Zhao, M. K.; Andrews, A. M.; Weber, S. G., Capillary Ultrahigh Performance Liquid Chromatography with Elevated Temperature for Sub-One Minute Separations of Basal Serotonin in Submicroliter Brain Microdialysate Samples. *Analytical Chemistry* **2010,** *82* (23), 9611-9616.

86. Chefer, V. I.; Thompson, A. C.; Zapata, A.; Shippenberg, T. S., Overview of Brain Microdialysis. *Current Protocols in Neuroscience* **2009,** *Chapter 7*, Unit7.1-Unit7.1.
87. Wood, D. L.; Chlistunoff, J.; Majewski, J.; Borup, R. L., Nafion Structural Phenomena at Platinum and Carbon Interfaces. *Journal of the American Chemical Society* **2009,** *131* (50), 18096-18104.
88. Wiedemann, D. J.; Basse-Tomusk, A.; Wilson, R. L.; Rebec, G. V.; Wightman, R. M., Interference by DOPAC and Ascorbate During Attempts to Measure Drug-induced Changes in Neostriatal Dopamine with Nafion-coated, Carbon-fiber Electrodes. *Journal of Neuroscience Methods* **1990,** *35* (1), 9-18.
89. Singh, Y. S.; Sawarynski, L. E.; Dabiri, P. D.; Choi, W. R.; Andrews, A. M., Head-to-head Comparisons of Carbon Fiber Microelectrode Coatings for Sensitive and Selective Neurotransmitter Detection by Voltammetry. *Analytical Chemistry* **2011,** *83* (17), 6658-6666.
90. Hulicova-Jurcakova, D.; Seredych, M.; Lu, G. Q.; Kodiweera, N. K. A. C.; Stallworth, P. E.; Greenbaum, S.; Bandosz, T. J., Effect of Surface Phosphorus Functionalities of Activated Carbons Containing Oxygen and Nitrogen on Electrochemical Capacitance. *Carbon* **2009,** *47* (6), 1576-1584.
91. Heien, M. L. A. V.; Phillips, P. E. M.; Stuber, G. D.; Seipel, A. T.; Wightman, R. M., Overoxidation of Carbon-fiber Microelectrodes Enhances Dopamine Adsorption and Increases Sensitivity. *Analyst* **2003,** *128* (12), 1413-1419.

Chapter 2 References

1. Friedrich, M. Depression Is The Leading Cause of Disability Around the World. *Global Health* **2017,** *317* (15), 1517-1517.
2. Leonard, B. J. Antidepressants. Current Concepts of Mode of Action. *Encephale* **1991,** *17*, 127-131.
3. Sulser, F., Mode of Action of Antidepressant Drugs. *Jornal of Clinical Psychiatry* **1983**. *17*, 127-131.
4. Pigott, H. E.; Leventhal, A. M.; Alter, G. S.; Boren, J., Efficacy and Effectiveness of Antidepressants: Current Status of Research. *Psychother Psychosom* **2010,** *79* (5), 267-279.
5. Moncrieff, J.; Kirsch, I., Efficacy of Antidepressants in Adults. *Journal of Medical Genetics* **2005,** *331* (7509), 155-157.
6. Stassen, H. H.; Angst, J. J., Delayed Onset of Action of Antidepressants. *European Psychiatry* **1998,** *9* (3), 177-184.
7. Gourion, D., Antidepressants and Their Onset of Action: A Major Clinical, Methodological and Pronostical Issue. *Encephale* **2008,** *34* (1), 73-81.
8. McEwen, B. S.; Chattarji, S.; Diamond, D. M.; Jay, T. M.; Reagan, L. P.; Svenningsson, P.; Fuchs, A, The Neurobiological Properties of Tianeptine (Stablon): From Monoamine Hypothesis to Glutamatergic Modulation. *Moleuclar Psychiatry* **2010,** *15* (3), 237-249.

9. Goldberg, J. S.; Bell Jr, C. E.; Pollard, D., Revisiting the Monoamine Hypothesis of Depression: A New Perspective. *Perspect Medicencinal Chemistry* **2014,** *6*, PMC. S11375.
10. Khan, A. S.; Michael, A. C., Invasive Consequences of Using Micro-electrodes and Microdialysis Probes in the Brain. *Trends in Analytical Chemistry* **2003,** *22* (8), 503-508.
11. Silvani, A.; Bojic, T.; Cianci, T.; Franzini, C.; Lenzi, P.; Lucchi, M. L.; Zoccoli, G., Brain Capillary Perfusion in the Spontaneously Hypertensive Rat During the Wake-sleep Cycle. *Experimental Brain Research* **2004,** *154* (1), 44-9.
12. David, D. J. P.; Renard, C. E.; Jolliet, P.; Hascoët, M.; Bourin, M., Antidepressant-like Effects in Various Mice Strains in the Forced Swimming Test. *Psychopharmacology* **2003,** *166* (4), 373-382.
13. Czachura, J. F.; Rasmussen, K., Effects of Acute and Chronic Administration of Fluoxetine on the Activity of Serotonergic Neurons in the Dorsal Raphe Nucleus of the Rat. *Naunyn Schmiedebergs Arch Pharmacology* **2000,** *362* (3), 266-275.
14. Riad, M.; Zimmer, L.; Rbah, L.; Watkins, K. C.; Hamon, M.; Descarries, L. J., Acute Treatment with the Antidepressant Fluoxetine Internalizes 5-HT1A Autoreceptors and Reduces the In Vivo Binding of the PET Radioligand [18F] MPPF in the Nucleus Raphe Dorsalis of Rat. *Journal of Neuroscience* **2004,** *24* (23), 5420-5426.
15. Hashemi, P.; Dankoski, E. C.; Petrovic, J.; Keithley, R. B.; Wightman, R. M., Voltammetric Detection of 5-Hydroxytryptamine Release in the Rat Brain. *Analytical Chemistry* **2009,** *81* (22), 9462-9471.
16. Jackson, B. P.; Dietz, S. M.; Wightman, R. M., Fast-scan Cyclic Voltammetry of 5-hydroxytryptamine. *Analytical Chemistry* **1995,** *67* (6), 1115-1120.
17. Hashemi, P.; Dankoski, E. C.; Lama, R.; Wood, K. M.; Takmakov, P.; Wightman, R. M., Brain Dopamine and Derotonin Differ in Regulation and Its Consequences. *Proceedings of the National Academy of Sciences of the United States of America* **2012,** *109* (29), 11510-5.
18. Wood, K. M.; Hashemi, P., Fast-Scan Cyclic Voltammetry Analysis of Dynamic Serotonin Reponses to Acute Escitalopram. *ACS Chemical Neuroscience* **2013,** *4* (5), 715-720.
19. Wood, K. M.; Zeqja, A.; Nijhout, H. F.; Reed, M. C.; Best, J.; Hashemi, P., Voltammetric and Mathematical Evidence for Dual Transport Mediation of Serotonin Clearance In Vivo. *Journal of Neurochemistry* **2014,** *130* (3), 351-359.
20. Saylor, R. A.; Hersey, M.; West, A.; Buchanan, A. M.; Berger, S. N.; Nijhout, H. F.; Reed, M. C.; Best, J.; Hashemi, P., Corrigendum: In Vivo Hippocampal Serotonin Dynamics in Male and Female Mice: Determining Effects of Acute Escitalopram Using Fast Scan Cyclic Voltammetry. *Front Neuroscience* **2019,** *13*, 726-726.
21. West, A.; Best, J.; Abdalla, A.; Nijhout, H. F.; Reed, M.; Hashemi, P., Voltammetric Evidence for Discrete Serotonin Circuits, Linked to Specific Reuptake Domains, in the Mouse Medial Prefrontal Cortex. *Neurochemistry International* **2019,** *123*, 50-58.
22. Abdalla, A.; West, A.; Jin, Y.; Saylor, R. A.; Qiang, B.; Peña, E.; Linden, D. J.; Nijhout, H. F.; Reed, M. C.; Best, J.; Hashemi, P., Fast Serotonin Voltammetry as a Versatile Tool for Mapping Dynamic Tissue Architecture: I. Responses at Carbon Fibers Describe Local Tissue Physiology. *Journal of Neurochemistry* **2020,** *153* (1), 33-50.

23. Hirschfeld, R., History and Evolution of the Monoamine Hypothesis of Depression. *Journal of Clincal Psychiatry* **2000,** *61* (6), 4-6.
24. Lee, S.; Jeong, J.; Kwak, Y.; Park, S. K., Depression Research: Where Are We Now? *Molecular Brain* **2010,** *3* (1), 8.
25. Owens, M. J.; Nemeroff, C., Role of Serotonin in the Pathophysiology of Depression: Focus on the Serotonin Transporter. *Clinical Chemistry* **1994,** *40* (2), 288-295.
26. Coppen, A.; Doogan, D. J. T. J. o. c. p., Serotonin and Its Place in the Pathogenesis of Depression. *Journal of Clinical Psychiatry* **1988**, *49 (1)*, 4-11.
27. Lacasse, J. R.; Leo, J., Serotonin and Depression: A Disconnect Between the Advertisements and the Scientific Literature. *PLOS Medicine* **2005,** *2* (12), e392.
28. Anderson, I. M., SSRIS Versus Tricyclic Antidepressants in Depressed Inpatients: a Meta-analysis of Efficacy and Tolerability. *Depression and Anxiety* **1998,** *7 (1)*, 11-7.
29. Schmidt, F. M.; Sander, C.; Dietz, M. E.; Nowak, C.; Schröder, T.; Mergl, R.; Schönknecht, P.; Himmerich, H.; Hegerl, U., Brain Arousal Regulation as Response Predictor for Antidepressant Therapy in Major Depression. *Scientific Reports* **2017,** *7*, 45187.
30. Anderson, I. M., Selective Serotonin Reuptake Inhibitors Versus Tricyclic Antidepressants: a Meta-analysis of Efficacy and Tolerability. *Journal of Affective Disorders* **2000,** *58* (1), 19-36.31.
31. Mellerup, E. T.; Plenge, P. J. P., High Affinity Binding of 3 H-paroxetine and 3 H-imipramine to Rat Neuronal Membranes. *Psychooharmacology* **1986,** *89* (4), 436-439.
32. Gepertz, S.; Nevéus, T., Imipramine for Therapy Resistant Enuresis: A Retrospective Evaluation. *The Journal of Urology* **2004,** *171* (6), 2607-2610.
33. Anderson, I. M., Selective Serotonin Reuptake Inhibitors Versus Tricyclic Antidepressants: a Meta-analysis of Efficacy and Tolerability. *Journal of Affective Disorders* **2000,** *58* (1), 19-36.
34. Ramachandraih, C. T.; Subramanyam, N.; Bar, K. J.; Baker, G.; Yeragani, V. K., Antidepressants: from MAOIs to SSRIs and More. *Indian Journal of Psychaitry* **2011,** *53* (2), 180.
35. Nutt, D., Beyond Psychoanaleptics–Can We Improve Antidepressant Drug Nomenclature? *Journal of Psychopharmacology* **2009,** *23* (4), 343-345.
36. Yáñez, M.; Fernando Padin, J.; Alberto Arranz-Tagarro, J.; Camiña, M.; Laguna, R., History and Therapeutic Use of MAO-A Inhibitors: A Perspective of Mao-a Inhibitors as Antidepressant Drug. *Current Topics in Medicinal Chemistry* **2012,** *12* (20), 2275-2282.
37. Wender, P. H.; Wood, D. R.; Reimherr, F. W.; Ward, M., An Open Trial of Pargyline in the Treatment of Attention Deficit Disorder, Residual Type. *Psychiatry Research* **1983,** *9* (4), 329-336.
38. Cristancho, M. A.; Thase, M. E., Critical Appraisal of Selegiline Transdermal System for Major Depressive Disorder. *Expert Opinion on Drug Delivery* **2016,** *13* (5), 659-665.
39. Hillhouse, T. M.; Porter, J. H., A Brief History of the Development of Antidepressant Drugs: From Monoamines to Glutamate. *Experimental and Clinical Psychopharmacology* **2015,** *23* (1), 1-21.

40. Coleman, J. A.; Gouaux, E., Structural Basis for Recognition of Diverse Antidepressants by the Human Serotonin Transporter. *Natural Structructure Molecular Biology* **2018,** *25* (2), 170-175.
41. Zhou, Z.; Zhen, J.; Karpowich, N. K.; Law, C. J.; Reith, M. E.; Wang, D. N., Antidepressant Specificity of Serotonin Transporter Suggested by Three LeuT-SSRI Structures. *Natural Structucture Molecular Biology* **2009,** *16* (6), 652-7.
42. Ferguson, J. M., SSRI Antidepressant Medications: Adverse Effects and Tolerability. *Primary Care Companion Journal of Clininical Psychiatry* **2001,** *3* (1), 22-27.
43. Bambico, F. R.; Nguyen, N.-T.; Gobbi, G. J. E. N., Decline in Serotonergic Firing Activity and Desensitization of 5-HT1A Autoreceptors After Chronic Unpredictable Stress. *European Neuropsychopharmacology* **2009,** *19* (3), 215-228.
44. Hervás, I.; Vilaró, M. T.; Romero, L.; Scorza, M. C.; Mengod, G.; Artigas, F. J. N., Desensitization of 5-HT1A Autoreceptors by a Low Chronic Fluoxetine Dose Effect of the Concurrent Administration of WAY-100635. *Europe PMC* **2001,** *24* (1), 11-20.
45. Chavda, N.; Kantharia, N. D.; Jaykaran, Effects of Fluoxetine and Escitalopram on C-reactive Protein in Patients of Depression. *Journal of Pharmacology Pharmacother* **2011,** *2* (1), 11-16.
46. Lee, C. H.; Giuliani, F., The Role of Inflammation in Depression and Fatigue. *Frontiers in Immunology* **2019,** *10*, 1696.
47. Cipriani, A.; Furukawa, T. A.; Salanti, G.; Chaimani, A.; Atkinson, L. Z.; Ogawa, Y.; Leucht, S.; Ruhe, H. G.; Turner, E. H.; Higgins, J. P. T.; Egger, M.; Takeshima, N.; Hayasaka, Y.; Imai, H.; Shinohara, K.; Tajika, A.; Ioannidis, J. P. A.; Geddes, J. R., Comparative Efficacy and Acceptability of 21 Antidepressant Drugs for the Acute Treatment of Adults With Major Depressive Disorder: A Systematic Review and Network Meta-Analysis. *Focus American Psychiatry Publishing* **2018,** *16* (4), 420-429.
48. Li, Q. S.; Tian, C.; Hinds, D.; andMe Research, T., Genome-wide Association Studies of Antidepressant Class Response and Treatment-resistant Depression. *Translantic Psychiatry* **2020,** *10* (1), 360.
49. Ryan, G. B.; Majno, G., Acute inflammation. A Review. *Amercian Journal of Pathology* **1977,** *86* (1), 183-276.
50. Salim, S., Oxidative Stress and the Central Nervous System. *Journal of Pharmacology Experiments* **2017,** *360* (1), 201-205.
51. Bajpai, A.; Verma, A. K.; Srivastava, M.; Srivastava, R., Oxidative Stress and Major Depression. *Journal of Clinical Diagnosis* **2014,** *8* (12), CC04-7.
52. Ribaudo, G.; Bortoli, M.; Ongaro, A.; Oselladore, E.; Gianoncelli, A.; Zagotto, G.; Orian, L., Fluoxetine Scaffold to Design Tandem Molecular Antioxidants and Green Catalysts. *RSC Advances* **2020,** *10* (32), 18583-18593.
53. Wong, E. H.; Sonders, M. S.; Amara, S. G.; Tinholt, P. M.; Piercey, M. F.; Hoffmann, W. P.; Hyslop, D. K.; Franklin, S.; Porsolt, R. D.; Bonsignori, A. J. B. p., Reboxetine: A Pharmacologically Potent, Selective, and Specific Norepinephrine Reuptake Inhibitor. *Biological Psychiatry* **2000,** *47* (9), 818-829.
54. Millan, M. J.; Gobert, A.; Lejeune, F.; Newman-Tancredi, A.; Rivet, J.-M.; Auclair, A.; Peglion, A Novel Ligand at Both Serotonin and Norepinephrine Transporters: I. Receptor Binding, Electrophysiological, and Neurochemical Profile in

Comparison with Venlafaxine, Reboxetine, Citalopram, and Clomipramine. *Journal of Pharmacology Experimental Theories* **2001,** *298* (2), 565-580.
55. Szabo, S. T.; Blier, P., Effects of the Selective Norepinephrine Reuptake Inhibitor Reboxetine on Norepinephrine and Serotonin Transmission in the Rat Hippocampus. *Neuropsychopharmacology* **2001,** *25* (6), 845-857.
56. Singh, I.; Morgan, C.; Curran, V.; Nutt, D.; Schlag, A.; McShane, Ketamine Treatment for Depression: Opportunities for Clinical Innovation and Ethical Foresight. *Biological Psychiatry* **2017,** *4* (5), 419-426.
57. Anand, A.; Charney, D. S.; Oren, D. A.; Berman, R. M.; Hu, X. S.; Cappiello, A.; Krystal, J., Attenuation of the Neuropsychiatric Effects of Ketamine with Lamotrigine: Support for Hyperglutamatergic Effects of N-methyl-D-aspartate Receptor Antagonists. *JAMA Psychiatry* **2000,** *57* (3), 270-276.
58. Grunebaum, M. F.; Galfalvy, H. C.; Choo, T.-H.; Keilp, J. G.; Moitra, V. K.; Parris, M. S.; Marver, J. E.; Burke, A. K.; Milak, M. S.; Sublette, M., Ketamine for Rapid Reduction of Suicidal Thoughts in Major Depression: A Midazolam-controlled Randomized Clinical Trial. **2018,** *175* (4), 327-335.
59. Feder, A.; Parides, M. K.; Murrough, J. W.; Perez, A. M.; Morgan, J. E.; Saxena, S.; Kirkwood, K.; Aan Het Rot, M.; Lapidus, K. A.; Wan, L.-B. J. J. p., Efficacy of intravenous ketamine for treatment of chronic posttraumatic stress disorder: a randomized clinical trial. *Journal of Neuroscience* **2014,** *71* (6), 681-688.
60. Phillips, J. L.; Norris, S.; Talbot, J.; Hatchard, T.; Ortiz, A.; Birmingham, M.; Owoeye, O.; Batten, L. A.; Blier, P. J. N., Single and Repeated Ketamine Infusions for Reduction of Suicidal Ideation in Treatment-resistant Depression. *Neuropsychopharmacology* **2020,** *45* (4), 606-612.
61. Johnson, J. W.; Glasgow, N. G.; Povysheva, N., Recent Insights Into the Mode of Action of Memantine and Ketamine. *Current Opinions in Pharmacology* **2015,** *20*, 54-63.
62. Skolnick, P.; Popik, P.; Trullas, R., Glutamate-based Antidepressants: 20 Years On. *Trends in Pharmacological Sciences* **2009,** *30* (11), 563-569.
63. Zanos, P.; Moaddel, R.; Morris, P. J.; Georgiou, P.; Fischell, J.; Elmer, G. I.; Alkondon, M.; Yuan, P.; Pribut, H. J.; Singh, N., NMDAR Inhibition-independent Antidepressant Actions of Ketamine Metabolites. *Nature* **2016,** *533* (7604), 481-486.
64. Liu, D.; Wang, Z.; Gao, Z.; Xie, K.; Zhang, Q.; Jiang, H.; Pang, Q., Effects of Curcumin on Learning and Memory Deficits, BDNF, and ERK Protein Expression in rats Exposed to Chronic Unpredictable Stress. *Behavioural Brain Research* **2014,** *271*, 116-121.
65. Samaranayake, S.; Abdalla, A.; Robke, R.; Nijhout, H. F.; Reed, M. C.; Best, J.; Hashemi, P., A Voltammetric and Mathematical Analysis of Histaminergic Modulation of Serotonin in the Mouse Hypothalamus. *Journal of Neurochemistry* **2016,** *138* (3), 374-383.
66. Hersey, M.; Samaranayake, S.; Berger, S. N.; Tavakoli, N.; Mena, S.; Nijhout, H. F.; Reed, M. C.; Best, J.; Blakely, R. D.; Reagan, Inflammation-induced Histamine Impairs the Capacity of Escitalopram to Increase Hippocampal Extracellular Serotonin. *Journal of Neuroscience* **2021,** *41* (30), 6564-6577.
67. Sattar, Y.; Wilson, J.; Khan, A. M.; Adnan, M.; Larios, D. A.; Shrestha, S.; Rahman, Q.; Mansuri, Z.; Hassan, A.; Patel, N., A Review of the Mechanism of

Antagonism of N-methyl-D-aspartate Receptor by Ketamine in Treatment-resistant Depression. *Cureus* **2018,** *10* (5).
68. Beurel, E.; Song, L.; Jope, R., Inhibition of Glycogen Synthase Kinase-3 is Necessary for the Rapid Antidepressant Effect of Ketamine in Mice. *Molecular Psychiatry* **2011,** *16* (11), 1068-1070.
69. Browne, C.; Lucki, I., Antidepressant Effects of Ketamine: Mechanisms Underlying Fast-acting Novel Antidepressants. *Frontiers Pharmacol.* **2013,** *4,* 1–18.
70. Fukumoto, K.; Iijima, M.; Chaki, S. J. N., The Antidepressant Effects of an mGlu2/3 Eeceptor Antagonist and Ketamine Require AMPA Receptor Stimulation in the mPFC and Subsequent Activation of the 5-HT Neurons in the DRN. *Neuropsychopharmacology* **2016,** *41* (4), 1046-1056.
71. Taniguchi, T.; Shibata, K.; Yamamoto, K., Ketamine Inhibits Endotoxin-induced Shock in Rats. *Anesthesiology* **2001,** *95* (4), 928-932.
72. Corriger, A.; Pickering, G., Ketamine and Depression: A Narrative Review. *Drug Design, Development and Therapy* **2019,** *13*, 3051-3067.
73. Carreno, F. R.; Lodge, D. J.; Frazer, A., Ketamine: Leading us into the future for development of antidepressants. *Behavioural Brain Research* **2020,** *383*, 112532.
74. Clapp-Lilly, K. L.; Roberts, R. C.; Duffy, L. K.; Irons, K. P.; Hu, Y.; Drew, K. L., An Ultrastructural Analysis of Tissue Surrounding a Microdialysis Probe. *Journal of Neuroscience Methods* **1999,** *90* (2), 129-142.
75. Khan, A. S.; Michael, A. C., Invasive Consequences of Using Micro-electrodes and Microdialysis Probes in the Brain. *Trends in Analytical Chemistry* **2003,** *22* (8), 503-508.
76. Silvani, A.; Bojic, T.; Cianci, T.; Franzini, C.; Lenzi, P.; Lucchi, M. L.; Zoccoli, G., Brain Capillary Perfusion in the Spontaneously Hypertensive Rat During the Wake-sleep Cycle. *Experimental Brain Research* **2004,** *154* (1), 44-9.
77. Stamford, J. A.; Kruk, Z. L.; Millar, J.; Wightman, R. M., Striatal Dopamine Uptake in the Rat: In Vivo Analysis by Fast Cyclic Voltammetry. *Neuroscience Letters* **1984,** *51* (1), 133-8.
78. Kurbanoglu, S.; Ozkan, S. A., Electrochemical Carbon Based Nanosensors: A Promising Tool in Pharmaceutical and Biomedical Analysis. *Journal of Pharmaceutical and Biomedical Analysis* **2018,** *147*, 439-457.

Chapter 3 References

1. Rakofsky, J.; Rapaport, M. J. Mood Disorders. *Continuum* **2018,** *24* (3), 804-827.
2. Ou, Y.; Buchanan, A. M.; Witt, C. E.; Hashemi, P. J. A. M., Frontiers in Electrochemical Sensors for Neurotransmitter Detection: Towards Measuring Neurotransmitters as Chemical Diagnostics for Brain Disorders. *Analytical Methods* **2019,** *11* (21), 2738-2755.
3. Hirschfeld, R. M. History and Evolution of the Monoamine Hypothesis of Depression. *Journal of Clinical Psychiatry* **2000,** *61* (6), 4-6.
4. Venton, B. J.; Cao, Q., Fundamentals of Fast-scan Cyclic Voltammetry for Dopamine Detection. *Analyst* **2020,** *145* (4), 1158-1168.

5. Hashemi, P.; Dankoski, E. C.; Petrovic, J.; Keithley, R. B.; Wightman, R. M., Voltammetric Detection of 5-Hydroxytryptamine Release in the Rat Brain. *Analytical Chemistry* **2009,** *81* (22), 9462-9471.
6. Yang, H.; Thompson, A. B.; McIntosh, B. J.; Altieri, S. C.; Andrews, A. M., Physiologically Relevant Changes in Serotonin Resolved by Fast Microdialysis. *ACS Chemical Neuroscience* **2013,** *4* (5), 790-8.
7. Yang, H.; Sampson, M. M.; Senturk, D.; Andrews, A. M., Sex- and SERT-Mediated Differences in Stimulated Serotonin Revealed by Fast Microdialysis. *ACS Chemical Neuroscience* **2015,** *6* (8), 1487-1501.
8. Abdalla, A.; Atcherley, C. W.; Pathirathna, P.; Samaranayake, S.; Qiang, B.; Peña, E.; Morgan, S. L.; Heien, M. L.; Hashemi, P., In Vivo Ambient Serotonin Measurements at Carbon-Fiber Microelectrodes. *Analytical Chemistry* **2017,** *89* (18), 9703-9711.
9. Jackson, B. P.; Dietz, S. M.; Wightman, R. M., Fast-scan Cyclic Voltammetry of 5-hydroxytryptamine. *Analytical Chemistry* **1995,** *67* (6), 1115-1120.
10. Atcherley, C. W.; Wood, K. M.; Parent, K. L.; Hashemi, P.; Heien, M. L., The Coaction of Tonic and Phasic Dopamine Dynamics. *Chemical Communications* **2015,** *51* (12), 2235-2238.
11. Honari, H.; Choe, A. S.; Pekar, J. J.; Lindquist, M. A., Investigating the Impact of Autocorrelation on Time-varying Connectivity. *NeuroImage* **2019,** *197*, 37-48.
12. Rahi, P. K.; Mehra, R. J. I. J. o. E. T.; Engineering, Analysis of Power Spectrum Estimation Using Welch Method for Various Window Techniques. *International Journal of Emerging Technologies and Engineering* **2014,** *2* (6), 106-109.
13. Virtanen, P.; Gommers, R.; Oliphant, T. E.; Haberland, M.; Reddy, T.; Cournapeau, D.; Burovski, E.; Peterson, P.; Weckesser, W.; Bright, SciPy 1.0: Fundamental Algorithms for Scientific Computing in Python. *Nature Methods* **2020,** *17* (3), 261-272.
14. Iversen, L. L., Uptake Processes for Biogenic Amines. *Biochemistry of Biogenic Amines* **1975**, pp 381-442.
15. Wood, K. M.; Zeqja, A.; Nijhout, H. F.; Reed, M. C.; Best, J.; Hashemi, P., Voltammetric and Mathematical Evidence for Dual Transport Mediation of Serotonin Clearance In Vivo. *Journal of Neurochemistry* **2014,** *130* (3), 351-359.
16. Daws, L. C.; Toney, G. High-speed Chronoamperometry to Study Kinetics and Mechanisms for Serotonin Clearance In Vivo. *Electrochemical Methods for Neuroscience* **2007**. Chapter 5.
17. Daws, L. C.; Koek, W.; Mitchell, N. C., Revisiting Serotonin Reuptake Inhibitors and the Therapeutic Potential of "Uptake-2" in Psychiatric Disorders. *ACS Chemical Neuroscience* **2013,** *4* (1), 16-21.
18. Corriger, A.; Pickering, G., Ketamine and Depression: A Narrative Review. *Drug Design, Development and Therapy* **2019,** *13*, 3051-3067.
19. Johnson, J. W.; Glasgow, N. G.; Povysheva, Recent Insights Into the Mode of Action of Memantine and Ketamine. *Current Opininions in Pharmacology* **2015,** *20*, 54-63.
20. Oreland, L.; Kinemuchi, H.; Yoo, B. Y., The Mechanism of Action of the Monoamine Oxidase Inhibitor Pargyline. *Life Sciences* **1973,** *13* (11), 1533-1541.

21. Aronson, S.; Delgado, P. J. Escitalopram. *Durgs Today (Barc)* **2004,** *40* (2), 121-131.
22. Braestrup, C.; Sanchez, C. Escitalopram: A Unique Mechanism of Action. *Internation Journal of Psychiatry Clinical Practice* **2004,** *8* (sup1), 11-13.
23. First, M.; Gil-Ad, I.; Taler, M.; Tarasenko, I.; Novak, N.; Weizman, A. J. J. o. M. N., The Effects of Fluoxetine Treatment in a Chronic Mild Stress Rat Model on Depression-related Behavior, Brain Neurotrophins and ERK Expression. *Journal of Molecular Neuroscience* **2011,** *45* (2), 246-255.
24. First, M.; Gil-Ad, I.; Taler, M.; Tarasenko, I.; Novak, N.; Weizman, A. The Effects of Reboxetine Treatment on Depression-like Behavior, Brain Neurotrophins, and ERK Expression in Rats Exposed to Chronic Mild Stress. *Journal of Molecular Neuroscience* **2013,** *50* (1), 88-97.
25. Russo-Neustadt, A. A.; Alejandre, H.; Garcia, C.; Ivy, A. S.; Chen, M. J. J. N., Hippocampal Brain-derived Neurotrophic Factor Expression Following Treatment with Reboxetine, Citalopram, and Physical Exercise. *Neuropsychopharmacology* **2004,** *29* (12), 2189-2199.

Chapter 4 References

1. Friedrich, M. Depression Is The Leading Cause of Disability Around the World. *Global Health* **2017,** *317* (15), 1517-1517.
2. Leonard, B. J. Antidepressants. Current Concepts of Mode of Action. *Encephale* **1991,** *17*, 127-131.
3. Sulser, F., Mode of Action of Antidepressant Drugs. *Jornal of Clinical Psychiatry* **1983**. *17*, 127-131.
4. Pigott, H. E.; Leventhal, A. M.; Alter, G. S.; Boren, J., Efficacy and Effectiveness of Antidepressants: Current Status of Research. *Psychother Psychosom* **2010,** *79* (5), 267-279.
5. Moncrieff, J.; Kirsch, I., Efficacy of Antidepressants in Adults. *Journal of Medical Genetics* **2005,** *331* (7509), 155-157.
6. Stassen, H. H.; Angst, J. J., Delayed Onset of Action of Antidepressants. *European Psychiatry* **1998,** *9* (3), 177-184.
7. Gourion, D., Antidepressants and Their Onset of Action: A Major Clinical, Methodological and Pronostical Issue. *Encephale* **2008,** *34* (1), 73-81.
8. McEwen, B. S.; Chattarji, S.; Diamond, D. M.; Jay, T. M.; Reagan, L. P.; Svenningsson, P.; Fuchs, A, The Neurobiological Properties of Tianeptine (Stablon): From Monoamine Hypothesis to Glutamatergic Modulation. *Moleuclar Psychiatry* **2010,** *15* (3), 237-249.
9. Goldberg, J. S.; Bell Jr, C. E.; Pollard, D., Revisiting the Monoamine Hypothesis of Depression: A New Perspective. *Perspect Medicencinal Chemistry* **2014,** *6*, PMC. S11375.
10. Khan, A. S.; Michael, A. C., Invasive Consequences of Using Micro-electrodes and Microdialysis Probes in the Brain. *Trends in Analytical Chemistry* **2003,** *22* (8), 503-508.

11. Silvani, A.; Bojic, T.; Cianci, T.; Franzini, C.; Lenzi, P.; Lucchi, M. L.; Zoccoli, G., Brain Capillary Perfusion in the Spontaneously Hypertensive Rat During the Wake-sleep Cycle. *Experimental Brain Research* **2004,** *154* (1), 44-9.
12. David, D. J. P.; Renard, C. E.; Jolliet, P.; Hascoët, M.; Bourin, M., Antidepressant-like Effects in Various Mice Strains in the Forced Swimming Test. *Psychopharmacology* **2003,** *166* (4), 373-382.
13. Czachura, J. F.; Rasmussen, K., Effects of Acute and Chronic Administration of Fluoxetine on the Activity of Serotonergic Neurons in the Dorsal Raphe Nucleus of the Rat. *Naunyn Schmiedebergs Arch Pharmacology* **2000,** *362* (3), 266-275.
14. Riad, M.; Zimmer, L.; Rbah, L.; Watkins, K. C.; Hamon, M.; Descarries, L. J., Acute Treatment with the Antidepressant Fluoxetine Internalizes 5-HT1A Autoreceptors and Reduces the In Vivo Binding of the PET Radioligand [18F] MPPF in the Nucleus Raphe Dorsalis of Rat. *Journal of Neuroscience* **2004,** *24* (23), 5420-5426.
15. Hashemi, P.; Dankoski, E. C.; Petrovic, J.; Keithley, R. B.; Wightman, R. M., Voltammetric Detection of 5-Hydroxytryptamine Release in the Rat Brain. *Analytical Chemistry* **2009,** *81* (22), 9462-9471.
16. Jackson, B. P.; Dietz, S. M.; Wightman, R. M., Fast-scan Cyclic Voltammetry of 5-hydroxytryptamine. *Analytical Chemistry* **1995,** *67* (6), 1115-1120.
17. Hashemi, P.; Dankoski, E. C.; Lama, R.; Wood, K. M.; Takmakov, P.; Wightman, R. M., Brain Dopamine and Derotonin Differ in Regulation and Its Consequences. *Proceedings of the National Academy of Sciences of the United States of America* **2012,** *109* (29), 11510-5.
18. Wood, K. M.; Hashemi, P., Fast-Scan Cyclic Voltammetry Analysis of Dynamic Serotonin Reponses to Acute Escitalopram. *ACS Chemical Neuroscience* **2013,** *4* (5), 715-720.
19. Wood, K. M.; Zeqja, A.; Nijhout, H. F.; Reed, M. C.; Best, J.; Hashemi, P., Voltammetric and Mathematical Evidence for Dual Transport Mediation of Serotonin Clearance In Vivo. *Journal of Neurochemistry* **2014,** *130* (3), 351-359.
20. Saylor, R. A.; Hersey, M.; West, A.; Buchanan, A. M.; Berger, S. N.; Nijhout, H. F.; Reed, M. C.; Best, J.; Hashemi, P., Corrigendum: In Vivo Hippocampal Serotonin Dynamics in Male and Female Mice: Determining Effects of Acute Escitalopram Using Fast Scan Cyclic Voltammetry. *Front Neuroscience* **2019,** *13*, 726-726.
21. West, A.; Best, J.; Abdalla, A.; Nijhout, H. F.; Reed, M.; Hashemi, P., Voltammetric Evidence for Discrete Serotonin Circuits, Linked to Specific Reuptake Domains, in the Mouse Medial Prefrontal Cortex. *Neurochemistry International* **2019,** *123*, 50-58.
22. Abdalla, A.; West, A.; Jin, Y.; Saylor, R. A.; Qiang, B.; Peña, E.; Linden, D. J.; Nijhout, H. F.; Reed, M. C.; Best, J.; Hashemi, P., Fast Serotonin Voltammetry as a Versatile Tool for Mapping Dynamic Tissue Architecture: I. Responses at Carbon Fibers Describe Local Tissue Physiology. *Journal of Neurochemistry* **2020,** *153* (1), 33-50.
23. Hirschfeld, R., History and Evolution of the Monoamine Hypothesis of Depression. *Journal of Clincal Psychiatry* **2000,** *61* (6), 4-6.
24. Lee, S.; Jeong, J.; Kwak, Y.; Park, S. K., Depression Research: Where Are We Now? *Molecular Brain* **2010,** *3* (1), 8.

25. Owens, M. J.; Nemeroff, C., Role of Serotonin in the Pathophysiology of Depression: Focus on the Serotonin Transporter. *Clinical Chemistry* **1994,** *40* (2), 288-295.
26. Coppen, A.; Doogan, D. J. T. J. o. c. p., Serotonin and Its Place in the Pathogenesis of Depression. *Journal of Clinical Psychiatry* **1988**, *49 (1)*, 4-11.
27. Lacasse, J. R.; Leo, J., Serotonin and Depression: A Disconnect Between the Advertisements and the Scientific Literature. *PLOS Medicine* **2005,** *2* (12), e392.
28. Anderson, I. M., SSRIS Versus Tricyclic Antidepressants in Depressed Inpatients: a Meta-analysis of Efficacy and Tolerability. *Depression and Anxiety* **1998,** *7 (1)*, 11-7.
29. Schmidt, F. M.; Sander, C.; Dietz, M. E.; Nowak, C.; Schröder, T.; Mergl, R.; Schönknecht, P.; Himmerich, H.; Hegerl, U., Brain Arousal Regulation as Response Predictor for Antidepressant Therapy in Major Depression. *Scientific Reports* **2017,** *7*, 45187.
30. Anderson, I. M., Selective Serotonin Reuptake Inhibitors Versus Tricyclic Antidepressants: a Meta-analysis of Efficacy and Tolerability. *Journal of Affective Disorders* **2000,** *58* (1), 19-36.31.
31. Mellerup, E. T.; Plenge, P. J. P., High Affinity Binding of 3 H-paroxetine and 3 H-imipramine to Rat Neuronal Membranes. *Psychooharmacology* **1986,** *89* (4), 436-439.
32. Gepertz, S.; Nevéus, T., Imipramine for Therapy Resistant Enuresis: A Retrospective Evaluation. *The Journal of Urology* **2004,** *171* (6), 2607-2610.
33. Anderson, I. M., Selective Serotonin Reuptake Inhibitors Versus Tricyclic Antidepressants: a Meta-analysis of Efficacy and Tolerability. *Journal of Affective Disorders* **2000,** *58* (1), 19-36.
34. Ramachandraih, C. T.; Subramanyam, N.; Bar, K. J.; Baker, G.; Yeragani, V. K., Antidepressants: from MAOIs to SSRIs and More. *Indian Journal of Psychaitry* **2011,** *53* (2), 180.
35. Nutt, D., Beyond Psychoanaleptics–Can We Improve Antidepressant Drug Nomenclature? *Journal of Psychopharmacology* **2009,** *23* (4), 343-345.
36. Yáñez, M.; Fernando Padin, J.; Alberto Arranz-Tagarro, J.; Camiña, M.; Laguna, R., History and Therapeutic Use of MAO-A Inhibitors: A Perspective of Mao-a Inhibitors as Antidepressant Drug. *Current Topics in Medicinal Chemistry* **2012,** *12* (20), 2275-2282.
37. Wender, P. H.; Wood, D. R.; Reimherr, F. W.; Ward, M., An Open Trial of Pargyline in the Treatment of Attention Deficit Disorder, Residual Type. *Psychiatry Research* **1983,** *9* (4), 329-336.
38. Cristancho, M. A.; Thase, M. E., Critical Appraisal of Selegiline Transdermal System for Major Depressive Disorder. *Expert Opinion on Drug Delivery* **2016,** *13* (5), 659-665.
39. Hillhouse, T. M.; Porter, J. H., A Brief History of the Development of Antidepressant Drugs: From Monoamines to Glutamate. *Experimental and Clinical Psychopharmacology* **2015,** *23* (1), 1-21.
40. Coleman, J. A.; Gouaux, E., Structural Basis for Recognition of Diverse Antidepressants by the Human Serotonin Transporter. *Natural Structructure Molecular Biology* **2018,** *25* (2), 170-175.

41. Zhou, Z.; Zhen, J.; Karpowich, N. K.; Law, C. J.; Reith, M. E.; Wang, D. N., Antidepressant Specificity of Serotonin Transporter Suggested by Three LeuT-SSRI Structures. *Natural Structucture Molecular Biology* **2009,** *16* (6), 652-7.
42. Ferguson, J. M., SSRI Antidepressant Medications: Adverse Effects and Tolerability. *Primary Care Companion Journal of Clininical Psychiatry* **2001,** *3* (1), 22-27.
43. Bambico, F. R.; Nguyen, N.-T.; Gobbi, G. J. E. N., Decline in Serotonergic Firing Activity and Desensitization of 5-HT1A Autoreceptors After Chronic Unpredictable Stress. *European Neuropsychopharmacology* **2009,** *19* (3), 215-228.
44. Hervás, I.; Vilaró, M. T.; Romero, L.; Scorza, M. C.; Mengod, G.; Artigas, F. J. N., Desensitization of 5-HT1A Autoreceptors by a Low Chronic Fluoxetine Dose Effect of the Concurrent Administration of WAY-100635. *Europe PMC* **2001,** *24* (1), 11-20.
45. Chavda, N.; Kantharia, N. D.; Jaykaran, Effects of Fluoxetine and Escitalopram on C-reactive Protein in Patients of Depression. *Journal of Pharmacology Pharmacother* **2011,** *2* (1), 11-16.
46. Lee, C. H.; Giuliani, F., The Role of Inflammation in Depression and Fatigue. *Frontiers in Immunology* **2019,** *10*, 1696.
47. Cipriani, A.; Furukawa, T. A.; Salanti, G.; Chaimani, A.; Atkinson, L. Z.; Ogawa, Y.; Leucht, S.; Ruhe, H. G.; Turner, E. H.; Higgins, J. P. T.; Egger, M.; Takeshima, N.; Hayasaka, Y.; Imai, H.; Shinohara, K.; Tajika, A.; Ioannidis, J. P. A.; Geddes, J. R., Comparative Efficacy and Acceptability of 21 Antidepressant Drugs for the Acute Treatment of Adults With Major Depressive Disorder: A Systematic Review and Network Meta-Analysis. *Focus American Psychiatry Publishing* **2018,** *16* (4), 420-429.
48. Li, Q. S.; Tian, C.; Hinds, D.; andMe Research, T., Genome-wide Association Studies of Antidepressant Class Response and Treatment-resistant Depression. *Translantic Psychiatry* **2020,** *10* (1), 360.
49. Ryan, G. B.; Majno, G., Acute inflammation. A Review. *Amercian Journal of Pathology* **1977,** *86* (1), 183-276.
50. Salim, S., Oxidative Stress and the Central Nervous System. *Journal of Pharmacology Experiments* **2017,** *360* (1), 201-205.
51. Bajpai, A.; Verma, A. K.; Srivastava, M.; Srivastava, R., Oxidative Stress and Major Depression. *Journal of Clinical Diagnosis* **2014,** *8* (12), CC04-7.
52. Ribaudo, G.; Bortoli, M.; Ongaro, A.; Oselladore, E.; Gianoncelli, A.; Zagotto, G.; Orian, L., Fluoxetine Scaffold to Design Tandem Molecular Antioxidants and Green Catalysts. *RSC Advances* **2020,** *10* (32), 18583-18593.
53. Wong, E. H.; Sonders, M. S.; Amara, S. G.; Tinholt, P. M.; Piercey, M. F.; Hoffmann, W. P.; Hyslop, D. K.; Franklin, S.; Porsolt, R. D.; Bonsignori, A. J. B. p., Reboxetine: A Pharmacologically Potent, Selective, and Specific Norepinephrine Reuptake Inhibitor. *Biological Psychiatry* **2000,** *47* (9), 818-829.
54. Millan, M. J.; Gobert, A.; Lejeune, F.; Newman-Tancredi, A.; Rivet, J.-M.; Auclair, A.; Peglion, A Novel Ligand at Both Serotonin and Norepinephrine Transporters: I. Receptor Binding, Electrophysiological, and Neurochemical Profile in Comparison with Venlafaxine, Reboxetine, Citalopram, and Clomipramine. *Journal of Pharmacology Experimental Theories* **2001,** *298* (2), 565-580.

55. Szabo, S. T.; Blier, P., Effects of the Selective Norepinephrine Reuptake Inhibitor Reboxetine on Norepinephrine and Serotonin Transmission in the Rat Hippocampus. *Neuropsychopharmacology* **2001,** *25* (6), 845-857.
56. Singh, I.; Morgan, C.; Curran, V.; Nutt, D.; Schlag, A.; McShane, Ketamine Treatment for Depression: Opportunities for Clinical Innovation and Ethical Foresight. *Biological Psychiatry* **2017,** *4* (5), 419-426.
57. Anand, A.; Charney, D. S.; Oren, D. A.; Berman, R. M.; Hu, X. S.; Cappiello, A.; Krystal, J., Attenuation of the Neuropsychiatric Effects of Ketamine with Lamotrigine: Support for Hyperglutamatergic Effects of N-methyl-D-aspartate Receptor Antagonists. *JAMA Psychiatry* **2000,** *57* (3), 270-276.
58. Grunebaum, M. F.; Galfalvy, H. C.; Choo, T.-H.; Keilp, J. G.; Moitra, V. K.; Parris, M. S.; Marver, J. E.; Burke, A. K.; Milak, M. S.; Sublette, M., Ketamine for Rapid Reduction of Suicidal Thoughts in Major Depression: A Midazolam-controlled Randomized Clinical Trial. **2018,** *175* (4), 327-335.
59. Feder, A.; Parides, M. K.; Murrough, J. W.; Perez, A. M.; Morgan, J. E.; Saxena, S.; Kirkwood, K.; Aan Het Rot, M.; Lapidus, K. A.; Wan, L.-B. J. J. p., Efficacy of intravenous ketamine for treatment of chronic posttraumatic stress disorder: a randomized clinical trial. *Journal of Neuroscience* **2014,** *71* (6), 681-688.
60. Phillips, J. L.; Norris, S.; Talbot, J.; Hatchard, T.; Ortiz, A.; Birmingham, M.; Owoeye, O.; Batten, L. A.; Blier, P. J. N., Single and Repeated Ketamine Infusions for Reduction of Suicidal Ideation in Treatment-resistant Depression. *Neuropsychopharmacology* **2020,** *45* (4), 606-612.
61. Johnson, J. W.; Glasgow, N. G.; Povysheva, N., Recent Insights Into the Mode of Action of Memantine and Ketamine. *Current Opinions in Pharmacology* **2015,** *20*, 54-63.
62. Skolnick, P.; Popik, P.; Trullas, R., Glutamate-based Antidepressants: 20 Years On. *Trends in Pharmacological Sciences* **2009,** *30* (11), 563-569.
63. Zanos, P.; Moaddel, R.; Morris, P. J.; Georgiou, P.; Fischell, J.; Elmer, G. I.; Alkondon, M.; Yuan, P.; Pribut, H. J.; Singh, N., NMDAR Inhibition-independent Antidepressant Actions of Ketamine Metabolites. *Nature* **2016,** *533* (7604), 481-486.
64. Liu, D.; Wang, Z.; Gao, Z.; Xie, K.; Zhang, Q.; Jiang, H.; Pang, Q., Effects of Curcumin on Learning and Memory Deficits, BDNF, and ERK Protein Expression in rats Exposed to Chronic Unpredictable Stress. *Behavioural Brain Research* **2014,** *271*, 116-121.
65. Samaranayake, S.; Abdalla, A.; Robke, R.; Nijhout, H. F.; Reed, M. C.; Best, J.; Hashemi, P., A Voltammetric and Mathematical Analysis of Histaminergic Modulation of Serotonin in the Mouse Hypothalamus. *Journal of Neurochemistry* **2016,** *138* (3), 374-383.
66. Hersey, M.; Samaranayake, S.; Berger, S. N.; Tavakoli, N.; Mena, S.; Nijhout, H. F.; Reed, M. C.; Best, J.; Blakely, R. D.; Reagan, Inflammation-induced Histamine Impairs the Capacity of Escitalopram to Increase Hippocampal Extracellular Serotonin. *Journal of Neuroscience* **2021,** *41* (30), 6564-6577.
67. Sattar, Y.; Wilson, J.; Khan, A. M.; Adnan, M.; Larios, D. A.; Shrestha, S.; Rahman, Q.; Mansuri, Z.; Hassan, A.; Patel, N., A Review of the Mechanism of Antagonism of N-methyl-D-aspartate Receptor by Ketamine in Treatment-resistant Depression. *Cureus* **2018,** *10* (5).

68. Beurel, E.; Song, L.; Jope, R., Inhibition of Glycogen Synthase Kinase-3 is Necessary for the Rapid Antidepressant Effect of Ketamine in Mice. *Molecular Psychiatry* **2011,** *16* (11), 1068-1070.
69. Browne, C.; Lucki, I., Antidepressant Effects of Ketamine: Mechanisms Underlying Fast-acting Novel Antidepressants. *Frontiers Pharmacol.* **2013,** *4,* 1–18.
70. Fukumoto, K.; Iijima, M.; Chaki, S. J. N., The Antidepressant Effects of an mGlu2/3 Eeceptor Antagonist and Ketamine Require AMPA Receptor Stimulation in the mPFC and Subsequent Activation of the 5-HT Neurons in the DRN. *Neuropsychopharmacology* **2016,** *41* (4), 1046-1056.
71. Taniguchi, T.; Shibata, K.; Yamamoto, K., Ketamine Inhibits Endotoxin-induced Shock in Rats. *Anesthesiology* **2001,** *95* (4), 928-932.

Chapter 5 References

1. Rakofsky, J.; Rapaport, Mood Disorders. *Continuum* **2018,** *24* (3), 804-827.
2. Ou, Y.; Buchanan, A. M.; Witt, C. E.; Hashemi, P. J. A. M., Frontiers in Electrochemical Sensors for Neurotransmitter Detection: Towards Measuring Neurotransmitters as Chemical Diagnostics for Brain Disorders. *Analytical Methods* **2019,** *11* (21), 2738-2755.
3. Hirschfeld, R. M. J. J. o. c. p., History and Evolution of the Monoamine Hypothesis of Depression. *Journal of Neuroscience* **2000,** *61* (6), 4-6.
4. Venton, B. J.; Cao, Q., Fundamentals of Fast-Scan Cyclic Voltammetry for Dopamine Detection. *Analyst* **2020,** *145* (4), 1158-1168.
5. Hashemi, P.; Dankoski, E. C.; Petrovic, J.; Keithley, R. B.; Wightman, R. M., Voltammetric Detection of 5-Hydroxytryptamine Release in the Rat Brain. *Analytical Chemistry* **2009,** *81* (22), 9462-9471.
6. Yang, H.; Thompson, A. B.; McIntosh, B. J.; Altieri, S. C.; Andrews, A. M., Physiologically relevant changes in serotonin resolved by fast microdialysis. *ACS Chemical Neuroscience* **2013,** *4* (5), 790-8.
7. Yang, H.; Sampson, M. M.; Senturk, D.; Andrews, A. M., Sex- and SERT-Mediated Differences in Stimulated Serotonin Revealed by Fast Microdialysis. *ACS Chemical Neuroscience* **2015,** *6* (8), 1487-1501.
8. Abdalla, A.; Atcherley, C. W.; Pathirathna, P.; Samaranayake, S.; Qiang, B.; Peña, E.; Morgan, S. L.; Heien, M. L.; Hashemi, P., In Vivo Ambient Serotonin Measurements at Carbon-Fiber Microelectrodes. *Analytical Chemistry* **2017,** *89* (18), 9703-9711.
9. Jackson, B. P.; Dietz, S. M.; Wightman, R. M., Fast-scan Cyclic Voltammetry of 5-hydroxytryptamine. *Analytical Chemistry* **1995,** *67* (6), 1115-1120.
10. Atcherley, C. W.; Wood, K. M.; Parent, K. L.; Hashemi, P.; Heien, M. L., The Coaction of Tonic and Phasic Dopamine Dynamics. *Chemistry Communcations* **2015,** *51* (12), 2235-2238.
11. Honari, H.; Choe, A. S.; Pekar, J. J.; Lindquist, M. A., Investigating the Impact of Autocorrelation on Time-varying Connectivity. *NeuroImage* **2019,** *197*, 37-48.

12. Rahi, P. K.; Mehra, R. J. I. J. o. E. T.; Engineering, Analysis of Power Spectrum Estimation Using Welch Method for Various Window Techniques. *International Journal of Emerging Technologies and Engineering* **2014,** *2* (6), 106-109.
13. Virtanen, P.; Gommers, R.; Oliphant, T. E.; Haberland, M.; Reddy, T.; Cournapeau, D.; Burovski, E.; Peterson, P.; Weckesser, W.; Bright, SciPy 1.0: Fundamental Algorithms for Scientific Computing in Python. National Methods **2020,** *17* (3), 261-272.
14. Iversen, L. L., Uptake Processes for Biogenic Amines. In *Biochemistry of Biogenic Amines* **1975**; pp 381-442.
15. Wood, K. M.; Zeqja, A.; Nijhout, H. F.; Reed, M. C.; Best, J.; Hashemi, P., Voltammetric and Mathematical Evidence for Dual Transport Mediation of Serotonin Clearance In Vivo. *Journal of Neurochemistry* **2014,** *130* (3), 351-359.
16. Daws, L. C.; Toney, G. M., High-Speed Chronoamperometry to Study Kinetics and Mechanisms for Serotonin Clearance In Vivo. *Electrochemical Methods for Neruoscience* **2007**. Chapter 5.
17. Daws, L. C.; Koek, W.; Mitchell, N. C., Revisiting Serotonin Reuptake Inhibitors and the Therapeutic Potential of "Uptake-2" in Psychiatric Disorders. *ACS Chemical Neuroscience* **2013,** *4* (1), 16-21.
18. Corriger, A.; Pickering, G., Ketamine and Depression: A Narrative Review. *Drug Design, Development and Therapy* **2019,** *13*, 3051-3067.
19. Johnson, J. W.; Glasgow, N. G.; Povysheva, N., Recent Insights Into the Mode of Action of Memantine and Ketamine. *Current Opinion in Pharmacology* **2015,** *20*, 54-63.
20. Oreland, L.; Kinemuchi, H.; Yoo, B. Y., The Mechanism of Action of the Monoamine Oxidase Inhibitor Pargyline. *Life Sciences* **1973,** *13* (11), 1533-1541.
21. Aronson, S.; Delgado, P. J., Escitalopram. *Drugs Today (Barc)* **2004,** *40* (2), 121-131.
22. Braestrup, C.; Sanchez, C. Escitalopram: A Unique Mechanism of Action. *International Journal of Psychiatry Clinical Pracitice* **2004,** *8* (sup1), 11-13.
23. First, M.; Gil-Ad, I.; Taler, M.; Tarasenko, I.; Novak, N.; Weizman, A., The Effects of Fluoxetine Treatment in a Chronic Mild Stress Rat Model on Depression-related Behavior, Brain Neurotrophins and ERK Expression. *Journal of Molecular Neuroscience* **2011,** *45* (2), 246-255.
24. First, M.; Gil-Ad, I.; Taler, M.; Tarasenko, I.; Novak, N.; Weizman, A. J., The Effects of Reboxetine Treatment on Depression-like Behavior, Brain Neurotrophins, and ERK Expression in Rats Exposed to Chronic Mild Stress. *Journal of Molecular Neuroscience* **2013,** *50* (1), 88-97.
25. Russo-Neustadt, A. A.; Alejandre, H.; Garcia, C.; Ivy, A. S.; Chen, M. J., Hippocampal Brain-Derived Neurotrophic Factor Expression Following Treatment with Reboxetine, Citalopram, and Physical Exercise. *Neuropsychopharcology* **2004,** *29* (12), 2189-2199.
26. Johnson, C. F.; Williams, B.; MacGillivray, S. A.; Dougall, N. J.; Maxwell, M. J, 'Doing the Right Thing': Factors Influencing GP Prescribing of Antidepressants and Prescribed Doses. *BCM Family Pracitce* **2017,** *18* (1), 1-13.
27. Myers, E.; Calvert, E. J., Information, Compliance and Side-Effects: a Study of Patients on Antidepressant Medication. *The American Journal of Psychiatry* **1984,** *17* (1), 21-25.

28. Meltzer, H., Role of Serotonin in Depression. *ANNALS of the New York Academy of Sciences* **1990,** *600* (1), 486-499.

Appendix A

Supporting Information for

Chapter 2: Glutamate Electropolymerization on Carbon Increases Analytical Sensitivity to Dopamine and Serotonin: An Auspicious *In Vivo* Phenomenon in Mice?[1]

[1]Holmes, J., Witt, C. E., Keen, D., Buchanan, A. M., Batey, L., Hersey, M. & Hashemi P.

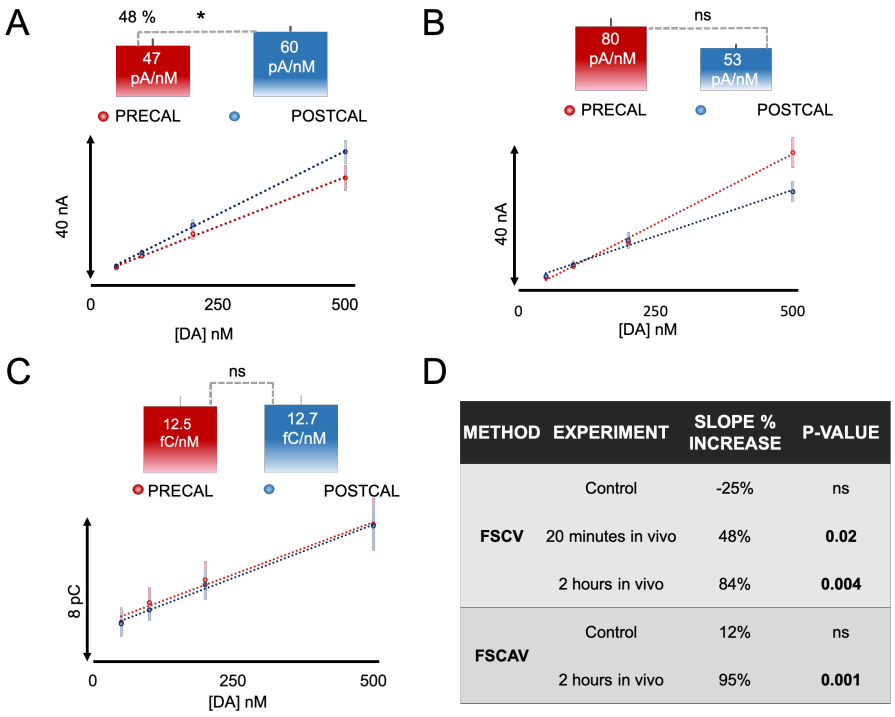

METHOD	EXPERIMENT	SLOPE % INCREASE	P-VALUE
FSCV	Control	-25%	ns
	20 minutes in vivo	48%	**0.02**
	2 hours in vivo	84%	**0.004**
FSCAV	Control	12%	ns
	2 hours in vivo	95%	**0.001**

Figure A.1: Pre- and Post-calibration Effects. Current (nA) or charge (pC) response to various concentrations of dopamine is plotted. (A) A pre-calibration was performed with FSCV, followed by implantation of the electrode *in vivo* for 20 min, and a post-calibration was performed after removal (n=5). All pre-calibrations are denoted in red and post-calibrations are denoted in blue. (B) A bare electrode is pre-calibrated with FSCV, then the DA waveform is cycled for 2 hours in PBS buffer, followed by a post-calibration (n=5). (C) The experimental paradigm is repeated with FSCAV where the electrode is pre-calibrated, cycled for 2 hours in TRIS buffer, and post-calibrated. These experiments were performed as a control (n=4). (D) A table of compiling data from Figure 1 and Figure S1 of experimental and control, FSCV, and FSCAV trails. Statistics: Error bars represent standard error of the mean. P-value was determined with a one-way paired T-test, ns = not significant.

To further support the results from **Fig. 2.1**, control pre-calibrations and post-calibrations were performed in **Fig. A.1**. When electrodes were implanted into brain tissue for between 20 minutes (to simulate the routine *in vivo* conditioning protocol) and 2 hours (the length of a typical *in vivo* experiment), there were significant increases in the slopes of post-calibrated electrodes with both FSCV and FSCAV, as shown in both **Fig. A.1** and **Fig. 2.1.** Electrodes were cycled for 2 hours with the DA waveform (+1.3 V positive potential limit) and calibrated before and after. When electrodes were cycled in PBS buffer for two hours, there was no change in the slope of the calibration curves before and after analysis with both FSCV and FSCAV. The percent increase in slope for each plot in **Fig. A.1** and **Fig. 2.1**, as well as the significance of each experiment, is compiled in the table within **Fig. A.1.D.** From these results, we conclude that the *in vivo* environment must be responsible for the increase in sensitivity, as the use of two different buffers and application of over-

oxidizing potential over time did not result in significant increases in the slopes of control calibration curves.

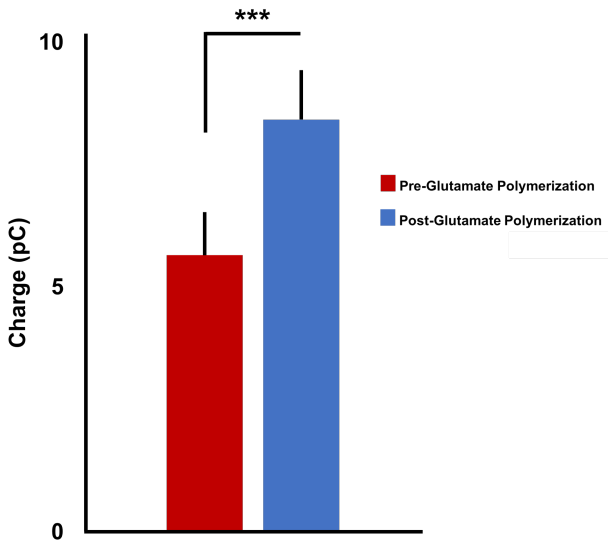

Figure A.2: Pre- and Post-Glutamate Polymerization Effects—FSCAV Analysis. Charge (pC) response to 1 μM of DA is displayed in the bar graph above. The red represents the responses of bare electrodes to 1 μM DA over 15 mins (n=6) of data acquisition using FSCAV. The bare electrodes were then cycled at 60 Hz on the DA waveform in a 1μM glutamate solution. The blue represents the responses of the now electropolymerized electrodes to 1 uM DA over 15 mins (n=6). A paired t-test and an ANOVA two-way test were performed on this data set; the two factors compared were the pre- and post-gluatmate polymerization in each test. Both tests indicate that glutamate polymerization produces a significant difference in sensitivity toward DA detection *via* FSCAV (p-value <0.00001).

Appendix B

Supporting Information for

Chapter 3: Novel, User-friendly Experimental and Analysis Strategies for Fast Voltammetry: 2. Methods for Improved FSCAV Analysis of Serotonin[1]

[1] Colby E. Witt‡, Sergio Mena‡, Lauren E. Honan, Marco Visentin, Lauren Batey, Nathan Robins, Yangguang Ou, & Parastoo Hashemi

1. Beaker Experiments Towards AA Surface Treatment. The following *in vitro* experiments were key findings toward the final amino acid surface modification and *in vivo* implantation.

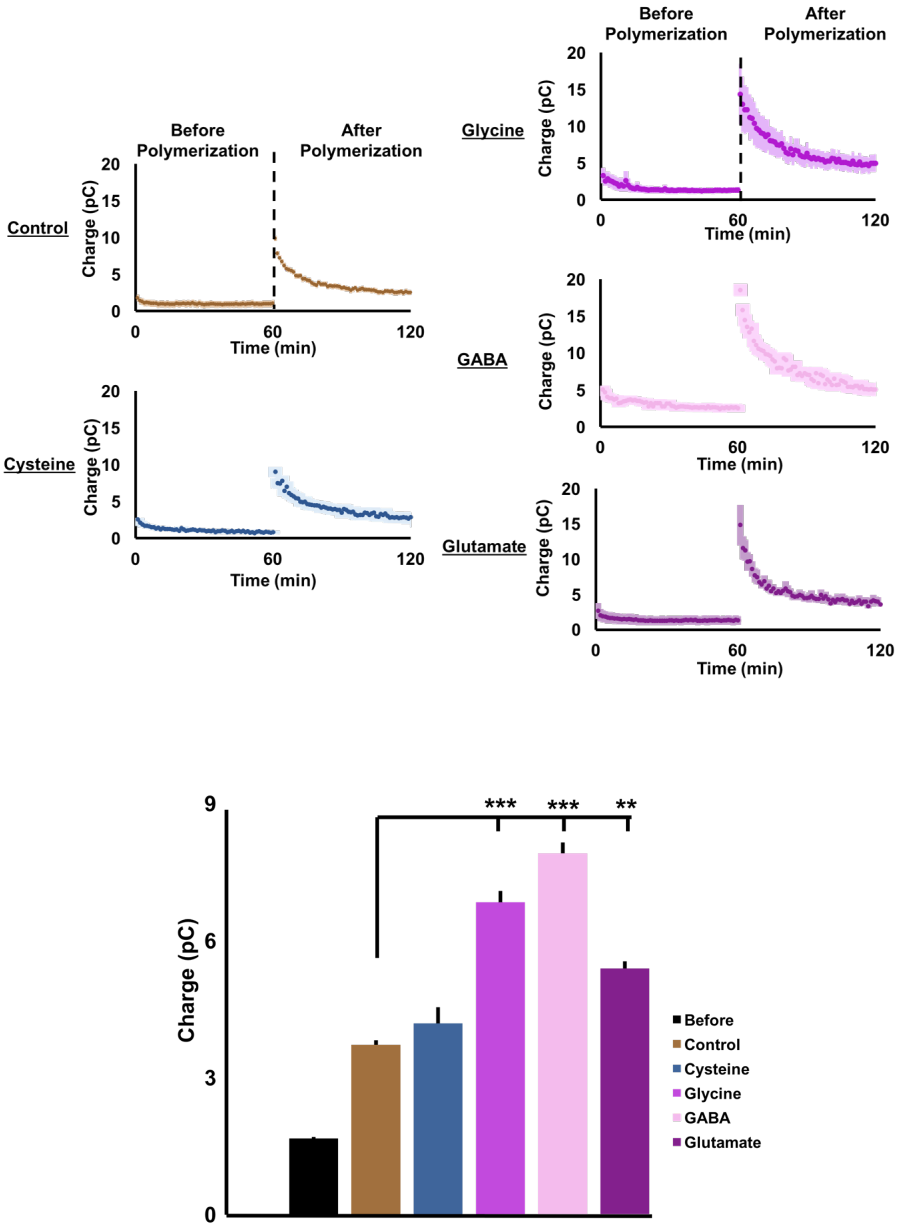

Figure B.1: Surface treatments of the carbon fibre with polymerized amino acids. (A, B, C, D, E) *In vitro* FSCAV acquisitions in PBS-buffered 75 nM serotonin solution together with the amino acid stated in the graph of each panel. Scatter points and error bars show the mean ± SEM across 5 electrodes. The gray bar shows the time at which the polymerization waveform is applied.

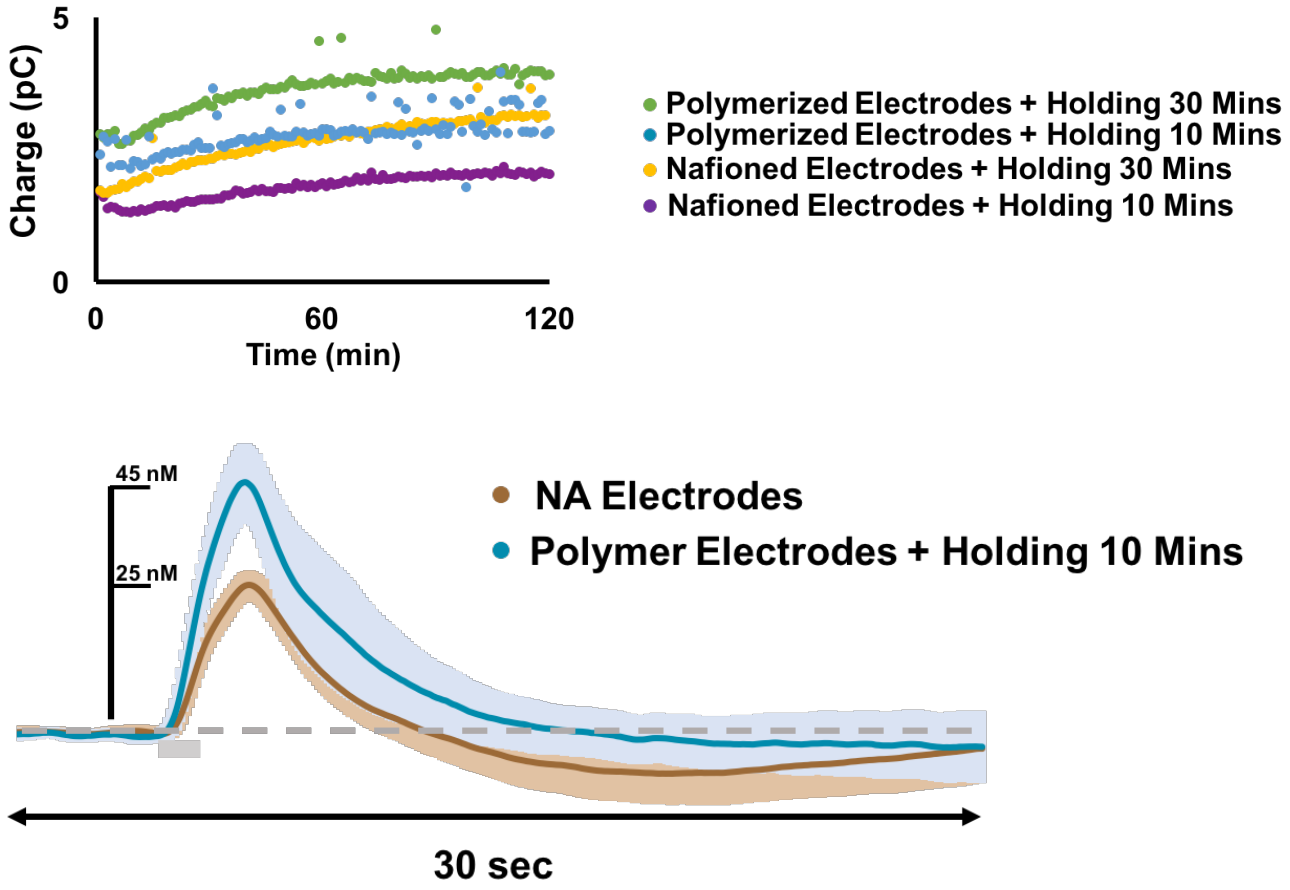

Figure B.2: Surface treatments of the carbon fibre with polymerized amino acids + wait time experiments. *In vitro* FSCAV acquisitions in AA acid + PBS-buffer 75 nM serotonin solution together. Across 3 electrodes, polymerized electrodes held for 10 mins at 0.2 V were the most stable. Below, current vs. time traces of serotonin collected *in vivo* are averaged (n=5) and compared: polymer application of the 3 AA pretreatment (blue) vs. the Jackson waveform on NA electrodes (brown) gray bar shows the time at which the polymerization waveform is applied.

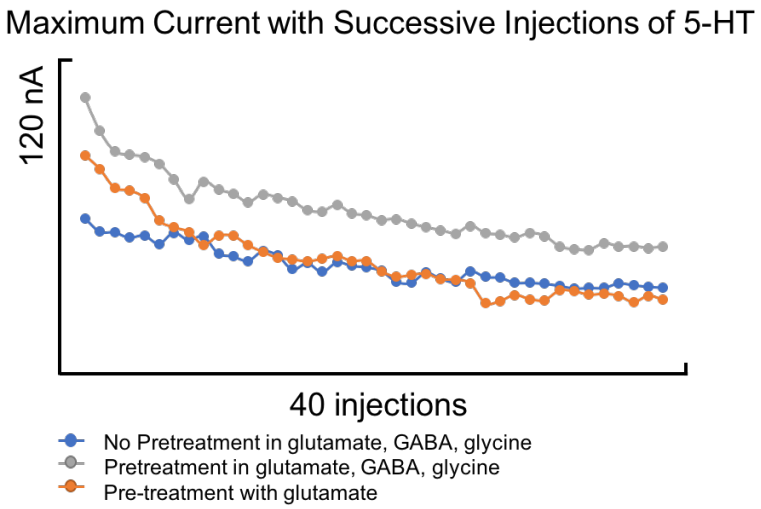

Pretreatment with Glutamate:
Carbon fiber micro-electrodes were hand fabricated and cut to 150 microns prior to coating with Nafion as previously described. The electrode was cycled in physiological buffer with 1uM glutamate for 10 minutes at 60hz and 10 minutes at 10hz using the extended Jackson waveform (0.2V to -0.1V to 1.3V to 0.2V at a scan rate of 1000V/s). After cycling with extended waveform for 20 minutes, the electrode was cycled for 10minutes at 60hz and 10 minutes at 10 Hz using the conventional Jackson waveform in physiological buffer with 1uM glutamate.
Pretreatment with Glutamate, Glycine, and GABA:
Carbon fiber micro-electrodes were hand fabricated and cut to 150 microns prior to coating with Nafion as previously described. The electrode was cycled in physiological buffer with 21.3 uM glutamate, 34uM Glycine, and 2.5uM GABA for 10 minutes at 60hz and 10 minutes at 10hz using the extended Jackson waveform (0.2V to -0.1V to 1.3V to 0.2V at a scan rate of 1000V/s). After cycling with extended waveform for 20 minutes, the electrode was cycled for 10minutes at 60hz and 10 minutes at 10 Hz using the conventional Jackson waveform in physiological buffer with 21.3 uM glutamate, 34uM Glycine, and 2.5uM GABA
Pretreatment with Glutamate, Glycine, and GABA:
Carbon fiber micro-electrodes were hand fabricated and cut to 150 microns prior to coating with Nafion as previously described. The electrode was cycled in physiological buffer with 21.3 uM glutamate, 34uM Glycine, and 2.5uM GABA for 10 minutes at 60hz and 10 minutes at 10 Hz using the conventional Jackson waveform.

Injection Protocol:
Pretreatment with Glutamate:
Following the Cycling paradigm, a bolus of 1uM serotonin was introduced to the electrode using the flow injection analysis system 40 times with 2 minutes between each injection. Between injections, the physiological buffer (with no glutamate) was permitted to flow through the system into contact with the electrode at a flow rate 1.7ml/min.

Pretreatment with Glutamate, Glycine, and GABA:
Following the Cycling paradigm, a bolus of 1uM serotonin was introduced to the electrode using the flow injection analysis system 40 times with 2 minutes between each injection. Between injections, the physiological buffer, with 21.3 uM glutamate, 34uM Glycine, and 2.5uM GABA, was permitted to flow through the system into contact with the electrode at a flow rate 1.7ml/min.
No Pretreatment with Glutamate, Glycine, and GABA:
Following the Cycling paradigm, a bolus of 1uM serotonin was introduced to the electrode using the flow injection analysis system 40 times with 2 minutes between each injection. Between injections, the physiological buffer, 21.3 uM glutamate, 34uM Glycine, and 2.5uM GABA, was permitted to flow through the system into contact with the electrode at a flow rate 1.7ml/min.

Figure B.3: FSCV confirmation of 3 AA treated electrode

Table B.1: List of names of groups and indexes of the analysis of variance.

Group	Number
Glutamate	1
GABA	2
Glycine	3
Glu + GABA + Gly	4
None (PBS only)	5

Table B.2: Analysis of variance results for the differences between pre and post sensitivity (**Figure 3**).

Source	Sum sq.	d.f.	Mean sq.	F statistic	Prob > F
Treatment	6.8698	4	1.7174	1.1650	0.3558
Error	29.4839	20	1.4742	-	-
Total	36.3537	24	-	-	-

As depicted in **Table B.2**, no significant effect of the treatment (polymerization of amino acids into the carbon fibre) was found in the variability of differences in sensitivity pre and post polymerization.

Table B3: Analysis of variance results for the differences between pre and post time constant (**Figure 3**).

Source	Sum sq.	d.f.	Mean sq.	F statistic	Prob > F
Treatment	8.4857e+03	4	2.1214e+03	8.2009	4.3827e-04
Error	5.1736e+03	20	25258.6814	-	-
Total	1.3659e+03	24	-	-	-

Table B.3 shows that a significant effect of the factor treatment was found in the variability of differences in time constant pre and post polymerization. After that, a *Tukey-Kramer post-hoc* multiple comparison test was performed. The full matrix of multiple comparisons p values are shown in **Table S.4**, and p values in bold are reported in the main manuscript.

Table B.4: Tukey-Kramer post-hoc test across ANOVA groups. Probabilities in bold text are of interest.

***Tukey-Kramer post-hoc* multiple tests** **Pr > |t| for H_0: Mean t63% (i) = Mean t63% (j)**					
i/j	**1**	**2**	**3**	**4**	**5**
1	-	0.2334	0.9457	0.9746	0.0005
2	0.2334	-	0.6173	0.5316	0.0636
3	0.9457	0.6173	-	0.9999	0.0028
4	0.9746	0.5316	0.9999	-	0.0021
5	**0.0005**	**0.0636**	**0.0028**	**0.0021**	-

Table B.5: List of names of groups and indexes of the analysis of variance.

Group	Number
In vivo, Nafion-only electrodes	1
In vivo, AA-polymerized electrodes	2
In vitro in AA matrix	3

Table B.6: Analysis of variance results for the t63%of experimental traces (**Figure 3**).

Source	**Sum sq.**	**d.f.**	**Mean sq.**	**F statistic**	**Prob > F**
Model	1406.6723	2	703.3362	5.3129	0.0161
Error	2250.5169	17	132.3833	-	-
Total	3657.1892	19	-	-	-

Table B.6 shows that a significant effect of the matrix and electrode surface treatment in the time constant of the experimental trace. After that, a *Tukey-Kramer post-hoc* multiple comparison test was performed. The full matrix of multiple comparisons p values are shown in **Table S.7**, and p values in bold are reported in the main manuscript.

Table B.7: Tukey-Kramer post-hoc test across ANOVA groups. Probabilities in bold text are of interest.

***Tukey-Kramer post-hoc* multiple tests** **Pr > |t| for H_0: Mean t63% (i) = Mean t63% (j)**			
i/j	**1**	**2**	**3**
1	-	0.9663	0.0216
2	**0.9663**	-	0.0290
3	0.0216	**0.0290**	-

Appendix C

Permission to Reprint

Chapter 2: Glutamate Electropolymerization on Carbon Increases Analytical Sensitivity to Dopamine and Serotonin: An Auspicious *In Vivo* Phenomenon in Mice?